

RILEM State-of-the-Art Reports

Øyvind Bjøntegaard  
Tor Arne Martius-Hammer  
Matias Krauss  
Harald Budelmann

# RILEM Technical Committee 195-DTD Recommendation for Test Methods for AD and TD of Early Age Concrete

Round Robin Documentation Report:  
Program, Test Results and Statistical  
Evaluation



 Springer

The Springer logo features a white chess knight icon on a blue background, followed by the word "Springer" in a white serif font.

**RILEM Technical Committee 195-DTD  
Recommendation for Test Methods  
for AD and TD of Early Age Concrete**

# RILEM STATE-OF-THE-ART REPORTS

## Volume 16

---

RILEM, The International Union of Laboratories and Experts in Construction Materials, Systems and Structures, founded in 1947, is a non-governmental scientific association whose goal is to contribute to progress in the construction sciences, techniques and industries, essentially by means of the communication it fosters between research and practice. RILEM's focus is on construction materials and their use in building and civil engineering structures, covering all phases of the building process from manufacture to use and recycling of materials. More information on RILEM and its previous publications can be found on [www.RILEM.net](http://www.RILEM.net).

The RILEM State-of-the-Art Reports (STAR) are produced by the Technical Committees. They represent one of the most important outputs that RILEM generates—high level scientific and engineering reports that provide cutting edge knowledge in a given field. The work of the TCs is one of RILEM's key functions.

Members of a TC are experts in their field and give their time freely to share their expertise. As a result, the broader scientific community benefits greatly from RILEM's activities.

RILEM's stated objective is to disseminate this information as widely as possible to the scientific community. RILEM therefore considers the STAR reports of its TCs as of highest importance, and encourages their publication whenever possible.

The information in this and similar reports are mostly pre-normative in the sense that it provides the underlying scientific fundamentals on which standards and codes of practice are based. Without such a solid scientific basis, construction practice will be less than efficient or economical.

It is RILEM's hope that this information will be of wide use to the scientific community.



Øyvind Bjøntegaard · Tor Arne Martius-Hammer  
Matias Krauss · Harald Budelmann

# RILEM Technical Committee 195-DTD Recommendation for Test Methods for AD and TD of Early Age Concrete

Round Robin Documentation Report:  
Program, Test Results and Statistical  
Evaluation



 Springer



Øyvind Bjøntegaard  
The Norwegian Public Roads  
Administration  
Trondheim  
Norway

Matias Krauss  
Bundesamt für Strahlenschutz  
Salzgitter  
Germany

Tor Arne Martius-Hammer  
SINTEF Building and Infrastructure  
Trondheim  
Norway

Harald Budelmann  
IBMB  
Braunschweig  
Germany

ISSN 2213-204X

ISBN 978-94-017-9265-3

DOI 10.1007/978-94-017-9266-0

ISSN 2213-2031 (electronic)

ISBN 978-94-017-9266-0 (eBook)

Library of Congress Control Number: 2014945780

Springer Dordrecht Heidelberg New York London

© RILEM 2015

No part of this work may be reproduced, stored in a retrieval system, or transmitted in any form or by any means, electronic, mechanical, photocopying, microfilming, recording or otherwise, without written permission from the Publisher, with the exception of any material supplied specifically for the purpose of being entered and executed on a computer system, for exclusive use by the purchaser of the work. Permission for use must always be obtained from the owner of the copyright: RILEM.

Printed on acid-free paper

Springer is part of Springer Science+Business Media ([www.springer.com](http://www.springer.com))

# Acknowledgments

The contribution from the RILEM TC195-DTD round robin participants is greatly acknowledged. The financial contribution of the Norwegian Research Council (the NOR-CRACK project) is also acknowledged as it was vital for the first author in the work on compilation of results and reporting.

# Contents

<b>1 Round Robin Documentation Report:</b>	
<b>Program, Test Results and Statistical Evaluation</b> . . . . .	1
1.1 Introduction and Background. . . . .	1
1.2 RR-participants. . . . .	1
1.3 Brief Description of the Dilation Rigs . . . . .	2
1.4 Round-Robin Tests, Plan and Execution . . . . .	4
1.4.1 Materials. . . . .	4
1.4.2 Mortar Tests . . . . .	4
1.4.3 Cement Paste Tests . . . . .	6
1.5 Mortar Test Results. . . . .	9
1.5.1 Fresh Properties and 28-Days Strength . . . . .	9
1.5.2 Supporting Test Results . . . . .	12
1.5.3 Dilation Rig Results, Autogenous Deformation. . . . .	17
1.6 Statistical Evaluation of the Dilation Rig Results . . . . .	18
1.6.1 Prerequisites, Objectives and Procedure . . . . .	20
1.6.2 A Concept for the Estimation of Candidates of Outliers from Unbiased Samples . . . . .	27
1.6.3 Analysis of the Data: Calculation of Outliers . . . . .	29
1.6.4 Statistical Attributes of AD and AS . . . . .	34
1.6.5 Summary and Conclusions. . . . .	37
1.7 Cement Paste Test Results . . . . .	39
1.7.1 Supporting Test Results . . . . .	39
1.7.2 Dilation Rig Test Results . . . . .	42
1.8 Summary and Conclusions. . . . .	44
References . . . . .	47

<b>Appendix A: Cement Analyses. . . . .</b>	<b>49</b>
<b>Appendix B: Sand Grading Curve . . . . .</b>	<b>51</b>
<b>Appendix C: Data Sheet, Scanflux AD18 . . . . .</b>	<b>53</b>
<b>Appendix D: Description of Equipment, Made by the Participants . . . . .</b>	<b>55</b>

# Notations

AD/AS	Autogenous deformation/autogenous shrinkage
COV	Coefficient of variation
CR	Creep
CS	Chemical shrinkage
CTE	Coefficient of Thermal Expansion (Greek symbol = $\alpha_T$ )
Dilation Rig	Set-up for longitudinal measurement of free strain of a sealed specimen
DS	Drying shrinkage
EA	Activation energy (two parameter law acc. to Freiesleben Hansen)
EOD	End of dormant phase
EOS	End of setting
H-Test	Hampel Test
KS-Test	Kolmogorov–Smirnov Test
MEAN	Mean value
MED	Median
N	Size of a sample
RH	Relative Humidity
RR	Round Robin
SD	Standard deviation
SP	Superplasticizer
SSD	Saturated, surface dry condition
$t_0$	End of dormant phase in real time domain
TD	Thermal Dilation
$t_{e0}$	End of dormant phase in equivalent time domain (maturity)
$t_{e0ad}$	Beginning of AD
$t_{e0as}$	Beginning of AS
TSTM	Temperature-Stress testing machine
$\epsilon_{ad}$	Estimated AD
$\epsilon_{as}$	Estimated AS
$\epsilon_{tot}$	Measured total strain

# RILEM Publications

The following list presents the global offer of RILEM Publications, sorted by series. Each publication is available in printed version and/or in online version.

## RILEM Proceedings

**PRO 1:** Durability of High Performance Concrete (ISBN: 2-912143-03-9); *Ed. H. Sommer*

**PRO 2:** Chloride Penetration into Concrete (ISBN: 2-912143-00-04); *Eds. L.-O. Nilsson and J.-P. Ollivier*

**PRO 3:** Evaluation and Strengthening of Existing Masonry Structures (ISBN: 2-912143-02-0); *Eds. L. Binda and C. Modena*

**PRO 4:** Concrete: From Material to Structure (ISBN: 2-912143-04-7); *Eds. J.-P. Bournazel and Y. Malier*

**PRO 5:** The Role of Admixtures in High Performance Concrete (ISBN: 2-912143-05-5); *Eds. J. G. Cabrera and R. Rivera-Villarreal*

**PRO 6:** High Performance Fiber Reinforced Cement Composites—HPFRCC 3 (ISBN: 2-912143-06-3); *Eds. H.W. Reinhardt and A.E. Naaman*

**PRO 7:** First International RILEM Symposium on Self-Compacting Concrete (ISBN: 2-912143-09-8); *Eds. Å. Skarendahl and Ö. Petersson*

**PRO 8:** International RILEM Symposium on Timber Engineering (ISBN: 2-912143-10-1); *Ed. L. Boström*

**PRO 9:** Second International RILEM Symposium on Adhesion between Polymers and Concrete ISAP '99 (ISBN: 2-912143-11-X); *Eds. Y. Ohama and M. Puterman*

**PRO 10:** Third International RILEM Symposium on Durability of Building and Construction Sealants (ISBN: 2-912143-13-6); *Eds. A.T. Wolf*

**PRO 11:** Fourth International RILEM Conference on Reflective Cracking in Pavements (ISBN: 2-912143-14-4); *Eds. A.O. Abd El Halim, D.A. Taylor and El H.H. Mohamed*

**PRO 12:** International RILEM Workshop on Historic Mortars: Characteristics and Tests (ISBN: 2-912143-15-2); *Eds. P. Bartos, C. Groot and J.J. Hughes*

**PRO 13:** Second International RILEM Symposium on Hydration and Setting (ISBN: 2 912143-16-0); *Ed. A. Nonat*

**PRO 14:** Integrated Life-Cycle Design of Materials and Structures—ILCDES 2000 (ISBN: 951-758-408-3); (ISSN: 0356-9403); *Ed. S. Sarja*

**PRO 15:** Fifth RILEM Symposium on Fibre-Reinforced Concretes (FRC)—BEFIB'2000 (ISBN: 2-912143-18-7); *Eds. P. Rossi and G. Chanvillard*

**PRO 16:** Life Prediction and Management of Concrete Structures (ISBN: 2-912143-19-5); *Ed. D. Naus*

**PRO 17:** Shrinkage of Concrete—Shrinkage 2000 (ISBN: 2-912143-20-9); *Eds. V. Baroghel-Bouny and P.-C. Aïtcin*

**PRO 18:** Measurement and Interpretation of the On-Site Corrosion Rate (ISBN: 2-912143-21-7); *Eds. C. Andrade, C. Alonso, J. Fullea, J. Polimon and J. Rodriguez*

**PRO 19:** Testing and Modelling the Chloride Ingress into Concrete (ISBN: 2-912143-22-5); *Eds. C. Andrade and J. Kropp*

**PRO 20:** First International RILEM Workshop on Microbial Impacts on Building Materials (CD 02) (e-ISBN 978-2-35158-013-4); *Ed. M. Ribas Silva*

**PRO 21:** International RILEM Symposium on Connections between Steel and Concrete (ISBN: 2-912143-25-X); *Ed. R. Eligehausen*

**PRO 22:** International RILEM Symposium on Joints in Timber Structures (ISBN: 2-912143-28-4); *Eds. S. Aicher and H.-W. Reinhardt*

**PRO 23:** International RILEM Conference on Early Age Cracking in Cementitious Systems (ISBN: 2-912143-29-2); *Eds. K. Kovler and A. Bentur*

**PRO 24:** Second International RILEM Workshop on Frost Resistance of Concrete (ISBN: 2-912143-30-6); *Eds. M.J. Setzer, R. Auberg and H.-J. Keck*

**PRO 25:** International RILEM Workshop on Frost Damage in Concrete (ISBN: 2-912143-31-4); *Eds. D.J. Janssen, M.J. Setzer and M.B. Snyder*

**PRO 26:** International RILEM Workshop on On-Site Control and Evaluation of Masonry Structures (ISBN: 2-912143-34-9); *Eds. L. Binda and R.C. de Vekey*

**PRO 27:** International RILEM Symposium on Building Joint Sealants (CD03); *Ed. A.T. Wolf*

**PRO 28:** Sixth International RILEM Symposium on Performance Testing and Evaluation of Bituminous Materials—PTEBM'03 (ISBN: 2-912143-35-7; e-ISBN: 978-2-912143-77-8); *Ed. M.N. Partl*

**PRO 29:** Second International RILEM Workshop on Life Prediction and Ageing Management of Concrete Structures (ISBN: 2-912143-36-5); *Ed. D.J. Naus*

**PRO 30:** 4th International RILEM Workshop on High Performance Fiber Reinforced Cement Composites—HPFRCC 4 (ISBN: 2-912143-37-3); *Eds. A.E. Naaman and H.W. Reinhardt*

**PRO 31:** International RILEM Workshop on Test and Design Methods for Steel Fibre Reinforced Concrete: Background and Experiences (ISBN: 2-912143-38-1); *Eds. B. Schnütgen and L. Vandewalle*

**PRO 32:** International Conference on Advances in Concrete and Structures 2 vol.(ISBN (set): 2-912143-41-1); *Eds. Ying-shu Yuan, Surendra P. Shah and Heng-lin Lü*

**PRO 33:** Third International Symposium on Self-Compacting Concrete (ISBN: 2-912143-42-X); *Eds. Ó. Wallevik and I. Nielsson*

**PRO 34:** International RILEM Conference on Microbial Impact on Building Materials (ISBN: 2-912143-43-8); *Ed. M. Ribas Silva*

**PRO 35:** International RILEM TC 186-ISA on Internal Sulfate Attack and Delayed Ettringite Formation (ISBN: 2-912143-44-6); *Eds. K. Scrivener and J. Skalny*

**PRO 36:** International RILEM Symposium on Concrete Science and Engineering—A Tribute to Arnon Bentur (ISBN: 2-912143-46-2); *Eds. K. Kovler, J. Marchand, S. Mindess and J. Weiss*

**PRO 37:** Fifth International RILEM Conference on Cracking in Pavements—Mitigation, Risk Assessment and Prevention (ISBN: 2-912143-47-0); *Eds. C. Petit, I. Al-Qadi and A. Millien*

**PRO 38:** Third International RILEM Workshop on Testing and Modelling the Chloride Ingress into Concrete (ISBN: 2-912143-48-9); *Eds. C. Andrade and J. Kropp*

**PRO 39:** Sixth International RILEM Symposium on Fibre-Reinforced Concretes—BEFIB 2004 (ISBN: 2-912143-51-9); *Eds. M. Di Prisco, R. Felicetti and G.A. Plizzari*

**PRO 40:** International RILEM Conference on the Use of Recycled Materials in Buildings and Structures (ISBN: 2-912143-52-7); *Eds. E. Vázquez, Ch. F. Hendriks and G.M.T. Janssen*

**PRO 41:** RILEM International Symposium on Environment-Conscious Materials and Systems for Sustainable Development (ISBN: 2-912143-55-1); *Eds. N. Kashino and Y. Ohama*

**PRO 42:** SCC'2005—China: First International Symposium on Design, Performance and Use of Self-Consolidating Concrete (ISBN: 2-912143-61-6); *Eds. Zhiwu Yu, Caijun Shi, Kamal Henri Khayat and Youjun Xie*

**PRO 43:** International RILEM Workshop on Bonded Concrete Overlays (e-ISBN: 2-912143-83-7); *Eds. J.L. Granju and J. Silfwerbrand*

**PRO 44:** Second International RILEM Workshop on Microbial Impacts on Building Materials (CD11) (e-ISBN: 2-912143-84-5); *Ed. M. Ribas Silva*

**PRO 45:** Second International Symposium on Nanotechnology in Construction, Bilbao (ISBN: 2-912143-87-X); *Eds. Peter J. M. Bartos, Yolanda de Miguel and Antonio Porro*

**PRO 46:** ConcreteLife'06—International RILEM-JCI Seminar on Concrete Durability and Service Life Planning: Curing, Crack Control, Performance in Harsh Environments (ISBN: 2-912143-89-6); *Ed. K. Kovler*

**PRO 47:** International RILEM Workshop on Performance Based Evaluation and Indicators for Concrete Durability (ISBN: 978-2-912143-95-2); *Eds. V. Baroghel-Bouny, C. Andrade, R. Torrent and K. Scrivener*

**PRO 48:** First International RILEM Symposium on Advances in Concrete through Science and Engineering (e-ISBN: 2-912143-92-6); *Eds. J. Weiss, K. Kovler, J. Marchand, and S. Mindess*



**PRO 49:** International RILEM Workshop on High Performance Fiber Reinforced Cementitious Composites in Structural Applications (ISBN: 2-912143-93-4); *Eds. G. Fischer and V.C. Li*

**PRO 50:** First International RILEM Symposium on Textile Reinforced Concrete (ISBN: 2-912143-97-7); *Eds. Josef Hegger, Wolfgang Brameshuber and Norbert Will*

**PRO 51:** Second International Symposium on Advances in Concrete through Science and Engineering (ISBN: 2-35158-003-6; e-ISBN: 2-35158-002-8); *Eds. J. Marchand, B. Bissonnette, R. Gagné, M. Jolin and F. Paradis*

**PRO 52:** Volume Changes of Hardening Concrete: Testing and Mitigation (ISBN: 2-35158-004-4; e-ISBN: 2-35158-005-2); *Eds. O. M. Jensen, P. Lura and K. Kovler*

**PRO 53:** High Performance Fiber Reinforced Cement Composites—HPFRCC5 (ISBN: 978-2-35158-046-2); *Eds. H.W. Reinhardt and A. E. Naaman*

**PRO 54:** Fifth International RILEM Symposium on Self-Compacting Concrete (ISBN: 978-2-35158-047-9); *Eds. G. De Schutter and V. Boel*

**PRO 55:** International RILEM Symposium Photocatalysis, Environment and Construction Materials (ISBN: 978-2-35158-056-1); *Eds. P. Baglioni and L. Cassar*

**PRO 56:** International RILEM Workshop on Integral Service Life Modelling of Concrete Structures (ISBN 978-2-35158-058-5); *Eds. R.M. Ferreira, J. Gulikers and C. Andrade*

**PRO 57:** RILEM Workshop on Performance of cement-based materials in aggressive aqueous environments (e-ISBN: 978-2-35158-059-2); *Ed. N. De Belie*

**PRO 58:** International RILEM Symposium on Concrete Modelling—CONMOD'08 (ISBN: 978-2-35158-060-8); *Eds. E. Schlungen and G. De Schutter*

**PRO 59:** International RILEM Conference on On Site Assessment of Concrete, Masonry and Timber Structures—SACoMaTiS 2008 (ISBN set: 978-2-35158-061-5); *Eds. L. Bindá, M. di Prisco and R. Felicetti*

**PRO 60:** Seventh RILEM International Symposium on Fibre Reinforced Concrete: Design and Applications—BEFIB 2008 (ISBN: 978-2-35158-064-6); *Ed. R. Gettu*

**PRO 61:** First International Conference on Microstructure Related Durability of Cementitious Composites 2 vol., (ISBN: 978-2-35158-065-3); *Eds. W. Sun, K. van Breugel, C. Miao, G. Ye and H. Chen*

**PRO 62:** NSF/ RILEM Workshop: In-situ Evaluation of Historic Wood and Masonry Structures (e-ISBN: 978-2-35158-068-4); *Eds. B. Kasal, R. Anthony and M. Drdácý*

**PRO 63:** Concrete in Aggressive Aqueous Environments: Performance, Testing and Modelling, 2 vol., (ISBN: 978-2-35158-071-4); *Eds. M.G. Alexander and A. Bertron*

**PRO 64:** Long Term Performance of Cementitious Barriers and Reinforced Concrete in Nuclear Power Plants and Waste Management—NUCPERF 2009 (ISBN: 978-2-35158-072-1); *Eds. V. L'Hostis, R. Gens, C. Gallé*

**PRO 65:** Design Performance and Use of Self-consolidating Concrete—SCC'2009 (ISBN: 978-2-35158-073-8); *Eds. C. Shi, Z. Yu, K.H. Khayat and P. Yan*

**PRO 66:** Second International RILEM Workshop on Concrete Durability and Service Life Planning—ConcreteLife'09 (ISBN: 978-2-35158-074-5); *Ed. K. Kovler*

**PRO 67:** Repairs Mortars for Historic Masonry (e-ISBN: 978-2-35158-083-7); *Ed. C. Groot*

**PRO 68:** Proceedings of the Third International RILEM Symposium on 'Rheology of Cement Suspensions such as Fresh Concrete (ISBN 978-2-35158-091-2); *Eds. O.H. Wallevik, S. Kubens and S. Oesterheld*

**PRO 69:** Third International PhD Student Workshop on 'Modelling the Durability of Reinforced Concrete (ISBN: 978-2-35158-095-0); *Eds. R.M. Ferreira, J. Gulikers and C. Andrade*

**PRO 70:** Second International Conference on 'Service Life Design for Infrastructure' (ISBN set: 978-2-35158-096-7, e-ISBN: 978-2-35158-097-4); *Ed. K. van Breugel, G. Ye and Y. Yuan*

**PRO 71:** Advances in Civil Engineering Materials—The 50-year Teaching Anniversary of Prof. Sun Wei' (ISBN: 978-2-35158-098-1; e-ISBN: 978-2-35158-099-8); *Eds. C. Miao, G. Ye, and H. Chen*

**PRO 72:** First International Conference on 'Advances in Chemically-Activated Materials—CAM'2010' (2010), 264 pp, ISBN: 978-2-35158-101-8; e-ISBN: 978-2-35158-115-5, *Eds. Caijun Shi and Xiaodong Shen*

**PRO 73:** Second International Conference on 'Waste Engineering and Management—ICWEM 2010' (2010), 894 pp, ISBN: 978-2-35158-102-5; e-ISBN: 978-2-35158-103-2, *Eds. J. Zh. Xiao, Y. Zhang, M.S. Cheung and R. Chu*

**PRO 74:** International RILEM Conference on 'Use of Superabsorbent Polymers and Other New Additives in Concrete' (2010) 374 pp., ISBN: 978-2-35158-104-9; e-ISBN: 978-2-35158-105-6; *Eds. O.M. Jensen, M.T. Hasholt, and S. Laustsen*

**PRO 75:** International Conference on 'Material Science—Second ICTRC—Textile Reinforced Concrete—Theme 1' (2010) 436 pp., ISBN: 978-2-35158-106-3; e-ISBN: 978-2-35158-107-0; *Ed. W. Brameshuber*

**PRO 76:** International Conference on 'Material Science—HetMat—Modelling of Heterogeneous Materials—Theme 2' (2010) 255 pp., ISBN: 978-2-35158-108-7; e-ISBN: 978-2-35158-109-4; *Ed. W. Brameshuber*

**PRO 77:** International Conference on 'Material Science—AdIPoC—Additions Improving Properties of Concrete—Theme 3' (2010) 459 pp., ISBN: 978-2-35158-110-0; e-ISBN: 978-2-35158-111-7; *Ed. W. Brameshuber*

**PRO 78:** Second Historic Mortars Conference and RILEM TC 203-RHM Final Workshop—HMC2010 (2010) 1416 pp., e-ISBN: 978-2-35158-112-4; *Eds J. Válek, C. Groot, and J.J. Hughes*

**PRO 79:** International RILEM Conference on Advances in Construction Materials Through Science and Engineering (2011) 213 pp., e-ISBN: 978-2-35158-117-9; *Eds Christopher Leung and K.T. Wan*

**PRO 80:** Second International RILEM Conference on Concrete Spalling due to Fire Exposure (2011) 453 pp., ISBN: 978-2-35158-118-6, e-ISBN: 978-2-35158-119-3; *Eds E.A.B. Koenders and F. Dehn*

**PRO 81:** Second International RILEM Conference on Strain Hardening Cementitious Composites (SHCC2-Rio) (2011) 451 pp., ISBN: 978-2-35158-120-9,

e-ISBN: 978-2-35158-121-6; *Eds R.D. Toledo Filho, F.A. Silva, E.A.B. Koenders and E.M.R. Fairbairn*

**PRO 82:** Second International RILEM Conference on Progress of Recycling in the Built Environment (2011) 507 pp., e-ISBN: 978-2-35158-122-3; *Eds V.M. John, E. Vazquez, S.C. Angulo and C. Ulsen*

**PRO 83:** Second International Conference on Microstructural-related Durability of Cementitious Composites (2012) 250 pp., ISBN: 978-2-35158-129-2; e-ISBN: 978-2-35158-123-0; *Eds G. Ye, K. van Breugel, W. Sun and C. Miao*

**PRO 85:** RILEM-JCI International Workshop on Crack Control of Mass Concrete and Related issues concerning Early-Age of Concrete Structures—ConCrack 3—Control of Cracking in Concrete Structures 3 (2012) 237 pp., ISBN: 978-2-35158-125-4; e-ISBN: 978-2-35158-126-1; *Eds F. Toutlemonde and J.-M. Torrenti*

**PRO 86:** International Symposium on Life Cycle Assessment and Construction (2012) 414 pp., ISBN: 978-2-35158-127-8, e-ISBN: 978-2-35158-128-5; *Eds A. Ventura and C. de la Roche*

**PRO 87:** UHPFRC 2013—RILEM-fib-AFGC International Symposium on Ultra-High Performance Fibre-Reinforced Concrete (2013), 832 pp ISBN: 978-2-35158-130-8, e-ISBN: 978-2-35158-131-5; *Eds F. Toutlemonde*

**PRO 88:** Eighth RILEM International Symposium on Fibre Reinforced Concrete (2012) 344 pp., ISBN: 978-2-35158-132-2, e-ISBN: 978-2-35158-133-9; *Eds Joaquim A.O. Barros*

**PRO 89:** RILEM International Workshop on Performance-based specification and control of concrete durability (2014) ISBN978-2-35158-135-3, e-ISBN: 978-2-35158-136-0, *Eds Dubraka Bjegović, Hans Beushausen and Marijana Serdar*

**PRO 90:** Seventh RILEM International Conference on Self-Compacting Concrete and of the First RILEM International Conference on Rheology and Processing of Construction Materials (2013) 396 pp, ISBN: 978-2-35158-137-7, e-ISBN: 978-2-35158-138-4, *Eds Nicolas Roussel and Hela Bessaies-Bey*

## RILEM Reports

**Report 19:** Considerations for Use in Managing the Aging of Nuclear Power Plant Concrete Structures (ISBN: 2-912143-07-1); *Ed. D.J. Naus*

**Report 20:** Engineering and Transport Properties of the Interfacial Transition Zone in Cementitious Composites (ISBN: 2-912143-08-X); *Eds. M.G. Alexander, G. Arliguie, G. Ballivy, A. Bentur and J. Marchand*

**Report 21:** Durability of Building Sealants (ISBN: 2-912143-12-8); *Ed. A.T. Wolf*

**Report 22:** Sustainable Raw Materials—Construction and Demolition Waste (ISBN: 2-912143-17-9); *Eds. C.F. Hendriks and H.S. Pietersen*

**Report 23:** Self-Compacting Concrete state-of-the-art report (ISBN: 2-912143-23-3); *Eds. Å. Skarendahl and Ö. Petersson*

**Report 24:** Workability and Rheology of Fresh Concrete: Compendium of Tests (ISBN: 2-912143-32-2); *Eds. P.J.M. Bartos, M. Sonebi and A.K. Tamimi*

**Report 25:** Early Age Cracking in Cementitious Systems (ISBN: 2-912143-33-0); *Ed. A. Bentur*

**Report 26:** Towards Sustainable Roofing (Joint Committee CIB/RILEM) (CD 07) (e-ISBN 978-2-912143-65-5); *Eds. Thomas W. Hutchinson and Keith Roberts*

**Report 27:** Condition Assessment of Roofs (Joint Committee CIB/RILEM) (CD 08) (e-ISBN 978-2-912143-66-2); *Ed. CIB W 83/RILEM TC166-RMS*

**Report 28:** Final report of RILEM TC 167-COM ‘Characterisation of Old Mortars with Respect to Their Repair’ (ISBN: 978-2-912143-56-3); *Eds. C. Groot, G. Ashall and J. Hughes*

**Report 29:** Pavement Performance Prediction and Evaluation (PPPE): Interlaboratory Tests (e-ISBN: 2-912143-68-3); *Eds. M. Partl and H. Piber*

**Report 30:** Final Report of RILEM TC 198-URM ‘Use of Recycled Materials’ (ISBN: 2-912143-82-9; e-ISBN: 2-912143-69-1); *Eds. Ch.F. Hendriks, G.M.T. Janssen and E. Vázquez*

**Report 31:** Final Report of RILEM TC 185-ATC ‘Advanced testing of cement-based materials during setting and hardening’ (ISBN: 2-912143-81-0; e-ISBN: 2-912143-70-5); *Eds. H.W. Reinhardt and C.U. Grosse*

**Report 32:** Probabilistic Assessment of Existing Structures. A JCSS publication (ISBN 2-912143-24-1); *Ed. D. Diamantidis*

**Report 33:** State-of-the-Art Report of RILEM Technical Committee TC 184-IFE ‘Industrial Floors’ (ISBN 2-35158-006-0); *Ed. P. Seidler*

**Report 34:** Report of RILEM Technical Committee TC 147-FMB ‘Fracture mechanics applications to anchorage and bond’ Tension of Reinforced Concrete Prisms—Round Robin Analysis and Tests on Bond (e-ISBN 2-912143-91-8); *Eds. L. Elfgren and K. Noghabai*

**Report 35:** Final Report of RILEM Technical Committee TC 188-CSC ‘Casting of Self Compacting Concrete’ (ISBN 2-35158-001-X; e-ISBN: 2-912143-98-5); *Eds. Å. Skarendahl and P. Billberg*

**Report 36:** State-of-the-Art Report of RILEM Technical Committee TC 201-TRC ‘Textile Reinforced Concrete’ (ISBN 2-912143-99-3); *Ed. W. Brameshuber*

**Report 37:** State-of-the-Art Report of RILEM Technical Committee TC 192-ECM ‘Environment-conscious construction materials and systems’ (ISBN: 978-2-35158-053-0); *Eds. N. Kashino, D. Van Gemert and K. Imamoto*

**Report 38:** State-of-the-Art Report of RILEM Technical Committee TC 205-DSC ‘Durability of Self-Compacting Concrete’ (ISBN: 978-2-35158-048-6); *Eds. G. De Schutter and K. Audenaert*

**Report 39:** Final Report of RILEM Technical Committee TC 187-SOC ‘Experimental determination of the stress-crack opening curve for concrete in tension’ (ISBN 978-2-35158-049-3); *Ed. J. Planas*

**Report 40:** State-of-the-Art Report of RILEM Technical Committee TC 189-NEC ‘Non-Destructive Evaluation of the Penetrability and Thickness of the Concrete Cover’ (ISBN 978-2-35158-054-7); *Eds. R. Torrent and L. Fernández Luco*

**Report 41:** State-of-the-Art Report of RILEM Technical Committee TC 196-ICC ‘Internal Curing of Concrete’ (ISBN 978-2-35158-009-7); *Eds. K. Kovler and O.M. Jensen*

**Report 42:** ‘Acoustic Emission and Related Non-destructive Evaluation Techniques for Crack Detection and Damage Evaluation in Concrete’—Final Report of RILEM Technical Committee 212-ACD (e-ISBN: 978-2-35158-100-1); *Ed. M. Ohtsu*

# Chapter 1

## Round Robin Documentation Report: Program, Test Results and Statistical Evaluation

### 1.1 Introduction and Background

The report presents the Round-Robin (RR) program and test results including a statistical evaluation, of the Rilem TC195-DTD committee named “Recommendation for test methods for autogenous deformation (AD) and thermal dilation (TD) of early age concrete”. The task of the committee was to *investigate the linear test set-up for AD and TD measurements (Dilation Rigs) in the period from setting to the end of the hardening phase some weeks after*. These are the “stress-inducing” deformations in a hardening concrete structure subjected to restraint conditions.

The main task was to carry out a RR program on testing of AD of one concrete at 20 °C isothermal conditions in Dilation Rigs. The concrete part materials were distributed to 10 laboratories (Canada, Denmark, France, Germany, Japan, The Netherlands, Norway, Sweden and USA), and totally 30 tests on AD were carried out. Some supporting tests were also performed, as well as a smaller RR on cement paste. The committee has worked out a *test procedure recommendation* which is reported separately and submitted acceptance as a RILEM method.

### 1.2 RR-participants

The list below gives the participants of the TC195-DTD RR test program. The acronym of each participant, which is used throughout the report, is given with bold letters. The list also contains the corresponding person(s) at each location.

**Delft** Delft University of Technology, Civil Engineering and Geosciences, Delft, The Netherlands. Contact Person: Eddy Koenders (e.a.b.koenders@tudelft.nl)

**DTU** Technical University of Denmark, Department of Civil Engineering, Lyngby, Denmark. Corresponding person: Ole Mejlhede Jensen (omj@byg.dtu.dk)

<b>IBMB</b>	Technical University of Braunschweig, Institute of Building Materials, Concrete Construction and Fire Protection, Braunschweig, Germany. Corresponding person: Harald Budelmann (h-budelmann@ibmb.tu-bs.de)
<b>Kanazawa</b>	Kanazawa University, Department of Civil Engineering, Kanazawa, Japan. Corresponding person: Shin-ichi Igarashi (igarashi@t.kanazawa-u.ac.jp)
<b>Laval</b>	Laval University, Department of Civil Engineering, Québec City, Canada. Corresponding person: Fabien Perez (fabien.perez@gci.ulaval.ca)
<b>LCPC</b>	Laboratoire Central des Ponts et Chaussées, Concrete and cementitious composites, Paris, France. Corresponding persons: Florent Baby (florent.baby@ifsttar.fr), Véronique Baroghel-Bouny (veronique.baroghel-bouny@ifsttar.fr)
<b>Lund</b>	Lund Institute of Technology, Department of Building Materials, Lund, Sweden. Corresponding person: Katja Fridh (katja.fridh@byggtek.lth.se)
<b>Munich</b>	Technical University of Munich, Centre for Building Materials, Munich, Germany. Corresponding person: Jürgen Huber (jhuber@cbm.bv.tum.de)
<b>NTNU</b>	The Norwegian University of Science and Technology (NTNU), Department of Structural Engineering., Trondheim, Norway. Corresponding person: Øyvind Bjøntegaard (oyvind.bjontegaard@vegvesen.no)
<b>SINTEF</b>	SINTEF Building and Infrastructure, Trondheim, Norway. Corresponding person: Tor Arne Martius-Hammer (tor.hammer@sintef.no)
<b>UIUC</b>	University of Illinois at Urbana-Champaign, Department of Civil and Environmental Engineering, Urbana, USA. Corresponding person: David A. Lange (dlange@illinois.edu)

Distribution of materials for the Round Robin tests:

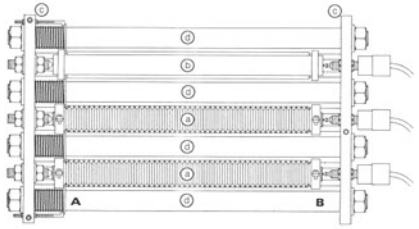
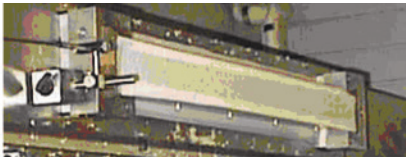
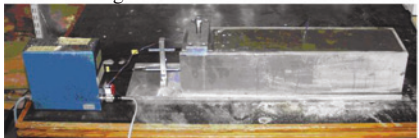


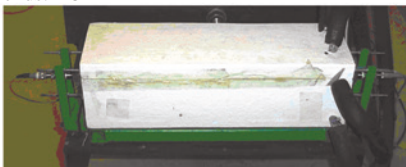
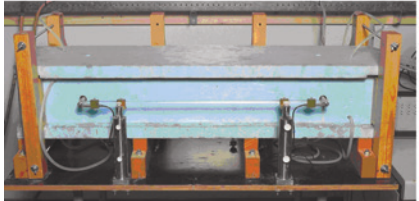

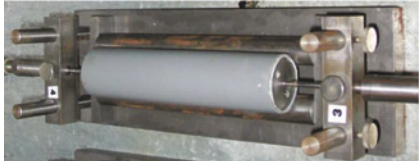

**NORCEM A.S. Brevik** (Norwegian cement producer): Corresponding person: Knut O. Kjellsen (knut.kjellsen@norcem.no)

### 1.3 Brief Description of the Dilation Rigs

All participating Dilation Rigs are given in the survey below (some with pictures and some with principal sketches). A short note on the measuring principle and temperature control is given for each rig. The short-term TC means “temperature-controlled” and NTC means “not temperature controlled”. TC or NTC describe whether or not the Dilation Rig is equipped with a special temperature control facility. All Dilation Rigs are placed in temperature controlled rooms.



A more detailed description of the equipment was made by each participant. These descriptions are given in Appendix D.

<p>DTU: LVDT fixed to one end. TC. (fig. shows two parallel spec. and one invar steel dummy)</p> 	<p>Kanazawa: LVDT fixed to one end plate. NTC.</p> 
<p>Lund: 3 LVDTs fixed to one end plate at different heights. NTC.</p> 	<p>UIUC: LVDT on a longitudinal steel rod with two top surface "forks". NTC.</p> 
<p>IBMB: Strain gauges glued to a cast-in quartz tube. TC.</p> 	<p>NTNU: LVDT fixed to cast-in bolts at both ends. TC</p> 
<p>Delft: LVDT on both longitudinal sides. Fixed between two transverse through-bolts. TC.</p> 	<p>Laval : LVDT on a longitudinal steel rod with two top surface "forks". TC.</p> 
<p>Munic : LVD fixed to both endplates. NTC</p> 	<p>LCPC: Vertical oriented. Digital transducer fixed to top ring. TC.</p> 



## 1.4 Round-Robin Tests, Plan and Execution

### 1.4.1 Materials

The materials listed below were sent out to the participants of the RR from NORCEM A.S. Brevik, in Norway. All materials were used in the mortar mixture, whereas only the cement was used for the cement paste mixture.

- Norcem Standardsement (CEM I-42.5 R) in 40 kg bags, see Appendix A
- Aggregate 0–8 mm (gneiss, granite) in plastic bags, see Appendix B
- Scanflux AD18 (superplasticizer) in plastic cans, see Appendix C

### 1.4.2 Mortar Tests

#### 1.4.2.1 Test Temperature and Test Series

The exact recipe was given in an Excel spreadsheet that was distributed to the participants. The mortar program, consisting totally of 30 dilation tests, was performed in two rounds (series). Prescribed target test temperature for the Dilation Rigs for both series was 20 °C *isothermal conditions*.

- In the first round, **Series I**, no requirements were set for the moisture state of the aggregate prior to mixing, and the amount of water to be added directly into the mix was then given by the spreadsheet considering the given moisture content in the sand. In SSD-condition the aggregate contains 0.8 % water, this was not regarded as free water. 7 of 10 participating laboratories (12 Dilation Rig tests) used moist aggregate (varying from 0.25 to 5.1 % moisture content) when mixing, while the remaining 3 laboratories (11 Dilation Rig tests) used pre-dried aggregate (zero moisture content). Slump after mixing varied from close to 0 to well above 200 mm in these mortar batches.
- In the second round, **Series II**, it was prescribed specifically that the aggregate was to be mixed with zero moisture, meaning pre-drying. The advantage with such requirement is that the recipe of the mortar is unique, see Sect. 1.5 laboratories participated in Series II (totally 5 batches, 7 Dilation Rig tests). In this series the slump after mixing varied from 150 to 255 mm.

The result was then that totally 18 Dilation Rig tests were cast with mortars based on pre-dried aggregate and totally 12 tests were based on moist aggregate.

#### 1.4.2.2 Prescribed Composition

The mortar composition was given in an Excel spreadsheet. The mortar has a water-to-cement ratio of 0.35–35 % paste volume. The detailed composition is given in Table 1.1

**Table 1.1** Round robin mortar composition

Constituent	kg/m <sup>3</sup>
Cement CEM I—42.5 R	521.78
Water added	187.90
Årdal sand 0–8 mm (SSD)	1,729.00
SP (Scanflux AD18)	10.44

The water absorption of the aggregate is 0.8 % (SSD-condition), therefore 13.8 l of water of the total added water (187.9 l) is absorbed and not regarded in the w/c-ratio. The SP contains 82 % water, meaning 8.56 l. It follows then that:  $w/c = (187.9 - 13.8 + 8.56)/521.78 = 0.35$

for the case with pre-dried aggregate. In SSD-condition the given aggregate contains 0.8 % water; this is not regarded as free water when calculating the amount of water to be added directly into the mix. The water (82 %) in the SP is regarded as free water. Initial testing at NTNU/SINTEF showed that the mortar developed no surface bleeding.

#### 1.4.2.3 Prescribed Mixing Procedure and Fresh Concrete Measurements

The following mixing procedure was prescribed:

- Add the water reducer Scanflux AD18 to the water prior to mixing
- Mix sand and cement for 1 min
- Add the mixture of Scanflux AD18 and water and mix for 2 min (included the time of adding)
- Stop the mixer and let rest for 2 min
- Mix for 1 min—end

The following fresh mortar measurements were prescribed:

- Slump, preferably according to EN 12350-2 (cone: bottom  $\varnothing$ 200 mm, top  $\varnothing$ 100 mm, height 300 mm)
- Air content, preferably according to EN 12350-7 (“pressure method”)
- Density, preferably according to EN 12350-6
- Bleeding every hour the first 5 h. The following simple method was suggested:
  - A. cast mortar in a separate container
  - B. tilt the container (gently) some cm during measurement with the help of a small block
  - C. suck up bleed water (if any) with a pipette and register the weight of water present
  - D. remove the block (gently) until the next measurement.

If bleed water was observed in the separate bleeding measurement, it was suggested to remove the bleed water from the top surface of the Dilation Rig specimen (when bleeding was completed) with the use of drying paper or a drying cloth, and then seal the specimen again.

#### 1.4.2.4 Prescribed Dilation Rig Test Procedure

- Target test temperature: 20 °C isothermal conditions.
- Protect the concrete against moisture loss between mixing and casting.
- Cast the mortar in the Dilation Rig within 45 min after mixing (remember the lining to avoid direct contact between specimen and mould).
- Describe the method used for compaction.
- Seal the specimen.
- Start the measurement as soon as possible (before setting).
- Measure over at least 2 weeks.

#### 1.4.2.5 Performed Mortar Test Program

The number of Dilation Rig tests at each location in *Series I* and *Series II* is given in Table 1.2. Supporting tests such as 28-days strength, heat development, TSTM-tests, RH, and setting (Vicat needle) were also performed among the participants. For 28-days compressive strength testing no exact curing conditions were described, but we assume that de-moulding was done after 1 day and then water curing until testing after 28 days.

### 1.4.3 Cement Paste Tests

#### 1.4.3.1 Prescribed Composition

The prescribed composition of the paste was similar to that of the mortar, i.e. same cement and w/c (0.35), but without any admixture.

#### 1.4.3.2 Prescribed Mixing Procedure

The following mixing procedure was prescribed:

Use an epicyclical mixer

- Put the cement into the bowl. Total mixing time from first water addition is 5 min.
- Mix at low speed for 1 min adding gradually about 3/4 of the mixing water (demineralised water). Continue mixing at high speed for 1 min. Stop mixing.
- Scrape off the paste from blade and walls of the bowl for 1 min.
- Resume mixing for 1 min at low speed and add the rest of the water.
- Turn mixer at high speed for the last minute of mixing.

**Table 1.2** Mortar test program overview

Laboratory	Series (batch)	Type of measurements	Comments, Dilation Rig tests
Delft	I	1 Dilation Rig	Wrong mixing procedure. Water added in two steps
	II	1 Dilation Rig 1 TSTM	
DTU	I	2 Dilation Rigs	Mortar contains only the 0–4 mm aggregate grains (intentional), the paste volume is correct. The specimen was rotated during the fresh state to avoid bleeding
	II	1 Dilation Rig	The specimen was rotated during the fresh state to avoid bleeding
IBMB	Ia	4 Dilation Rigs 1 Adiabatic calorimeter	Early T-control malfunction
	Ib	4 Dilation Rigs	Bleeding observed visually—no bleeding was seen
UIUC	I	1 Dilation Rig 1 TSTM Relative humidity	Test temperature was 26 °C. 8 l of SP used (and not 10.4 l as prescribed). Reported strain curve is already temperature compensated
Kanazawa	I	1 Dilation Rig 1 TSTM Mechanical properties ( $E$ , $f_t$ )	Test temperature was 16 °C
	II	1 Dilation Rig 1 TSTM	Test temperature was 18 °C
Laval	I	1 Dilation Rig 1 TSTM	
LCPC	I	2 Dilation Rigs 1 Semi-adiabatic calorimeter Setting: vicat needle, UPV and cyclic loading	8 l of SP used (and not 10.4 l as prescribed). Bleeding observed visually—no bleeding was seen. CTE measured after 350 h to be $15.2 \times 10^{-6}/^{\circ}\text{C}$ by changing the temperature rapidly between 23 and 17 °C
Lund	I	3 Dilation Rigs	$T_{\max}$ was 27 °C. Reported strain curves are already temperature compensated
	II	3 Dilation Rigs Relative humidity	
Munich	I	3 Dilation Rigs	
NTNU / SINTEF	I	1 Dilation Rig 1 TSTM 1 Semi-adiabatic calorimeter	Bleeding measurement showed no bleeding
	II	1 Dilation Rig	Bleeding measurement showed no bleeding

### 1.4.3.3 Prescribed Dilation Rig Test Procedure

- Target test temperature: 20 °C isothermal conditions.
- Protect the cement paste against moisture loss between mixing and casting.
- Cast the paste in the Dilation Rig within 30 min after mixing (remember the lining to avoid direct contact between specimen and mould).
- Describe the method used for compaction.
- Seal the specimen.
- Start the measurement as soon as possible (before setting).
- Measure over at least 2 weeks.

### 1.4.3.4 Prescribed Fresh Paste Measurement and Reporting

- Measure paste bleeding every hour the first hours according to the procedure given for the mortar, see Fig. 1.1. If bleeding, remove the bleed water from the surface of the Dilation Rig specimen when bleeding has stopped.
- Report only one strain curve per rig (the measured deformation must be divided by the measuring length).
- Report temperature in the core of the specimen (or from a parallel specimen with similar geometry subjected to similar temperature control). More temperature measurements are welcome, but then report the average temperature of the specimen.

### 1.4.3.5 Cement Paste Test Program

The number of Dilation Rig tests on cement paste at each location is given in the table below. Some supporting tests on heat development and RH were also performed (Table 1.3).

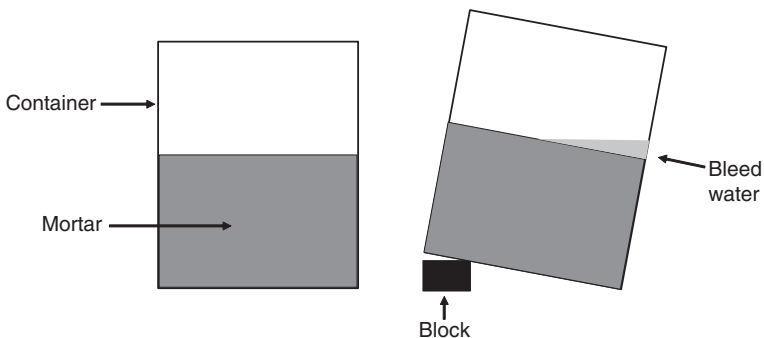


Fig. 1.1 Set-up for bleeding measurement

**Table 1.3** Cement paste tests

Laboratory	Batch volume (litres)	Type of measurements	Comments, Dilation Rig tests
DTU	1.33	2 Dilation Rigs relative humidity	The specimen was rotated during the fresh state to avoid bleeding
Laval	20.0	1 Dilation Rig	42 kg/m <sup>3</sup> bleeding was measured during the first 4 h. This is 8 % of the total water content, which means that the w/c-ratio of the remaining mix is (522 - 42)/1,491 = 0.32. The bleed water was not removed from the sample
NTNU/SINTEF	4.0	1 Dilation Rig 1 Calorimeter (1 l)	Bleed water (0.4 kg/m <sup>3</sup> ) was removed from the top surface of the sample after 3 h. CTE measured after 350 h to be $25.4 \times 10^{-6} \text{ } ^\circ\text{C}$ by changing the temperature rapidly between 23 and 17 °C

## 1.5 Mortar Test Results

### 1.5.1 Fresh Properties and 28-Days Strength

All fresh mortar measurements are given in Table 1.4. The table also gives the moisture in the sand prior to mixing and batch volume. It can be seen that slump, air and density varied considerably among the laboratories. The relation between density and air is plotted in Fig. 1.2.

All 28-days strength results are given in Table 1.5 and plotted in Fig. 1.3. Varying specimen geometries were used, this is accounted for by transforming (denoted “trans.”) the results to 100 mm cube strength using conversion factors from [1] and from the European Standard EN 206-1:

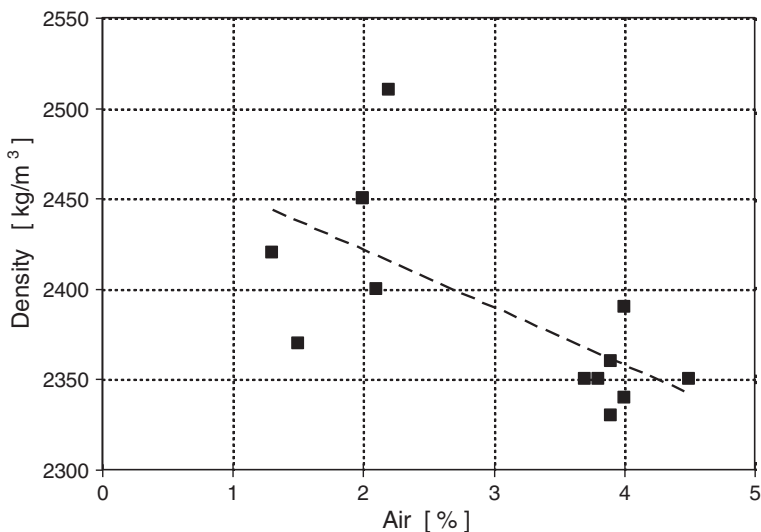
$$f_{c, \text{cube}100} = 1.09f_{c, \text{cube}150} \quad (5.1)$$

$$f_{c, \text{cube}100} = 1.22f_{c, \text{cyl}, h/D=2} \quad (5.2)$$

The average 100 mm (transformed) cube strength in the tests is 71 MPa with a COV of 11 %, when excluding the lowest value of 40 MPa (50 mm<sup>3</sup>). Average air content was 3 % and COV = 38 %. Note that the strength results have not been compensated for varying air content, but it is notable that such compensation would increase the deviation since higher air contents (see Fig. 1.3) mean added strength in the compensation. We note that this is not possible and merely indicates other variables not under control.

**Table 1.4** Fresh properties. The slump measurements are based on the “Abrams cone” (bottom  $\varnothing 200$  mm, top  $\varnothing 100$  mm, height 300 mm) except otherwise indicated

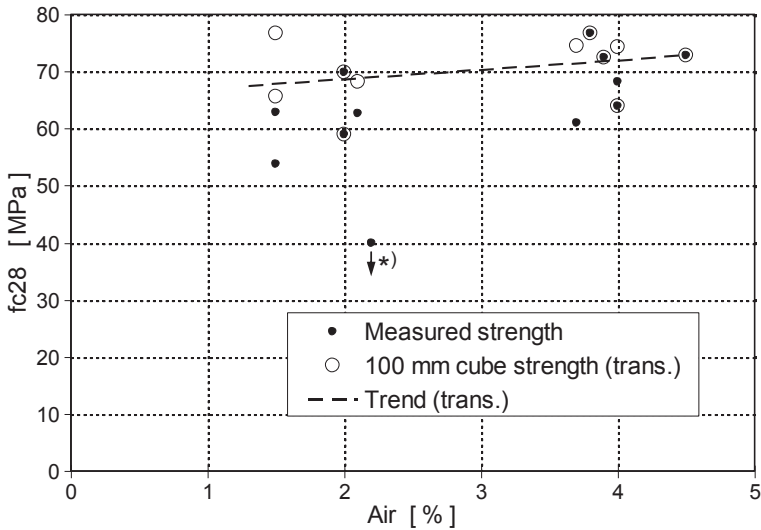
Laboratory	Mix no.	Moisture in sand (%)	Batch volume (litres)	Slump (mm)	Air (%)	Density ( $\text{kg/m}^3$ )
Delft	I	2.7	40	20	3.8	2,350
	II	0	40	150	4.0	2,390
DTU	I	1.7	2.5	0 (mini-slump)	–	–
	II	0	2	–	–	–
IBMB	Ia	0	35	205	2.1	2,400
	Ib	0	35	215	1.3	2,420
UIUC	I	5.1	35	10	2.2	2,510
Kanazawa	I	0.8	30	230	1.5	2,370
	II	0	10	255	–	–
Laval	I	0	–	200	3.9	2,330
LCPC	I	0	28	60	3.7	2,350
Lund	I	3.1	25	45	4.2	2,350
	II	0	25	205	2.0	2,450
Munich	I	0.25	20	380 (flow table)	4.0	2,340
NTNU/ SINTEF	I	3.2	55	130	3.9	2,360
	II	0	25	180	4.5	2,350



**Fig. 1.2** Density versus air content (and trend line)

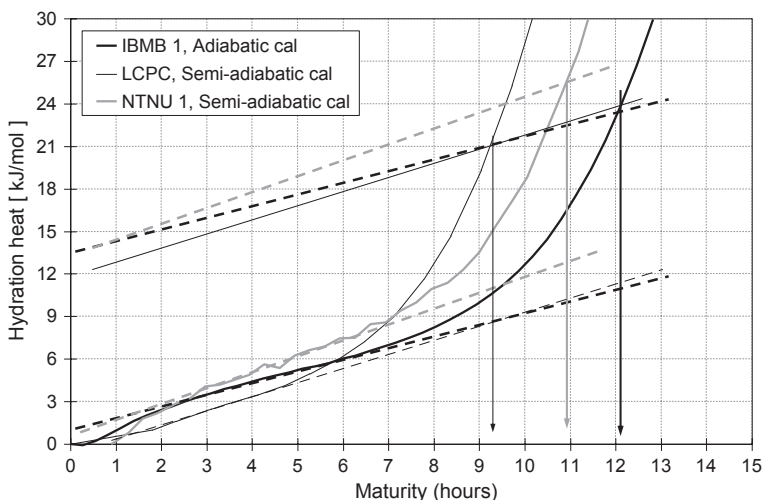
**Table 1.5** 28-days strength results \* very deviating result, since transformation to 100 mm<sup>3</sup> will give even lower value than the measured 40 MPa

Laboratory	Mix no.	$f_{c28}$ (MPa)	$f_{c28}$ transformed to 100 mm <sup>3</sup> (MPa)
Delft	I	76.7 (100 <sup>3</sup> )	76.7
	II	68.1 (150 <sup>3</sup> )	74.3
DTU	I	53.7 (60 × 120 cyl)	65.5
	II	–	–
IBMB	Ia	62.6 (150 <sup>3</sup> )	68.2
	Ib	–	–
UIUC	I	40 (50 <sup>3</sup> )	*
Kanazawa	I	62.9 (50 × 100 cyl)	76.7
	II	–	–
Laval	I	–	–
LCPC	I	61 (113 × 220 cyl)	74.4
Lund	I	59 (100 <sup>3</sup> )	59.0
	II	69.9 (100 <sup>3</sup> )	69.9
Munich	I	64 (100 <sup>3</sup> )	64.0
NTNU/SINTEF	I	72.4 (100 <sup>3</sup> )	72.4
	II	72.8 (100 <sup>3</sup> )	72.8



**Fig. 1.3**  $f_{c28}$  versus air (and trend line). \* 50 mm<sup>3</sup> test: will be even lower when transformed to 100 mm<sup>3</sup>—not considered by the trend line





**Fig. 1.4** Setting time according to the 12.5 kJ/kg heat release criteria (an activation energy parameter (EA) of 30 kJ/mole was used to plot the curves on a maturity scale)

## 1.5.2 Supporting Test Results

### 1.5.2.1 Results Indicating Setting Time

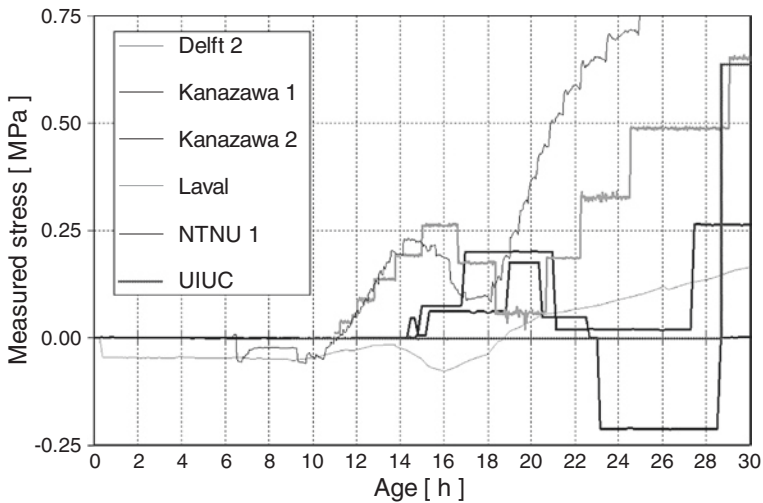
Early heat release versus maturity is shown in Fig. 1.4, and setting according to the so-called “12.5 kJ/kg criterion” [2] is indicated: the lower dotted lines are placed on the strait part of the heat release curve during the dormant period and the upper dotted lines are placed 12.5 kJ above (corresponds to around 3 °C temperature increase). The intersection with the upper dotted lines and the heat release curves then indicates time of setting, see arrows. According to this procedure setting is 9.3 maturity hours in the LCPC test, 11 h at NTNU and 12.1 h at IBMB. The result from LCPC corresponds rather well to end of setting from a parallel vicat needle test (showed setting after 8 h), see Table 1.6. The early stress development from supporting TSTM-tests (Fig. 1.5) also indicates setting time variations.

### 1.5.2.2 Adiabatic Temperature Development

The adiabatic temperature data shown in Fig. 1.6 was the basis for constructing the already discussed Fig. 1.4. The adiabatic calorimeter test data from IBMB in Fig. 1.6 served as a reference in the compensation of heat loss in the two semi-adiabatic tests at LCPC and NTNU. For these two tests the compensation (the “heat loss factor”) was adjusted to give an angle of the adiabatic curve similar to the IBMB-curve between 40 and 50 maturity hours (Fig 1.7).

**Table 1.6** Various measurements at LCPC indicating setting

Age (hh:mm) method used
04:40 Temperature rise in the center of the isothermal specimens
04:44 Vicat needle: start of setting (4 specimens at 20 °C)
05:00 The young modulus determined with the deformations under the cyclic loading takes off
05:30 Change in the slope of the celerity of a transmitted long. Wave (ultrasonic technique) versus the age
05:40 Coarse coincidence of the deformation shape curves of the two specimens
07:00 Fast delayed deformations under cyclic loading disappears
08:00 Amplitude of a transmitted long. wave (ultrasonic technique) begin to increase
08:05 Vicat needle: end of setting (4 specimens at 20 °C)
08:30 Change in the slope of the time propagation of a transmitted long. Wave (ultrasonic technique) versus the age
11:30 perfect coincidence of the deformation shape curves of the two specimens



**Fig. 1.5** Early stress development in TSTM-tests. The automatic strain control in the tests was started before/during setting, except at UIUC where the test was started at 24 h

**1.5.2.3 Relative Humidity**

RH-measurements were performed at UIUC and Lund, the results are given in the figures below.

**1.5.2.4 Additional 28-Days Mechanical Properties**

Some additional measurements of mechanical properties was reported from Kanazawa, see below. Note that all tensile strength results are from splitting tests

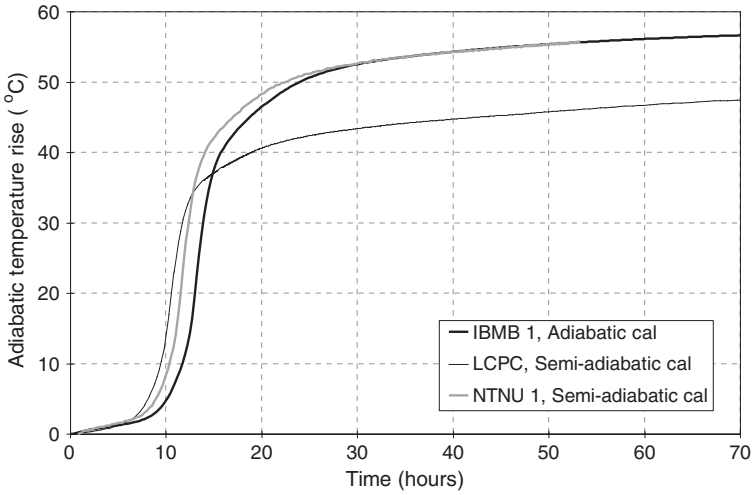


Fig. 1.6 Adiabatic temperature rise

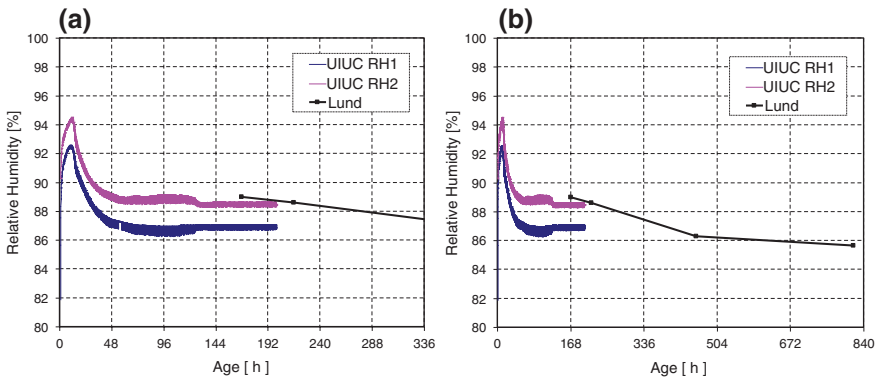


Fig. 1.7 RH-measurements a first 2 weeks, b all data

and modulus of elasticity is measured on cylinders in compression. The effect of curing condition is notable. The tensile strength test on the Dilation Rig- and TSTM test specimens were done after end of testing by sawing each specimen into three pieces..

Days	Sealed curing	Water curing
<i>Compressive strength (MPa)</i>		
7	48.4	54.9
28	60.2	62.9

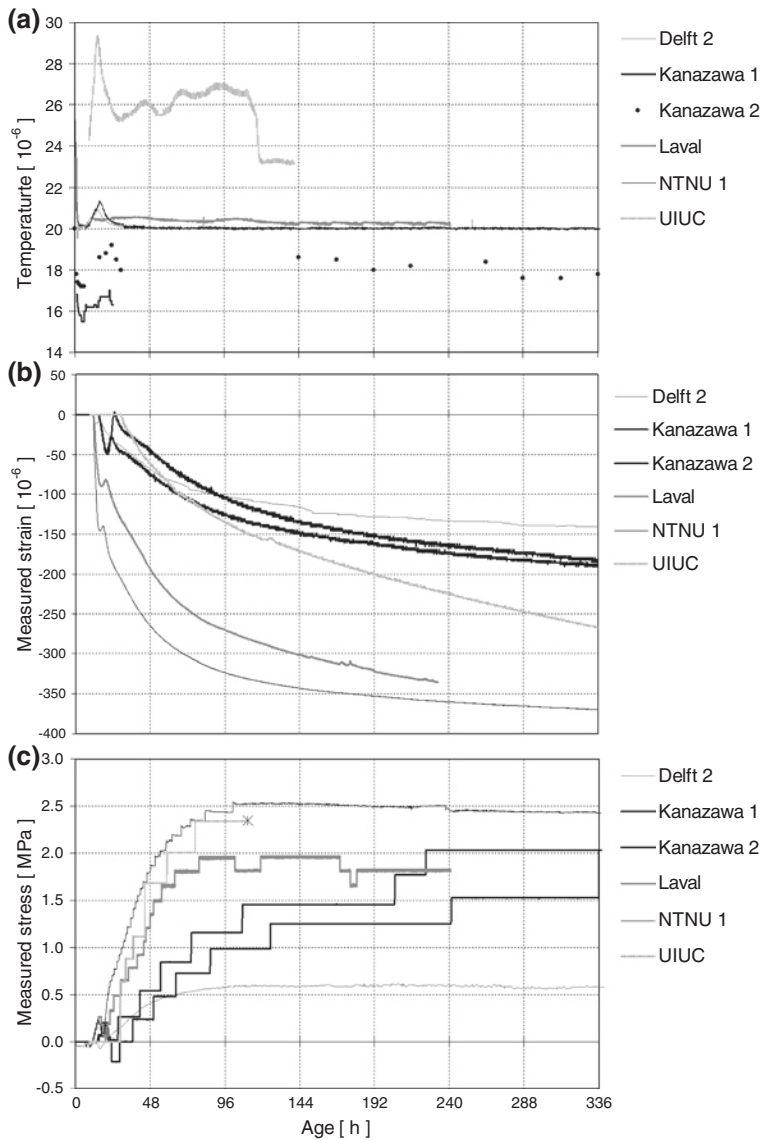
Days	Sealed curing	Water curing
<i>Splitting tensile strength (MPa)</i>		
7	3.38	4.15
28	3.96	4.57
<i>Modulus of elasticity (GPa)</i>		
7	29.4	30.4
28	30.5	33.4
Days	Free	Restrain
<i>Splitting tensile strength (Dilation Rig- and TSTM-test)</i>		
14	3.14	3.16

### 1.5.2.5 TSTM and Corresponding Dilation Rig Results

Five laboratories performed 20 °C isothermal full restraint stress tests (TSTM) in parallel with the Dilation Rigs. The results from parallel tests are shown in Fig. 1.8, together with the temperature in the Dilation Rig specimen (presumably the same as in the TSTM). The automatic strain control of the TSTM-rigs was started before/during setting, except at UIUC where the test was started at 24 h. The measured strain curves (AD) in the figure are zeroed when stresses are starting to develop in the TSTM. As can be seen, the results display considerable variation, but it is notable that there is coherence between AD and corresponding stress results. The temperature drop in the UIUC-test after 5 days caused failure in tension in the TSTM. It is reported from UIUC that the stress increase during this temperature drop was not recorded, hence the actual failure stress was probably somewhat higher than what is indicated in the figure.

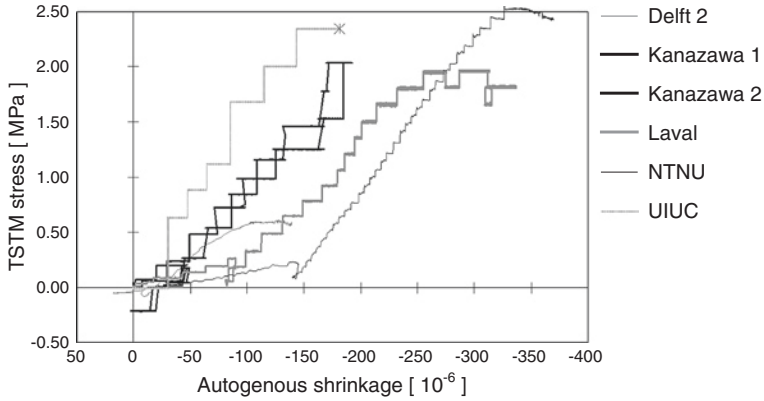
In Fig. 1.9 the stresses are plotted versus measured strain (denoted autogenous shrinkage) for the whole measuring period, while only the data between 30 and 100 h is plotted in Fig. 1.10 (except Delft 2 which is plotted from 25 to 40 h due to the distinct quality of the stress curve). The effective E-modulus is derived from the latter figure and the results show the coherence between AD and stress results in the sense that the effective E-modulus values are in the same range (average is 12.3 GPa). If the Delft 2 results were plotted over the same time range as the other results the E-modulus becomes about half of the average from the other results.

Three of the 5 participating TSTM-rigs were equipped with both strain control (zero strain as an average, i.e. 100 % restraint) and stress control (no change in stress between each strain compensation). With this facility the creep strain can be deduced from the tests. In the 3 TSTMs the strain control was activated each time the specimen had moved 6 to 8 × 10<sup>-6</sup> from the initial position. Calculated E-modulus from the 3 TSTM-tests are shown in Fig. 1.11. It is notable that the



**Fig. 1.8** Measured temperature in the Dilation rig specimens (a), measured free strain (autogenous shrinkage) from the Dilation Rigs (from the start of TSTM-stress) b and measured restraint stress in the TSTMs c. Symbol "\*" means failure in tension

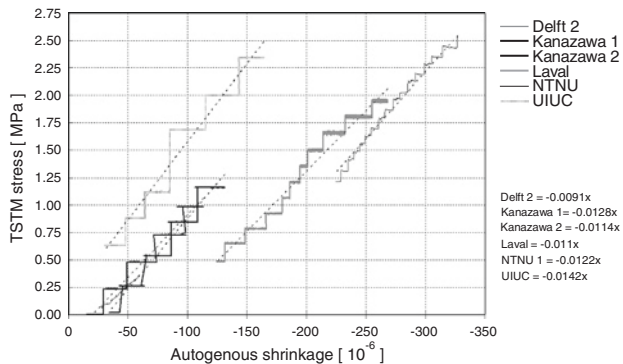
(elastic) E-modulus varies much more than the effective E-modulus in Fig. 1.10. The reason for this is not clear, but the procedure behind the data in Fig. 1.11 is "sensitive" because very small strain increments are involved in the calculation of the E-modulus.



**Fig. 1.9** Stress development in the TSTM-tests versus free strain (autogenous shrinkage) in the parallel Dilatation Rig test (zeroed at the start of TSTM-stress)

Effective E-modulus over the period from 30 to 100 hours:

- Delft 2<sup>\*)</sup>: 9.1 GPa
- Kanazawa 1: 12.8 GPa
- Kanazawa 2: 11.4 GPa
- Laval: 11.0 GPa
- NTNU I: 12.2 GPa
- UIUC: 14.2 GPa

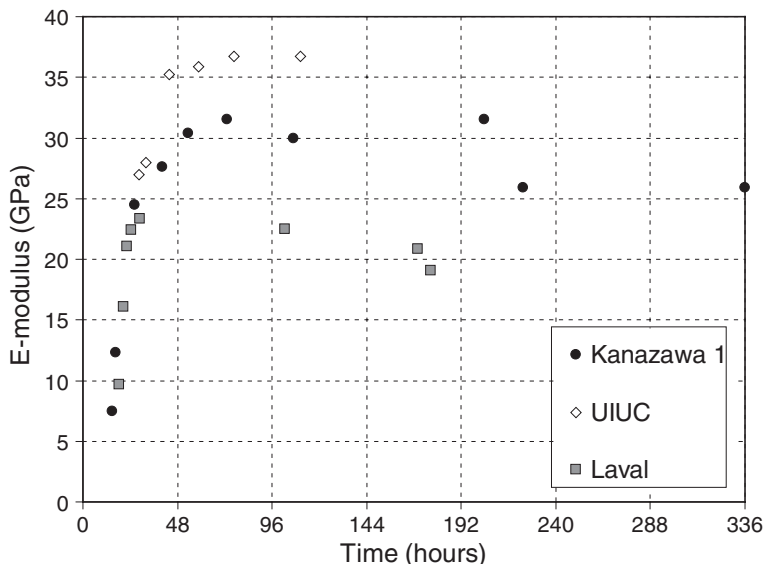


**Fig. 1.10** TSTM-tests versus autogenous shrinkage in the period from 30 to 100 h, except Delft 2<sup>\*)</sup> which is plotted from 25 to 45 h. Effective E-modulus is calculated from the angle of the trend lines (dotted lines)

The different strains involved (autogenous, elastic and creep) are shown in Fig. 1.12 for Laval and UIUC (the two reported the strain over time in the TSTM), whereas Fig. 1.13 compiles the creep strains (also including a reported curve from Kanazawa).

### 1.5.3 Dilatation Rig Results, Autogenous Deformation

Different plots of the Dilatation Rig tests on the RR-mortar are shown in the following figures. We note that it is difficult to distinguish between the different curves,



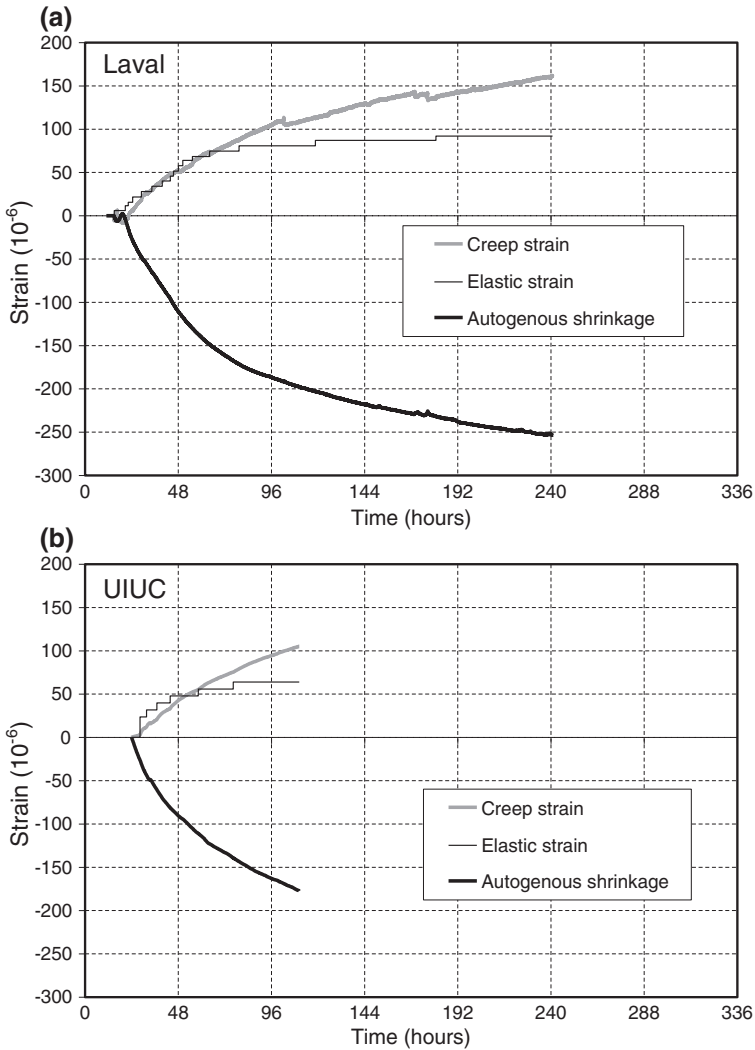
**Fig. 1.11** E-modulus development calculated at each step in the TSTM stress curves. The E-modulus is calculated as restraint stress divided by the accumulated elastic strain

but the main point in the figures is to show the time development and spread of the results. The plots give raw data results from the participants; hence no treatment is done except that the strain results are zeroed at different times. The term “free strain” in the figures is presumably mainly resulted from AD since the test temperatures are rather constant (i.e. TD is quite insignificant) in addition to possible errors/variables not under control. These issues are treated in Chap. 6 (statistical evaluation).

After the rather deviating results in the very early phase (first 10 h), all Dilation Rig results display a small expansion phase before “long term” shrinkage is measured. The duration of the expansion varies, but occur somewhere between 14 and 24 h, see Fig. 1.14a. The strain plot in Fig. 1.16 is made from the start of the expansion phase for each curve (Figs. 1.15 and 1.17).

## 1.6 Statistical Evaluation of the Dilation Rig Results

Measurements of autogenous deformations AD are influenced by a multiplicity of coincidental effects, which can cause a substantial variance in the results. The discussion of the Dilation Rig results in Sect. 1.5.3 shows this very clearly. The scatter in the graphs is around 3–4 times larger than the scatter of the compressive strength results tested at 28 days (see Table 1.7). This phenomenon has also been

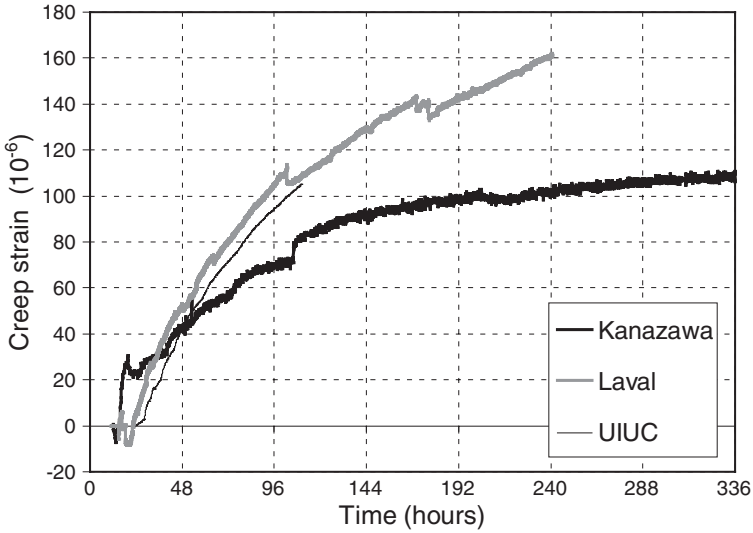


**Fig. 1.12** Autogenous shrinkage from the Dilation Rig and deduced elastic- and creep strain from the TSTM test at **a** Laval and **b** UIUC

reported earlier (e.g. [1]). The reasons for this are various. Some of the reasons were already called in the preceding sections—further ones are regarded here.

There is a lack of information regarding the variance of AD of hardening concrete—especially for early ages. The Table 1.7 shows some coincidental and unspecified values from different references. From the values in Table 1.7 one may suppose that the coefficient of variation of the AD can be estimated at least in the order of magnitude of the coefficient of variation of the elastic modulus in tension (viz. Figs. 1.10 and 1.11).





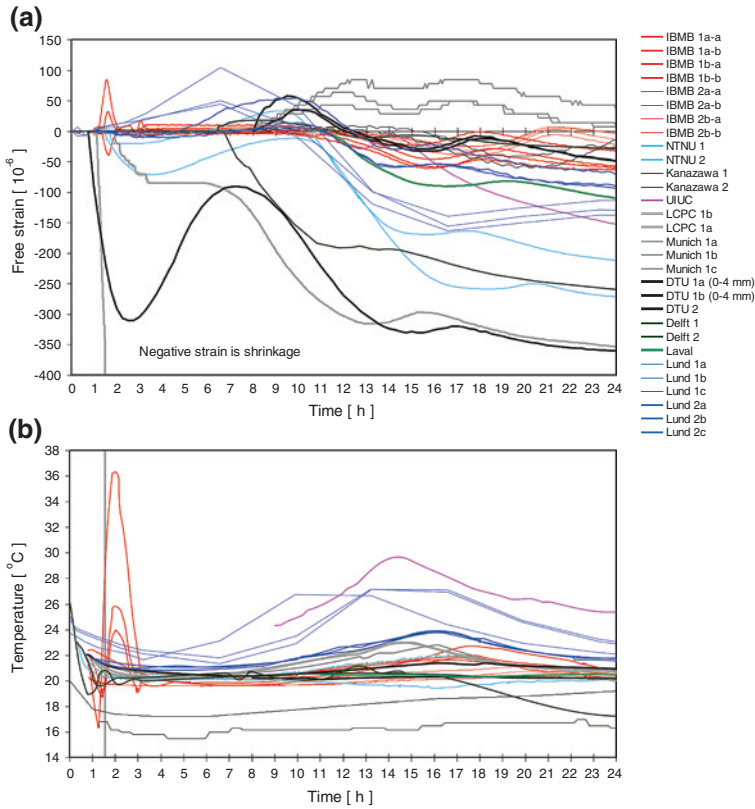
**Fig. 1.13** Deduced creep strain (same data as in Fig. 1.12 plus results reported from Kanazawa)

The statistical attributes of the mechanical and thermodynamic properties of early age concrete are considerably influenced by fresh concrete characteristics like temperature and air void content. Therefore these parameters are considered in this analysis.

### 1.6.1 Prerequisites, Objectives and Procedure

As discussed earlier, the initial situation for the following statistical investigations is the following: 30 individual measurements of AD of the RR-mortar under almost isotherms conditions from 10 different laboratories are present. The objective of the investigation is to estimate the statistical attributes of AD as function of time. This requires a representative and outliers free (homogeneous) sample of the population AD. Possible candidates of outliers are identified with the help of statistical test techniques and the information from the Tables 1.2 (possible biased errors), 1.5.1 (fresh concrete characteristics) and 1.5.2 (28-d compressive strength). The Table 1.8 shows indenture number (the index) of all data-sets and associated fresh concrete characteristics.

In this chapter the autogenous deformation curve is calculated from the measured total strain  $\epsilon_{\text{tot}}$  acc. to the equation  $\epsilon_{\text{ad}} = \epsilon_{\text{tot}} - \epsilon_{\text{T}}$ .  $\epsilon_{\text{ad}}$  is zeroed at time zero  $t_0$ .  $\epsilon_{\text{T}}$  denotes the temperature strain due to heat of hydration within the sample. Time  $t_0$  is estimated with the help of the end of dormant phase EOD. Furthermore the autogenous shrinkage curve is calculated from  $\epsilon_{\text{ad}}$ . It is stipulated, that  $\epsilon_{\text{as}}$  starts at the first maximum of the  $\epsilon_{\text{ad}}$ -curve. This means, that  $\epsilon_{\text{ad}}$ -curve is zeroed at  $t_{0\text{as}}$ . Details are given in Sect. 1.6.1.3.



**Fig. 1.14** Measured free strain in the Dilation Rig tests **a** and measured temperature in the specimens **b** all results, first 24 h

The large number of measurements recommends a computer aided analysis of the data. So all procedures described in this paper were implemented in a software tool, available by the authors. Unknown factors which influence the numerical analysis are the activation energy EA, the end of the dormant phase EOD and the coefficient of thermal expansion CTE as well as the measuring period and the measuring interval. Figure 1.18 shows the statistical framework at a glance.

### 1.6.1.1 Statistical Framework

With the high level of uncertainty of the measurements of AD in mind only a rather simple (in other words robust) statistical framework is defined. In descriptive statistics robust means, that the test dimensions that are used for determination of the test statistics are not or only little influenced by outliers. The Hampel-Test (H-Test)

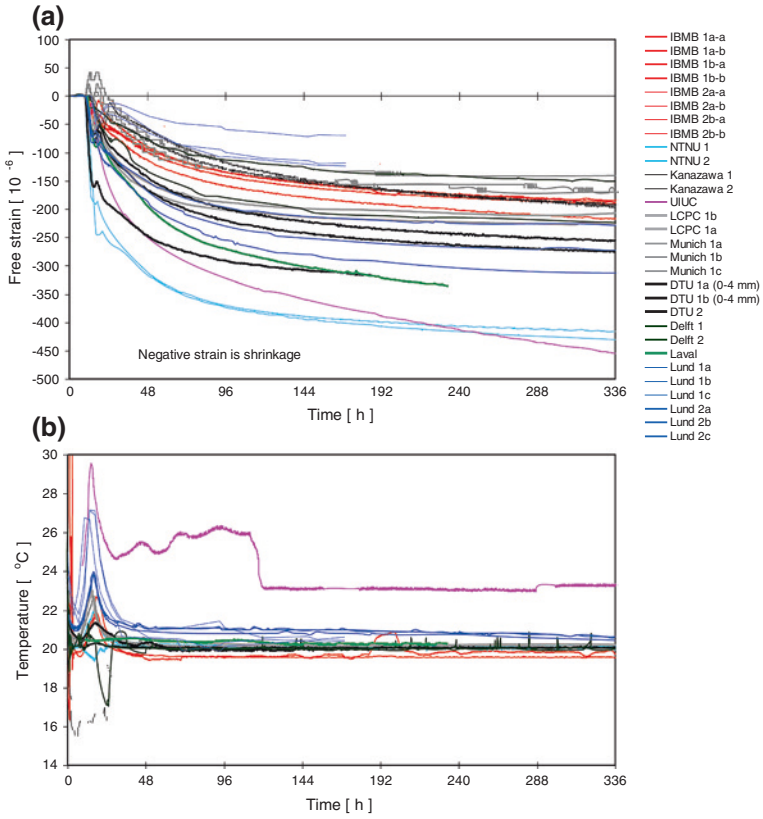


Fig. 1.15 Measured free strain when plotted (zeroed) from 10 h (a) and measured temperature in the specimens (b)

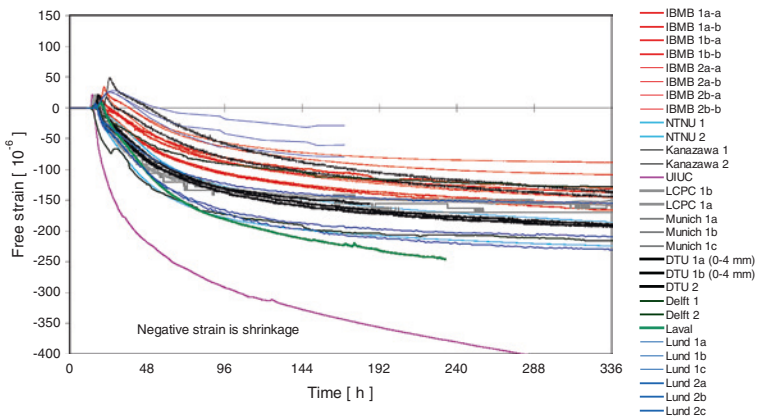


Fig. 1.16 Measured free strain when plotted (zeroed) from the start of the early expansion phase for each curve

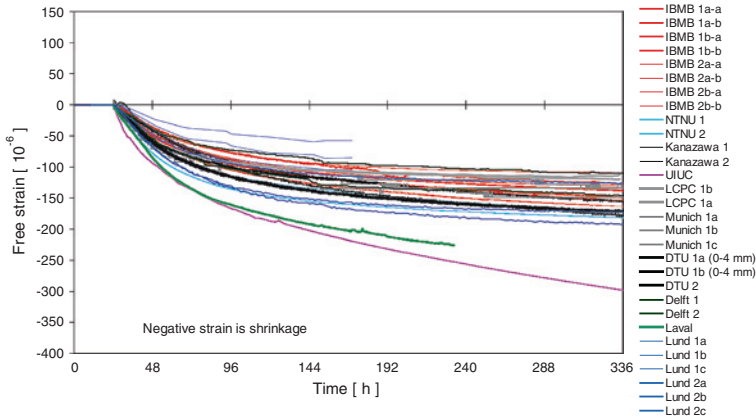


Fig. 1.17 Measured free strain when plotted (zeroed) from 24 h

Table 1.7 Statistical attributes of autogenous *AD*, *CS* chemical shrinkage; *DS* drying shrinkage and *CR* creep—unspecified values for the *COV* coefficient of variation taken from different literature sources

Source	Description	COV
[10]	AD, HSC, w/b = 0.40, $f_{cc,28} = 79.6 \pm 2.9$ MPa, isothermal 20 °C, N = 3, one laboratory	AD: COV $\approx$ 29 % AS: COV $\approx$ 15–18 %, age 6 days
[6]	AD, HSC, w/b = ?, N = 30, one laboratory	COV $\approx$ 4–11 % depending on age
[11]	AD, HSC, w/b = ?, N = 3, one laboratory	COV $\approx$ 10 % independent on age
[11]	CS, paste, w/b = 0.3, N = ?, one laboratory	COV $\approx$ 4 %, age 6 days
[11]	AD, HSC, w/b = 0.33, N = 4, one laboratory	COV $\approx$ 6 %, end value
[11]	AD, HSC, w/b = 0.22–0.4, N = ?, graphical summary of results from at least for different literature sources	COV $\approx$ 30 % independent on w/b-ratio
[1]	AD and CR, HSC, w/b = 0.4, N = 9, isothermal 20 °C, Round Robin Test with six laboratories	COV $\approx$ 22 %, age 6 days
[6]	CR, NSC, HSC, N $\geq$ 800, evaluation of different model codes	COV $\approx$ 37–56%, end values, dependent on model
[12]	CR and DS, HSC, N $\geq$ 800, evaluation of different model codes	COV $\approx$ 24–55%, end values, dependent on model

[3] for the calculation of outliers and the Kolmogorov-Smirnov Test (KS-Test) [4] for the estimation of the probability density function fulfil these requirements. All significant levels of statistical tests are predefined to 20 %. Furthermore it can be assumed that AD and CR are lognormal distributed random variables (cf. [5, 6]).

**Table 1.8** Indenture number (index) of all data-sets and associated fresh concrete characteristics

No.	Data-set name	$T_{e0}$ (°C)	Air cont. (Vol-%)
1	delft-1	23	3.8
2	delft-2	26.2	4.0
3	dtu-1-a	20.2	–
4	dtu-1-b	20.2	–
5	dtu-2	22.1	–
6	ibmb-1a-a	22.1	2.1
7	ibmb-1a-b	21.7	2.1
8	ibmb-1b-a	21.2	2.1
9	ibmb-1b-b	22.4	2.1
10	ibmb-2a-a	20.9	1.3
11	ibmb-2a-b	20.2	1.3
12	ibmb-2b-a	20.3	1.3
13	ibmb-2b-b	20.2	1.3
14	kana-1	16.8	1.5
15	kana-2	17.2	–
16	laval	20.5	3.9
17	lcpc-1-a	21.5	3.7
18	lcpc-1-b	21.6	3.7
19	lund-1-a	25.0	4.2
20	lund-1-b	23.7	4.2
21	lund-1-c	24.7	4.2
22	lund-2-a	21.8	2.0
23	lund-2-b	21.7	2.0
24	lund-2-c	21.7	2.0
25	munic-1-a	21.6	4.0
26	munic-1-b	21.0	4.0
27	munic-1-c	20.8	4.0
28	ntnu-1	22.2	3.9
29	ntnu-2	22.9	4.5
30	uiuc	24.3	2.2

It is necessary to estimate the size of a sample  $N$  in dependence of the coefficient of variation  $COV$  which can be expected. The size can be estimated with the help of the confidence interval of the  $COV$ . Further on the confidence interval depends on  $N$  and the assumed significance level (probability of error). According to [7] the upper and the lower bound  $COV_{UB}/COV_{LB}$  of the confidence interval can be approximately calculated with the following expressions, which hold for  $N > 10$  and  $\max COV_N \approx 0.4$ . Here  $COV_N$  denotes the coefficient of variation calculated from the sample of size  $N$  and  $z_\alpha$  denotes the quantile of the standard normal distribution on the significance level  $\alpha$  (two-sided).

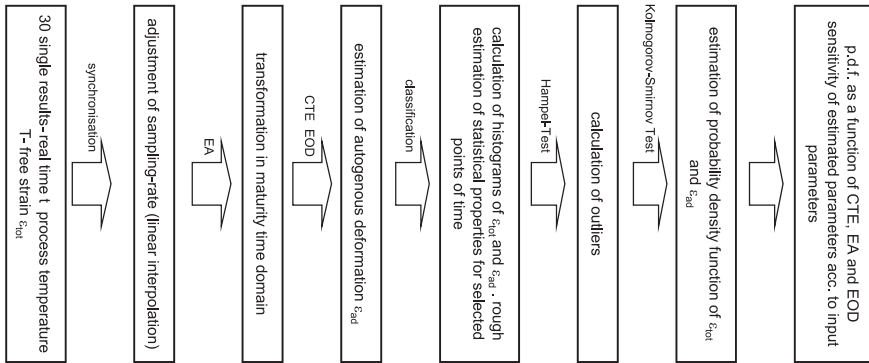


Fig. 1.18 Statistical framework for the evaluation of the dilation rig results at a glance

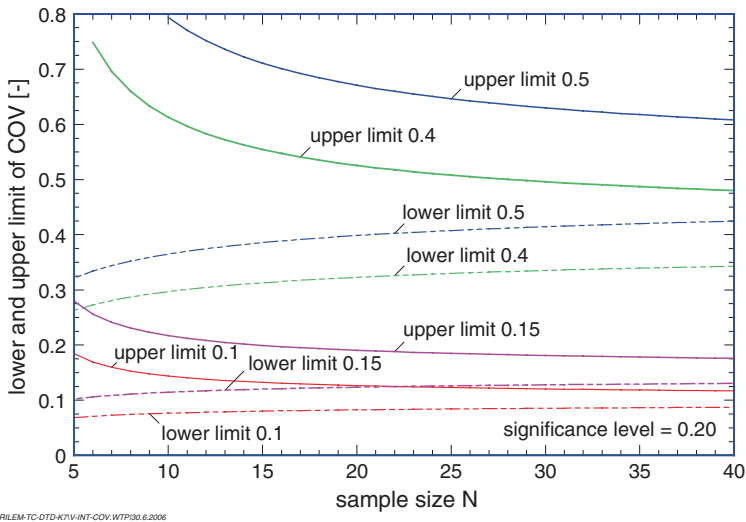


Fig. 1.19 Influence of the sample size N on the confidence interval of COV at a significance level of 20 %

$$COV_{UB} = \frac{COV_N}{1 - z_\alpha \cdot \sqrt{\frac{1 + 2 \cdot COV_N^2}{2N - 2}}} \tag{6.1}$$

$$COV_{LB} = \frac{COV_N}{1 + z_\alpha \cdot \sqrt{\frac{1 + 2 \cdot COV_N^2}{2N - 2}}} \tag{6.2}$$

The Fig. 1.19 shows a plot of the above equations for a significance level of 20 %. In order to estimate the reliability of the variance, it can be recognized that with an expected COV of 40 % the sample must contain of approximately 30 values.

For the available 30 measurements and an expected COV of 35 % this means that values of COV between 29 and 43 % describes the variation of the population statistically equivalently.

### 1.6.1.2 Sampling Rate

The numerical analysis requires a synchronisation of the sampling rate  $\Delta t$ . In the measurements the sampling rate varies between two minutes and two days. In the analysis  $\Delta t = 1 \text{ min}$  is chosen for numerical differentiation and  $\Delta t = 1 \text{ h}$  in the statistical procedures. For the sake of simplicity the calculations are performed for  $t_c = 1, 3, 5, 7, 14$  days. The adjustment of the sampling rate is calculated by linear interpolation.

### 1.6.1.3 Estimation of EA, CTE and EOD

The activation energy EA is estimated from cement composition. A modified Freisleben Hansen law (two parameter formula with  $A = 30.0 \text{ kJ/mol}$ ;  $B = 0.109 \text{ kJ/(mol/K)}$ , time invariant) is used. For details see e.g. [8]. CTE estimated to  $10^{-6} \text{ 1/K}$  (standard value for concrete, time invariant, independent from temperature).

The end of the dormant phase EOD is the most sensitive parameter for the definition of AD and this item is strongly correlated with the beginning of AD. So, in this analysis the EOD is regarded as an estimator for time zero  $t_0$ . For the estimation of the end of dormant phase a more sophisticated approach is chosen. A global value for EOD for all 30 results is not recommended, because EOD is a function of temperature.

In the numerical analysis the following approach has been used: The main idea is, that one can estimate a lower bound min EOD and a upper bound max EOD for EOD. The value min EOD is approximately the end of setting measured with Vicat-needle (LCPC-test) taking a safety measure into account—here  $8-2 \text{ h} = 6 \text{ h}$  (cf. Table 1.6). The parameter max EOD is calculated via min EOD + 12 h (derived from the influence of temperature). With the introduction of the definitions

- $\varepsilon_{\text{tot}} = 0$  if  $\text{abs}(\varepsilon_{\text{tot}}) < 5 \text{ } \mu\text{m/m}$  and
- if  $\partial\varepsilon_{\text{tot}}/\partial t$  reaches  $3 \text{ } \mu\text{m/m/h}$  then  $\text{EOD} = t_{c0}$

We can calculate automatically the EOD from the measurements. The thresholds  $5 \text{ } \mu\text{m/m}$  and  $3 \text{ } \mu\text{m/m/h}$  are user-defined and motivated from numerical reasons. In other words the AD-curve is calculated from the first significant change of the temperature corrected measured total strain.

These criteria agree well with the results of LCPC (time of setting, semi-adiabatic calorimeter), NTNU (semi-adiabatic calorimeter), and iBMB (adiabatic calorimeter) measurements. Figure 1.20 shows a result of this evaluation procedure

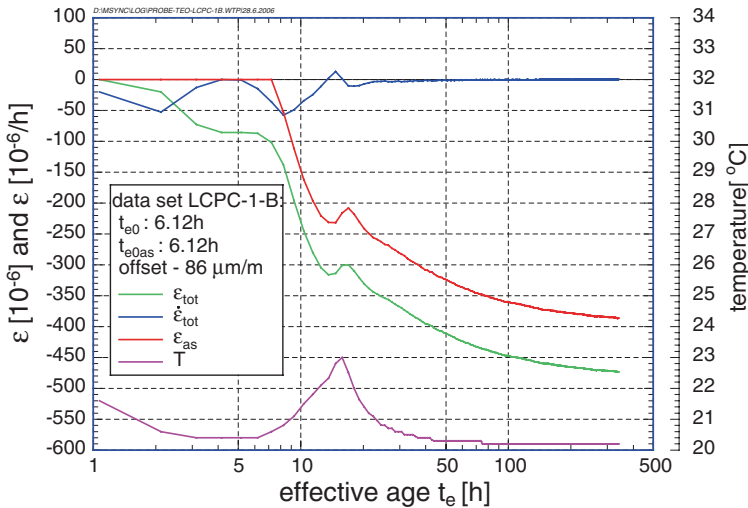


Fig. 1.20 Data set LCPC-1-B: numerical estimation of EOD (time zero  $t_{e0}$ )

for the data set LCPC-1-B. Here the EOD is estimated to 6.12 h and the curve of the total strain is zeroed at this point of time. The offset between  $\epsilon_{tot}$  and  $\epsilon_{as}$  is calculated to 86  $\mu\text{m/m}$ .

Table 1.9 shows all calculated values of EOD, the start of AS and the offset between total deformation and AS at time zero. Furthermore the values for the start and the end of measurements are documented in terms of equivalent age. It can be observed, that 13 partners stops their measurements before an equivalent age of 336 h (14 days) is reached. The start of the measurements indicates that in some cases the time between addition of water and start of measurement was not taken into account. It can be assumed, that a minimum error of 15 min exists. The very early AD and AS results varies significantly. The beginning of AD varies between 6 and 14 h with a mean value of 8.7 h and a standard deviation of 2.7 h; corresponding to a COV of 30 %. On the other hand the beginning of AS varies between 6.2 and 21.6 h with a mean value of 10.7 h and a standard deviation of 3.9 h; corresponding to a COV of 36 %.

### 1.6.2 A Concept for the Estimation of Candidates of Outliers from Unbiased Samples

One possible graphical representation of the population is to plot the quantity  $x$  of a sample in dependence of his index  $n$  in ascending order. The slope of the regression line  $n - x$  is a measure for the scatter of the sample [4].

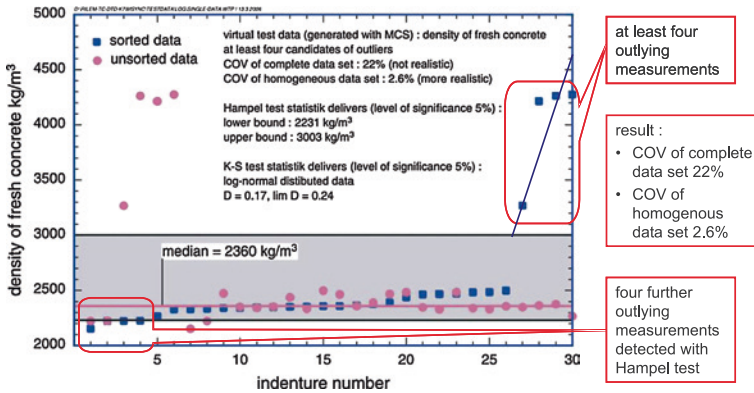
If the sample contains random values, which are unusual far away, the Hampel-Test is an appropriate method to calculate these outliers. In this method



**Table 1.9** a Calculated EOD for data-set 1–15, b Calculated EOD for data-set 16–30

No.	Data-set name	Effective age in hours			Begin of as in hours	
		Start of measurement	End of measurement	EOD $\approx t_{e0}$	$t_{e0,as}$	Offset ( $\mu\text{m}/\text{m}$ )
(a)						
1	delft-1	0.03	335	6.96	6.96	0
2	delft-2	0.01	336	6.60	8.22	18
3	dtu-1-a	7.0	337	8.37	9.88	35
4	dtu-1-b	1.0	337	8.17	9.58	58
5	dtu-2	0.5	186	6.07	7.50	-91
6	ibmb-1a-a	0.1	338	8.58	10.0	6.7
7	ibmb-1a-b	0.1	339	6.49	6.49	9.8
8	ibmb-1b-a	0.1	331	9.31	9.31	-3.9
9	ibmb-1b-b	0.1	334	10.28	10.28	-1.7
10	ibmb-2a-a	0.1	338	13.55	13.55	3.1
11	ibmb-2a-b	0.1	330	12.25	12.25	2.6
12	ibmb-2b-a	0.1	330	13.66	21.40	7.7
13	ibmb-2b-b	0.1	330	11.45	21.61	4.6
14	kana-1	0.3	286	9.89	9.97	7
15	kana-2	0.03	310	12.97	12.97	5
(b)						
16	laval	1.01	243	11.74	11.74	0
17	lcpc-1-a	0.1	340	6.78	6.78	0.6
18	lcpc-1-b	0.1	340	6.18	6.18	-86
19	lund-1-a	0.01	180	6.02	7.30	44
20	lund-1-b	0.01	177	6.08	7.32	105
21	lund-1-c	0.01	177	6.08	7.38	50
22	lund-2-a	0.6	350	6.03	9.62	53.6
23	lund-2-b	0.6	350	9.48	10.55	6.8
24	lund-2-c	0.6	348	6.10	9.98	13.6
25	munic-1-a	0.2	340	8.38	12.89	84.6
26	munic-1-b	0.23	340	8.48	11.93	63.7
27	munic-1-c	0.2	340	8.69	17.63	49.5
28	ntnu-1	0.6	338	6.66	9.09	33
29	ntnu-2	0.6	337	6.02	9.73	-22
30	uiuc	8.0	397	13.99	13.99	5

the outliers themselves do not have any influence on the estimator for location and variation. It uses the median as an estimator for the location and the MAD (Median Absolute Deviation; median of the absolute deviations from the median) as an estimator for the variation. The test is high reliable in detecting outliers, if the size of the sample is large enough [9]. To illustrate this approach and the effectiveness of Hampel-Test an example of virtual (calculated) data was created.



**Fig. 1.21** Virtual data to illustrate the functionality of the Hampel-test and the main concept for the estimation of candidates of outliers. The sample was calculated with MCS. The quantities were not derived from data of RR-test

### 1.6.2.1 Functionality of the Hampel-Test

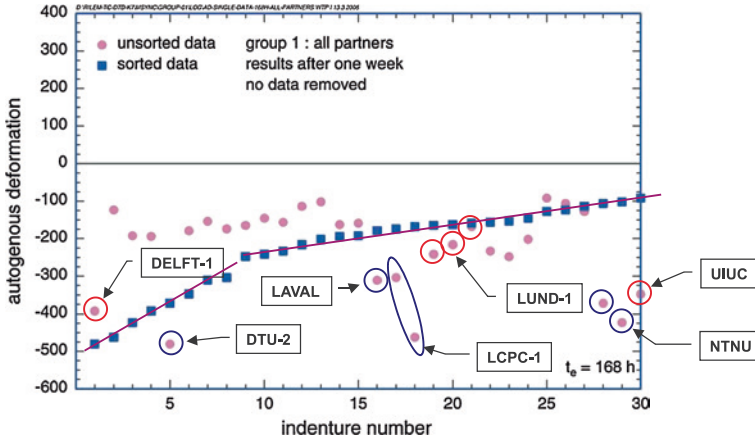
For the example 30 values of density of fresh concrete were calculated via Monte-Carlo simulation (MCS) with a median of 2,360 kg/m<sup>3</sup> and a COV of 2.6 %. The data of this example was not derived from the Round Robin Test.

Eight values of the sample were substituted to simulate outliers (four high and for low values). The sample is illustrated in Fig. 1.21 (circles).

If the data of this virtual sample is sorted and plotted in the same graph, one can detect at least four outlying measurements. The COV of the disturbed sample is 22 %—for density of fresh concrete an unacceptable value. Now the H-Test is applied to this. The test calculates a lower bound of 2,231 kg/m<sup>3</sup> and an upper bound of 3,003 kg/m<sup>3</sup> (shaded area in Fig. 1.21). The test detects all eight outliers and the COV of the reduced sample is 2.6 % again. In the graph one can plot three different regression lines. The first line is defined by the indices 1–4, the second from 5 to 26 and the third one from 27 to 30. The three lines differ significantly in their slope, and this indicates the candidates of outliers.

### 1.6.3 Analysis of the Data: Calculation of Outliers

The concept of Sect. 1.6.2 is used to analyze the measured data. Figure 1.22 shows the plot of sorted and unsorted data of AD from all laboratories for  $t_e = 168$  h. The indenture numbers are defined in Table 1.9. The Hampel-Test detects no outliers in the 30 measurements at significant levels of 5 and 20 %. This strongly indicates that no random error has occurred in the complete sample (or the sample size is too low). Other



**Fig. 1.22** Analysis of measured AD for  $t_e = 168$  h. Sorted and unsorted data of all laboratories (group 1). Indenter number acc. to Table 1.9

influencing factors have to be considered. According to Sect. 1.4.2.5 and Table 1.2 some errors/deviations occurred during the test program. The main problems were

- wrong w/b-ratio,
- test temperature to high (26 °C) or to low (16 °C),
- malfunction of temperature control,
- wrong aggregate size (0–4 mm),
- lower amount of superplasticizer
- and bleeding.

Figure 1.22 indicates that the data-sets DELFT-1, DTU-2, LAVAL, LCPC-1, NTNU and UIUC deliver unexpected high values for  $t_e = 7$  days (168 h), overall 8 quantities. Some of them fulfil single items of the listing above. But the results of NTNU, LAVAL and DTU-2 can not be explained by this. This situation holds for  $t_e = 1, 3, 5, 14$  days also (cf. Figs. 1.23, 1.24, 1.25, 1.26).

For a more detailed analysis the data is divided in some subsets. The subsets are defined in Table 1.10. These sets pool the data of non-outlier candidates acc. to Table 1.2 and other observations. In group 1 no data was removed. In group 2 the data of DELFT-1 (wrong mixing procedure), LUND-1 (maximum temperature 27 °C) and UIUC (test temperature 26 °C) was removed from the sample. In group 3 additional to group 2 the data of DTU-2 (bleeding?), LAVAL (no information) and LCPC (low SP-dosage) was removed from the sample. Group 4 is a subset of group 3. Here the complete LUND-data was not taken into account.

In general the data can be determined in two further subsets. The first set (group 5) contains all measurements, in which a low air content in the fresh concrete ( $\leq 2.5$  Vol-%) was determined. In the second set (group 6) all measurements are summarized, in which a high air content in the fresh concrete ( $> 2.5$  Vol-%) was determined (cf. Fig. 1.27). In the following figures time zero is EOD, acc. to Sect. 1.6.1.3.

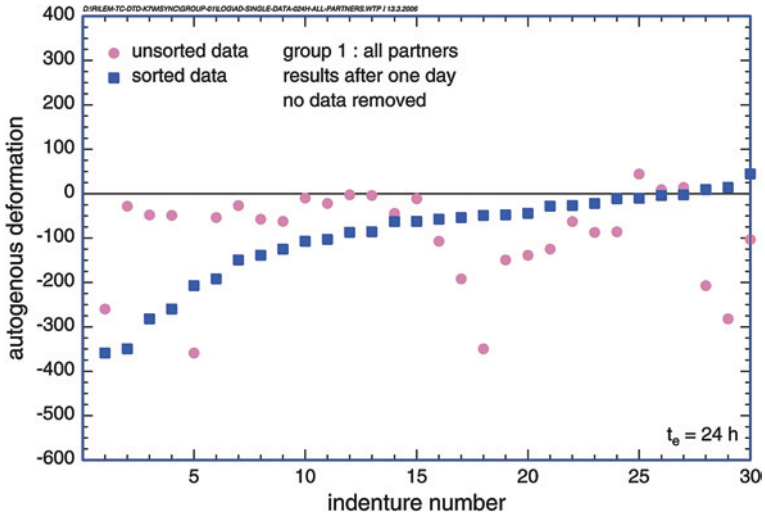


Fig. 1.23 Analysis of measured AD for  $t_e = 24$  h. Sorted and unsorted data of all laboratories. Indenture number acc. to Table 1.9

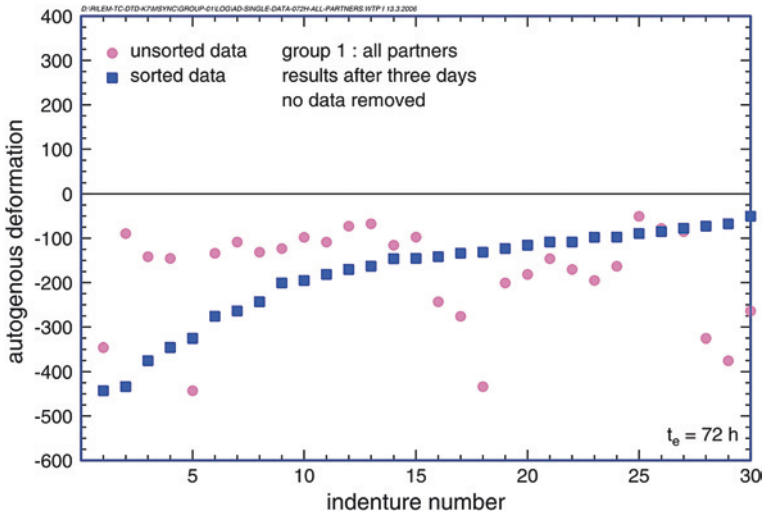


Fig. 1.24 Analysis of measured AD for  $t_e = 72$  h. Sorted and unsorted data of all laboratories. Indenture number acc. to Table 1.9

All these groups were analyzed with the same procedure as described above. The Figs. 1.28, 1.29, 1.30, 1.31, 1.32 show the data for AD at the age of 7 days equivalent time. In all cases which were analyzed, the Hampel-Test calculates

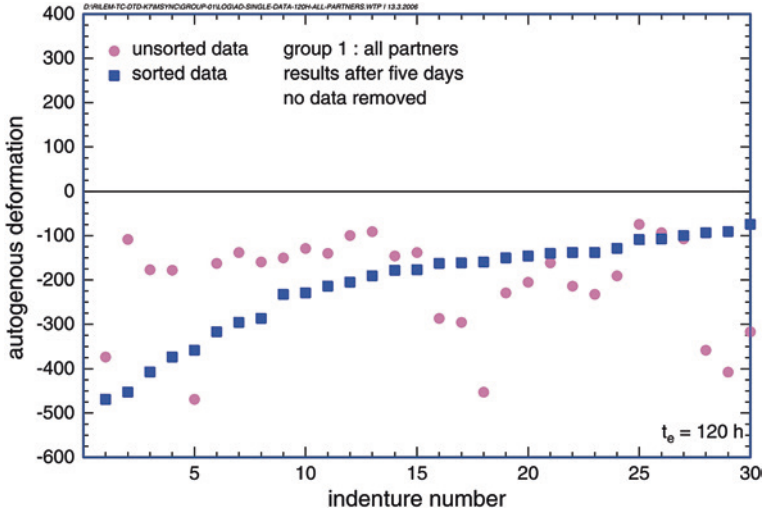


Fig. 1.25 Analysis of measured AD for  $t_e = 120$  h. Sorted and unsorted data of all laboratories. Indenture number acc. to Table 1.9

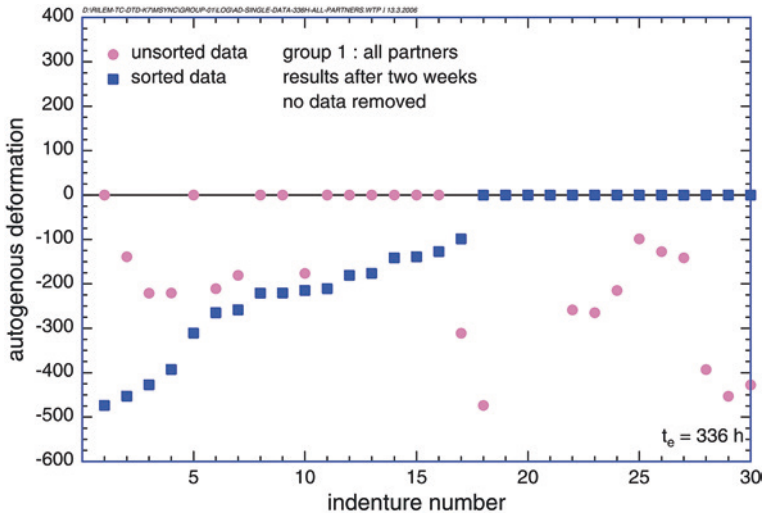
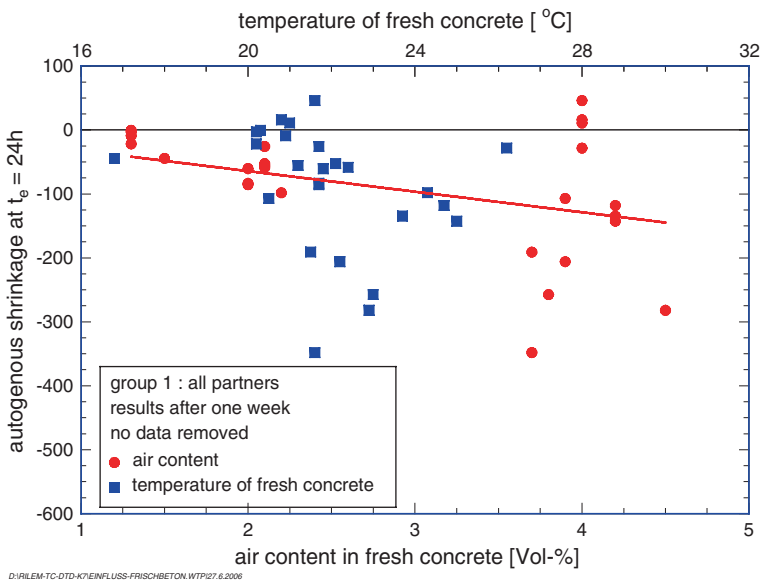


Fig. 1.26 Analysis of measured AD for  $t_e = 336$  h. Sorted and unsorted data of all laboratories. Indenture number acc. to Table 1.9

no outliers again. Figure 1.33 summarizes this analysis and gives the COV of all investigated subsets. Table 1.11 shows the statistical attributes of AD data for all groups for  $t_e = 7$  days. The results from Fig. 1.33 agree well with the data from

**Table 1.10** Definition of different subsets of the measured data

Group	N	Comment
1	30	No data removed
2	25	DELFT-1, LUND-1, UIUC removed from the sample
3	19	DELFT-1, DTU-2, LAVAL, LCPC, LUND-1, NTNU UIUC removed from the sample
4	16	DELFT-1, DTU-2, LAVAL, LCPC, LUND, NTNU, UIUC removed from the sample
5	13	Low air content : only IBMB, KANA, LUND-2
6	14	High air content : DELFT-2, DTU-1, LAVAL, LCPC, LUND-1, MUNIC, NTNU



**Fig. 1.27** Influence of fresh concrete characteristics on early age shrinkage ( $t_e = 24$  h)

the literature (cf. Table 1.7). For the COV of AD at 7 days equivalent time values between  $-52$  and  $-21$  % were calculated. The corresponding values for AS are  $-38$  and  $-15$  %.

It is notable that the COV of group 5 is only half of that of group 6. In first approximation this observation applies also to all other regarded times. Together with the regression analysis from Fig. 1.27 this indicates that the air void content possesses a significant (and unsystematic) influence on AD in the early age, while the effect is likely to be reduced at later times. The influence of the fresh temperature of concrete is not so strongly pronounced in this sense. This phenomenon is well-known also for other characteristics of concrete in the early age.

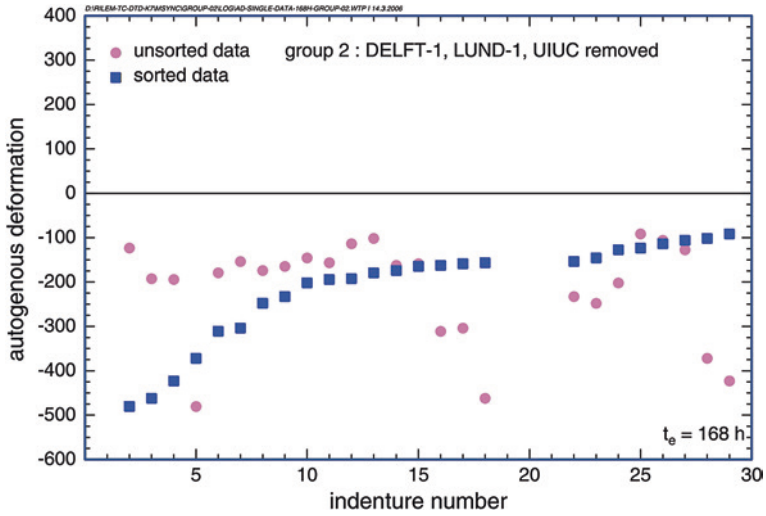


Fig. 1.28 Analysis of measured AD for  $t_e = 168$  h. Sorted and unsorted data of group 2. Indenture number acc. to Table 1.9

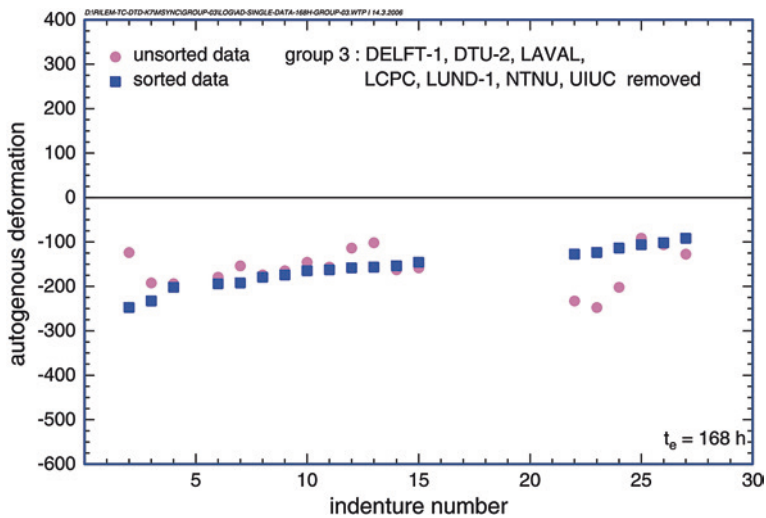


Fig. 1.29 Analysis of measured AD for  $t_e = 168$  h. Sorted and unsorted data of group 3. Indenture number acc. to Table 1.9

### 1.6.4 Statistical Attributes of AD and AS

The statistic characteristics of AD/AS are strongly time-dependent. The Fig. 1.34 points histograms of four different times for AD—all data. The estimated statistical attributes of AD and AS are given in the Tables 1.12 and 1.13.

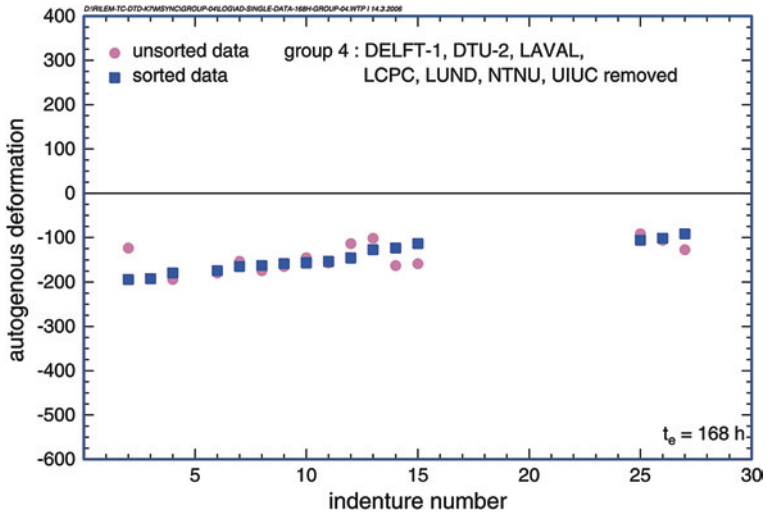


Fig. 1.30 Analysis of measured AD for  $t_e = 168 \text{ h}$ . Sorted and unsorted data of group 4. Indenture number acc. to Table 1.9

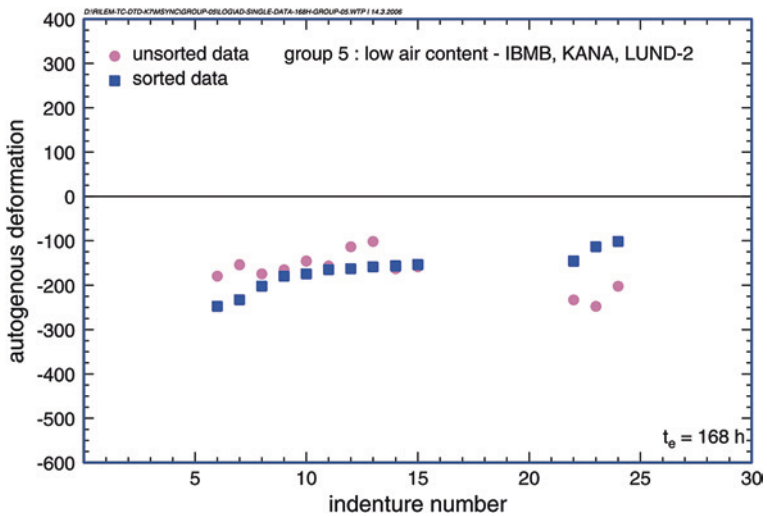


Fig. 1.31 Analysis of measured AD for  $t_e = 168 \text{ h}$ . Sorted and unsorted data of group 5. Indenture number acc. to Table 1.9

For the development of the COV a final value can be accepted. The increase of the scatter likewise converges to a final value. With the formula  $f(x) = a + b/x$  the final value of the COV for the AD becomes  $-38 \pm 1.3$  (Mean  $\pm$  SD) and AS  $-32 \pm 0.2$  (Mean  $\pm$  SD) percent. The KS-Test confirms that AD and AS can be



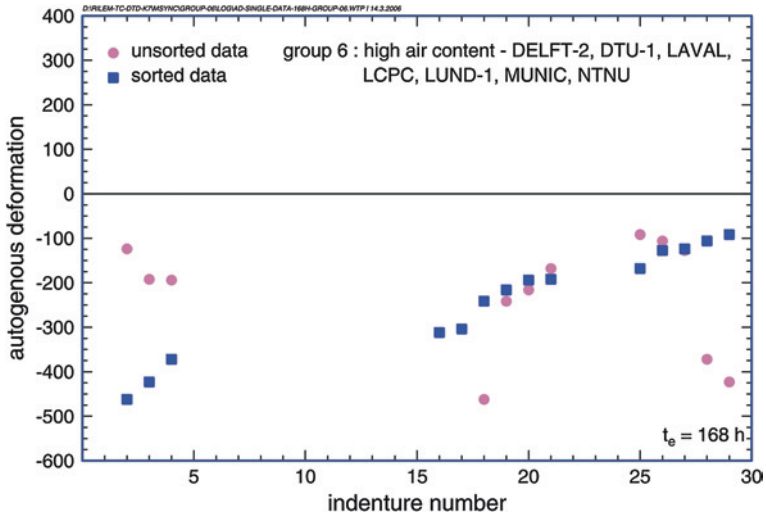


Fig. 1.32 Analysis of measured AD for  $t_e = 168 \text{ h}$ . Sorted and unsorted data of group 6. Indenture number acc. to Table 1.9

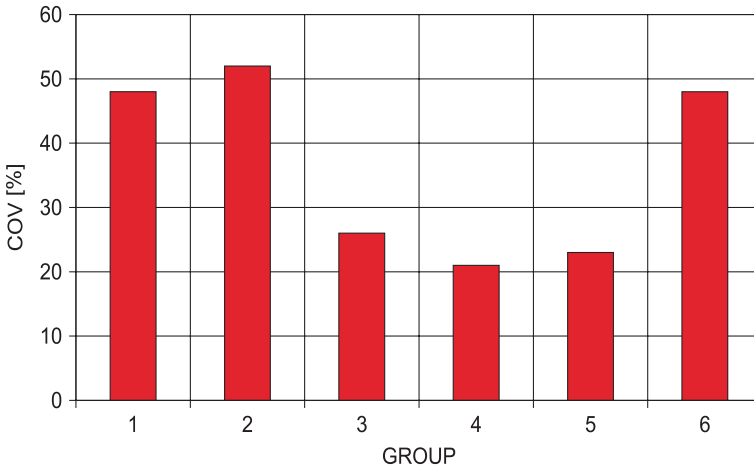


Fig. 1.33 Comparison of COV AD data at 7 days equivalent age

regarded as lognormal distributed random variables (cf. Fig. 1.34). This statement applies independently from time.

Normally the reproducibility within one lab is higher than the presented values which involve 10 laboratories. From the IBMB data (8 Dilation Rig measurements in total) it is notable that the end value of the COV for AS (14 days) is  $-11 \pm 1.4 \%$  (conf. interval =  $[-15, -7]$ ). Again this agrees well with the information of Table 1.8.

**Table 1.11** Statistical attributes of AD data for all groups for  $t_e = 7$  days

Group	N	MED	Mean	SD	COV
1	30	-186	-225	109	-48
2	25	-174	-215	111	-52
3	19	-158	-159	42	-26
4	16	-155	-147	31	-21
5	13	-163	-169	39	-23
6	14	-205	-238	115	-48

**Table 1.12** Calculated statistical attributes of AD for different ages—all partners

Equivalent age in days	N	$(\mu\text{m}/\text{m})$							(%)
		Min	Max	MED	Mean	Q05	Q95	SD	COV
1	30	-358	46	-57	-94	-353	13	104	-111
2	30	-414	-22	-110	-149	-411	-44	106	-72
3	30	-442	-51	-144	-180	-438	-70	108	-60
5	30	-469	-74	-170	-209	-387	-117	109	-52
7	30	-481	-92	-186	-225	-471	-104	110	-48
14	17	-474	-99	-221	-254	-457	-122	118	-46

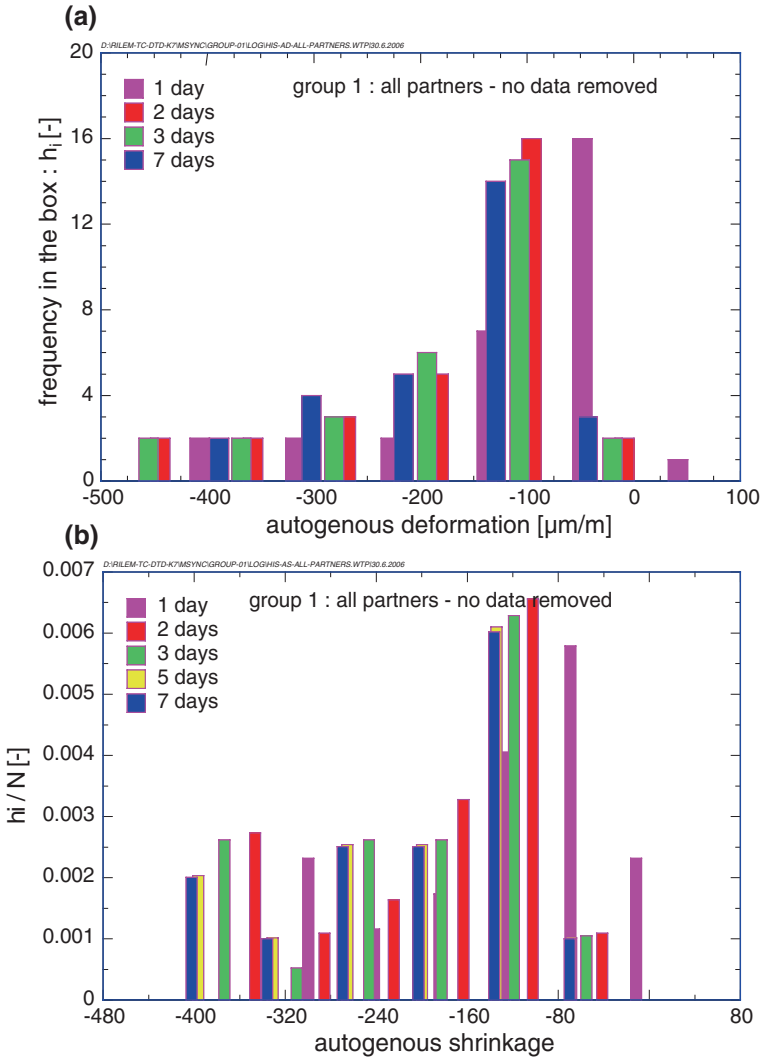
**Table 1.13** Calculated statistical attributes of AS for different ages—all partners

Equivalent age in days	N	$(\mu\text{m}/\text{m})$							(%)
		Min	Max	MED	Mean	Q05	Q95	SD	COV
1	30	-266	-7	-87	-108	-264	-10	86	-77
2	30	-322	-47	-144	-163	-321	-59	88	-54
3	30	-358	-71	-177	-195	-356	-91	90	-46
5	30	-390	-95	-205	-224	-387	-117	91	-41
7	30	-405	-106	-214	-239	-402	-131	92	-38
14	17	-431	-157	-256	-273	-433	-175	95	-35

### 1.6.5 Summary and Conclusions

The result of the evaluation can be summarized as follows:

- The literature review show that the time-dependent coefficient of variation (COV) of autogenous deformation (AD) and autogenous shrinkage (AS) is around 3–4 times larger than appropriate values for the mechanical properties. The present analysis confirms this trend.
- An estimate of the end of dormant period (EOD) of the reference mix was derived from all 30 measurements of AD. A mean value of 8.7 h and a standard deviation of 2.7 h were calculated.



**Fig. 1.34** **a** Calculated histograms of AD for different ages, equivalent time. **b** Calculated histograms of AS for different ages, equivalent time

- The COV of the end values for AD and AS are the following: All data (N = 30)—AD 38 %, AS 32 %; IBMB (N = 8)—AD 15 %, AS 11 %; LUND (N = 6)—AD 10 %, AS 9 %; MUNIC (N = 3)—AD 10 %, AS 1.3 %.
- The investigation underlines seriously the experience that the characteristics of fresh concrete has a very large influence on the AD in the early stages. An partitioning of the entire sample into the subsets “small air void content” and

“high air void content” showed that the COV of the group “small air void content” ( $N = 13$ , AD 14 %, AS 10 %) reaches only approximately half of the of the COV of the group “high air void content” ( $N = 14$ , AD 29 %, AS 21 %). This hypothesis remains even in later ages due to memory character of the void structure. The influence of the variations in fresh concrete temperature is not so strongly pronounced in this sense.

- It could be stated that the COV for the end value of AS is approximately 70 % lower than the value for AD.
- The sample contains values from faulty measurements. A reduction of the sample from these measurements did not bring improvements of the computed COV. Outliers test confirms that no unusual values are contained in the available sample. The large scatter cannot be explained thereby. Therefore a larger sample size is necessary.

From the above average sensitivity of the various measuring methods (presented in Chap. 3) in relation to the variation of the fresh concrete characteristics one can recommend that—independently of the selected measuring method—at least five individual measurements of the AD should become accomplished for a reliable forecast.

The RR-test obtained similar values for COV of AD and AS as found in the literature (22–56 %). From this point of view, the RR-test was successful. As the minimum number of tests depends on the expected COV it is therefore recommended to perform 8 tests for one laboratory and 20 tests for an inter-laboratory comparison are recommended.

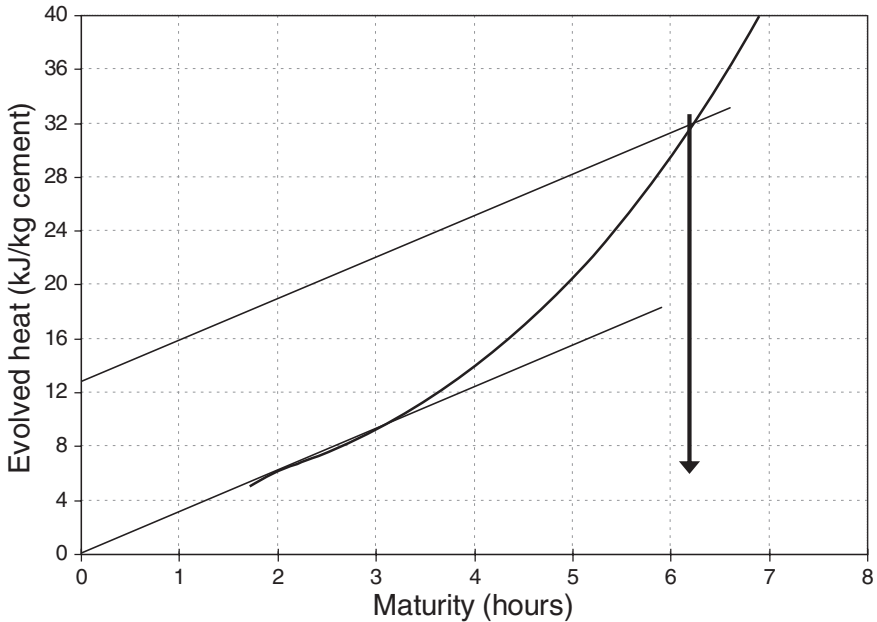
## 1.7 Cement Paste Test Results

### 1.7.1 Supporting Test Results

#### 1.7.1.1 Hydration Heat

Early hydration heat of the cement paste from the NTNU test is shown in Fig. 1.35. Setting according to the 12.5 kJ/kg criteria (see Sect. 1.5.2.1) is 6.2 (maturity) hours, which is 4.8 h earlier than in the corresponding NTNU-test on the mortar. The main reason for this difference is that the mortar is retarded by the SP, while the paste is made without SP.

Adiabatic temperature rise and heat development from the NTNU-tests on the cement paste as well as the mortar are shown in Fig. 1.36. The cement paste develops naturally very high adiabatic temperature rise. Note that the semi-adiabatic calorimeter used for the paste is relatively small (1 l sample) compared to the mortar (15 l sample). The calculation of adiabatic temperature of the paste is therefore rather inaccurate when the sample temperature becomes high because the heat loss to the surroundings is very dominant. However, the smaller calorimeter works well at least during the early hours when the temperature in the calorimeter is still



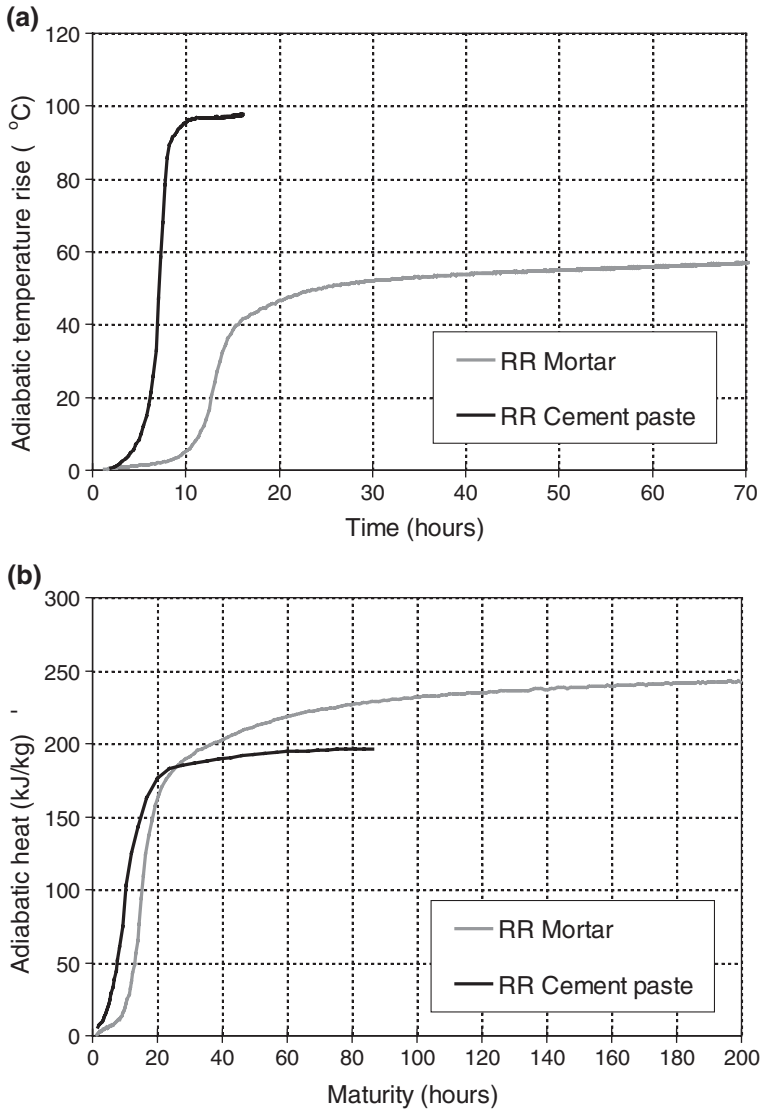
**Fig. 1.35** Early heat liberation of the cement paste (NTNU, semi-adiabatic calorimeter) and indication of setting according to the 12.5 kJ/kg criteria (EA of 30 kJ/mole was used to plot the curves on a maturity scale)

moderate. It is quite clear that the onset of rapid hydration occurs earlier in the paste than in the mortar, as already discussed. The results also indicate that the paste develops less total heat than the mortar which may be logic since the curing temperature was quite extreme in the paste (maximum temperature during the test was above 100 °C) something that obstructs hydration. But, again, it is reason to doubt the paste results over longer times, as already discussed.

Note that the conversion from adiabatic temperature to adiabatic heat in Fig. 1.36 requires the specific heat capacity ( $c_p$ ) of paste and mortar.  $c_p$  was calculated by assuming that water has a  $c_p$  of 4.2 kJ/kg and all solid materials 0.8 kJ/kg. The  $c_p$  of fresh paste and mortar then becomes 1.68 and 1.06 kJ/kg, respectively. Furthermore, the calculation then takes into account that the  $c_p$ -values decrease as water is bound chemically during hydration (degree of hydration over time was calculated as evolved heat divided by final heat and final degree of hydration was assumed to be 60 %).

### 1.7.1.2 Relative Humidity

Two RH-measurements performed in the same cement paste sample over 5 weeks at DTU are shown in Fig. 1.37. After a quite rapid decrease of the RH during



**Fig. 1.36** Adiabatic temperature **a** and heat developments **b** in the cement paste and mortar, as deduced from NTNU semi-adiabatic calorimeter tests. Note that the mortar sample is 15 l while the cement paste sample was only 1 l. (EA of 30 kJ/mole was used to plot the curves on a maturity scale)

the first 3–4 days it is notable that the RH increases from about 5 days to about 2.5 weeks until stabilizing from that point on. The RH-increase in the mid period is accompanied by autogenous expansion measured in a parallel Dilation Rig test at DTU, see next section.

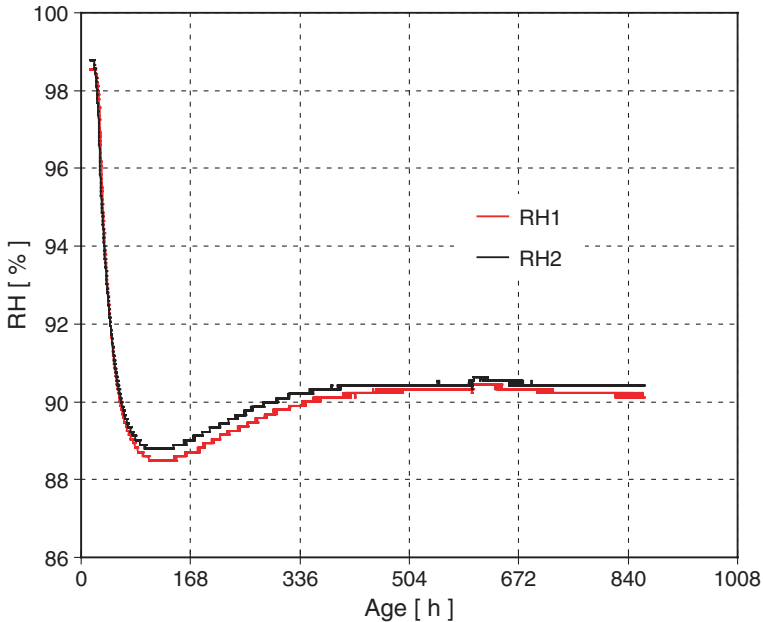


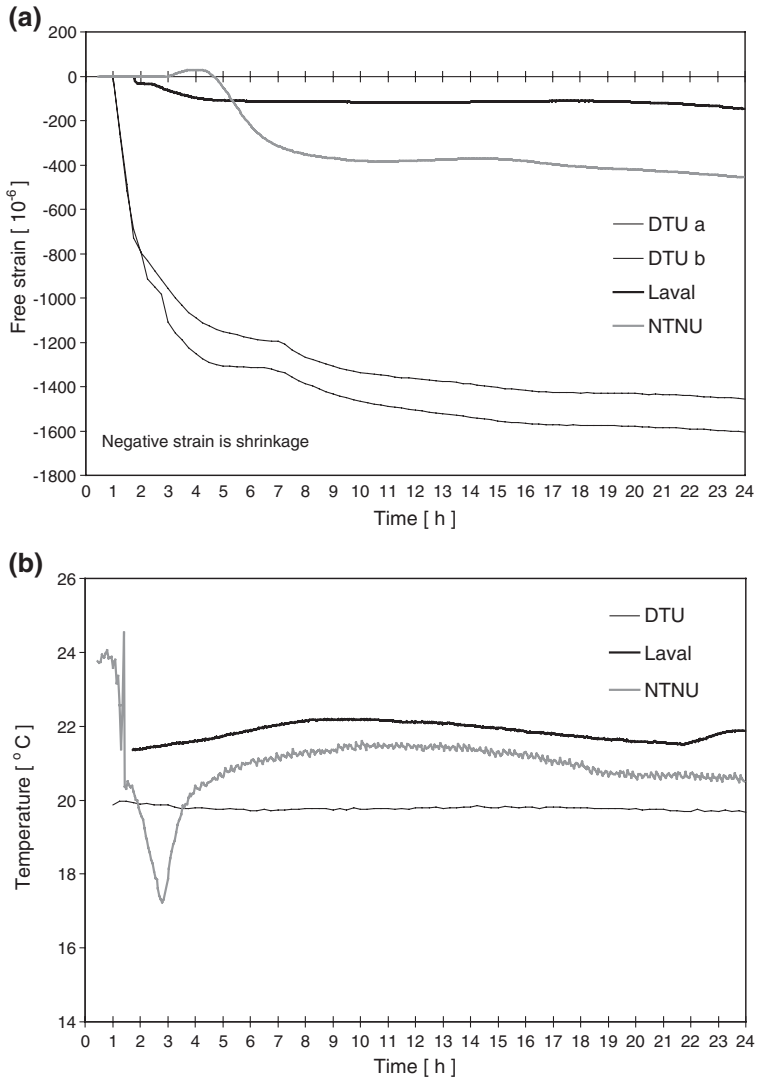
Fig. 1.37 RH-measurements at DTU on the cement paste

### 1.7.2 Dilation Rig Test Results

Different plots of the 20 °C isothermal Dilation Rig tests on the RR-cement paste are shown in the following figures. The plots give reported results from the participants; hence no treatment of the results is done except that the strain results are zeroed at different times. The term “free strain” in the figures is presumably mainly resulted from AD since the test temperatures were very constant (i.e. no TD), in addition to possible errors/variables not under control.

Bleeding and bleeding reabsorption is important in such measurements and it is therefore important to note that the specimens in the two DTU-tests were rotated until setting to avoid bleeding to form on the top surface. In the NTNU-test a small amount of bleed water (corresponds to 0.4 l/m<sup>3</sup> paste) was removed from the top surface of the specimen after 3 h. A substantial amount of bleeding (corresponds to 42 l/m<sup>3</sup> paste) was measured in the paste at Laval (separate measurement), but not removed from the surface of the specimen.

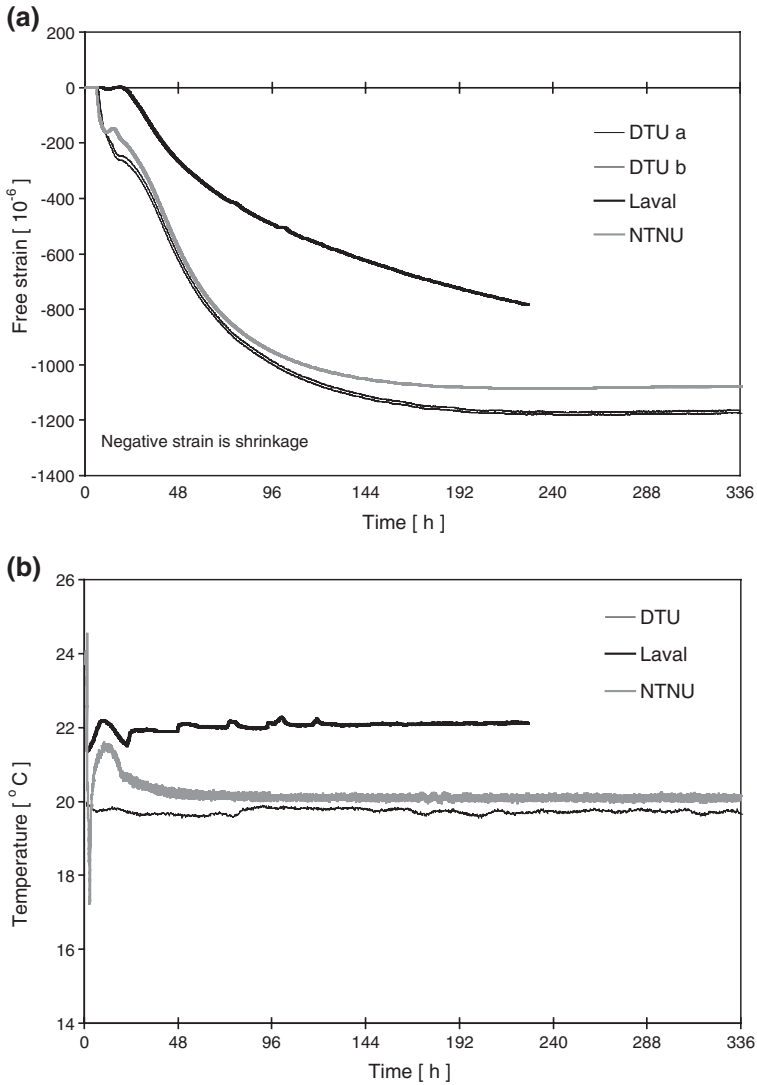
Measured temperature and free strain during the first 24 h are shown in Fig. 1.38, while Figs. 1.39 and 1.40 shows plots over the whole measuring period (when zeroed after 6 and 24 h, respectively). The results show that the DTU- and NTNU-results are in the same range, while lower shrinkage is measured at Laval.



**Fig. 1.38** Measured free strain in the Dilation Rig tests on cement paste **a** and measured temperature in the specimens **b** all results from the start of measurement, first 24 h

Figure 1.41 is a close-up of the late strain behaviour in the DTU and NTNU-tests and shows that there is expansion from about 10 days (240 h). The expansion occurs along with a RH-increase in the paste (as measured at DTU, see Fig. 1.37) which indicate that the under-pressure in the pore system of the cement paste is reduced. The RH-increase starts, however, from as early as about 5 days.

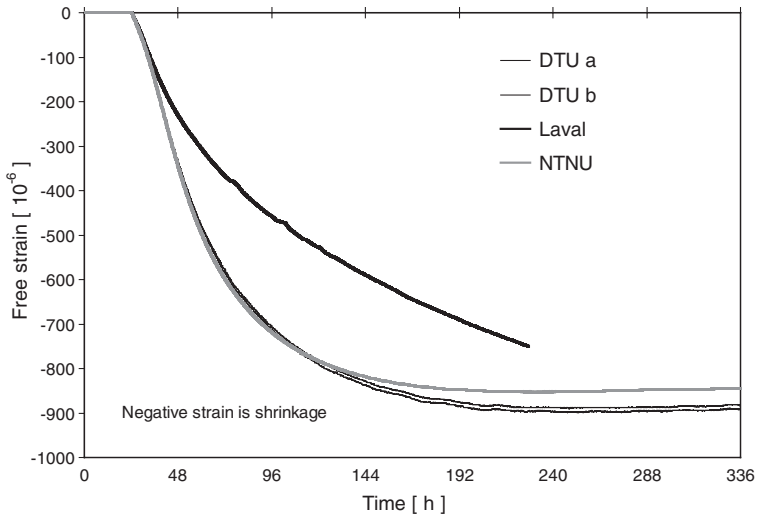




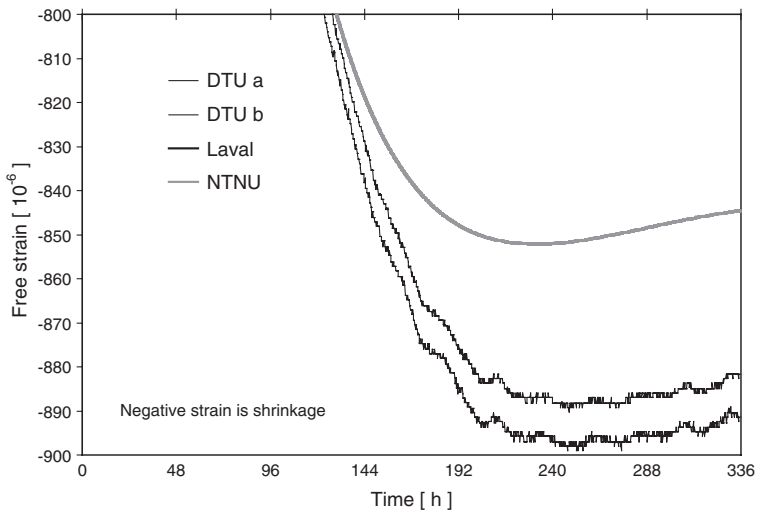
**Fig. 1.39** Measured free strain in the Dilation Rig tests on cement paste when plotted (zeroed) from 6 h (a) and measured temperature in the specimens (b)

### 1.8 Summary and Conclusions

The scope of the RILEM TC195-DTD committee was to study Dilation Rigs measuring thermal dilation (TD) and autogenous deformation (AD) of hardening cement paste, mortar and concrete in linear test set-ups, as basis for preparing a



**Fig. 1.40** Measured free strain in the Dilation Rig tests on cement paste when plotted (zeroed) from 24 h



**Fig. 1.41** Close-up of Fig. 1.40: expansion is measured in both the DTU- and NTNU-test from approximately 10 days

test procedure recommendation for AD and TD. The report presents the results from the round-robin (RR) test program that was carried out.

The RR mortar ( $w/c = 0.35$  and  $d_{max} = 8$  mm) was tested in 10 laboratories around the world. The intended test condition for the Dilation Rig tests was 20 °C *isothermal*

*temperature and protected against moisture exchange with the surroundings*, hence the intended situation is that the measured strain in the tests is caused by autogenous deformation. Totally 30 Dilation Rig tests were performed.

Supporting tests showed that the mortar slump and air content after mixing varied with a coefficient of variation (COV) of 58 and 38 %, respectively. The 28-days compressive strength varied with a COV of 11 %.

A statistical evaluation of the Dilation Rig results was performed and the following conclusions can be drawn:

The overall variation of AD in the RR in terms of coefficient of variation (COV) was similar to that found in the literature, and thus confirmed general experience. With a significance level of 20 % it implies that 8 individual measurements on one particular concrete are needed in each lab. The batch to batch variation between labs was large (seen as variation in fresh concrete properties) whereas the variation within each lab was less. This implies that the necessary number of individual measurements in each lab can be reduced. Therefore, it is recommended to execute pre-tests to find the number of tests needed by establishing a batch to batch variation for the procedure, and a specimen to specimen variation if concrete from the same batch is used in parallel specimens.

Based on the present and previous experience possible pitfalls/errors associated with Dilation Rig experiments and RR-programs can be listed:

*Dilation Rig tests, possible pitfalls:*

- friction between specimen and mould
- unwanted movement of measuring points (thermal disturbance, etc.)
- reabsorption of top surface bleed water into the specimen after setting (here: not observed, probably due to low w/c)
- malfunction/lack of temperature control, unwanted temperature increase due to hydration heat
- temperature gradients in the specimen
- moisture loss between mixing and casting, and during the measuring period.

*RR programs, possible pitfalls/errors (generally valid):*

- wrong mixing proportions and -procedure (here: in one batch the water was added in two steps)
- initial aggregate moisture state (here: a relation between moisture state and slump was found)
- aggregate size (here: one test used  $d_{\max} = 4$  mm instead of 8 mm due to the specimen geometry)
- wrong amount of superplasticizer (here: two labs. used 8 l/m<sup>3</sup> instead of 10.4 l/m<sup>3</sup>)
- varying test procedure (time between mixing and casting, casting procedure, etc.)
- varying reference time (time from water addition or time from casting)
- varying initial temperature and test temperature (here: 16–26 °C)
- degree of processing data (here: raw data was to be send, but some of the data where temperature compensated)

One of the success factors in a RR program is good planning, involving detailed descriptions on, for instance, initial aggregate moisture content, mixing- and test procedure, as well as supporting tests. Which data and how to report data should be well-defined. Such descriptions were made for the present RR, but there is room for improvements in possible future programs. Finally, the work has generated experience on how to organize and execute RR-tests. Experience from other RR-programs could be compiled with the present in order to help and secure high quality in future RR-programs. Such task could be undertaken by a RILEM-committee.

## References

1. Morabito, P., Bjøntegaard, Ø., van Breugel, K., Dalmagioni, P., Gram, H.-E., Gutsch, A., Hedlund, H., Jonasson, J.-E., Kanstad, K., Lura, P., Pellegrini, R., Rostasy, F., Sellevold, E.: Round robin testing program. equipment, testing methods, test results. IPACS report, Ed. by P. Morabito, 110 p, Luleå University of Technology, Sweden (2001) ISBN 91-89580-42-7
2. Helland, S.: Norwegian standards on activation energy and heat release. IPACS-report, 25 p, Luleå University of Technology, Sweden (2001), ISBN 91-89580-24-9
3. Hampel, F.R.: Robust statistics—the approach based on influence functions. Wiley, New York (1986). ISBN 0-471-82921-8 - ISBN 0-471-63238-4
4. Mandel, J.: The Statistical Analysis of Experimental Data. Dover publications, New York (1984), ISBN 0-486-64666-1
5. Krauß, M.: Probabilistic concept for the validation of the effectiveness of measures against early age cracking in massive concrete structures. Doctoral-Thesis. TU Braunschweig, (2004), (in German)
6. Tsubaki, T.: Sensitivity of factors in relation to prediction of creep and shrinkage of concrete. In: Bažant Z.P. and Carol I. (ed.) Creep and shrinkage of concrete. Proceedings of the International RILEM Symposium, pp. 611–622. Barcelona, E&FN Spon, London (1993)
7. Sachs, L.: Applied Statistics, Springer, Berlin, (2002) ISBN 3-540-42448-2
8. Springenschmidt, R. (ed.): Prevention of thermal cracking in concrete at early ages. RILEM Report 15, E&FN Spon, London (1998)
9. Kölling, W.: To Break the Rank. The identification of Outliers with the Hampel-Test. QZ, pp. 315 (2001), (in German)
10. Bjøntegaard, Ø.: Thermal dilation and autogenous deformation as driving forces to self-induced stresses in high performance concrete. Doctoral Thesis, Department of Structural Engineering, The Norwegian University of Science and Technology (1999), ISBN 82-7984-002-8
11. Tazawa, E.: (ed.) Proceedings of the int. workshop: autogenous shrinkage of concrete. organized by the Japan Concrete Institute, Hiroshima, Japan, (1998), © 1999 E & FN Spon, ISBN 0-419-23890-5
12. Bažant, Z.P., Zebich, S.: Statistical linear regression analysis of prediction models for creep and shrinkage. Cem. Concr. Res. **13**, 869–876 (1983). Pergamon Press

# Appendix A

## Cement Analyses

## REPORT ON QUALITY TEST

Sample marked: Norcem CEM I 42.5R RILEM TC-DTD

Our Ref.: BZ3-03

CHEMICAL ANALYSES			PHYSICAL TEST EN 196		
Loss on ignition	(L.O.I.)	2.49 %	<b>FINENESS</b>		
Silica	(SiO <sub>2</sub> )	20.28 %	Particle analysis	+90 mic.	1.6 %
Alumina	(Al <sub>2</sub> O <sub>3</sub> )	4.71 %	" "	+64 mic.	5.6 %
Ferric Oxide	(Fe <sub>2</sub> O <sub>3</sub> )	3.30 %	" "	-24 mic.	64.4 %
Lime	(CaO)	61.94 %	" "	-30 mic.	72.6 %
Magnesia	(MgO)	2.34 %	Sp.surface,	Blaine	363 m <sup>2</sup> /kg
Sulphur Trioxide		3.20 %			
Limestone		4.2 %			
Potassium Oxide	(K <sub>2</sub> O)	1.06 %	<b>STANDARD CONSISTENCY</b>		
Sodium Oxide	(Na <sub>2</sub> O)	0.36 %	Temperate climate	20°C	27.3 %
Free Lime		0.71 %	<b>SOUNDNESS</b>		
Chloride		0.03 %	Le Chatelier expansion		0.0 mm
Alkali	(Na <sub>2</sub> O Eq.)	1.05 %	<b>SETTING TIME</b>		
Phosphorus Pentoxide	(P <sub>2</sub> O <sub>5</sub> )	0.15 %	Initial		130 min.
			<b>COMPRESSIVE STRENGTH</b>		
			1 day		19.6 MPa
			2 days		31.9 MPa
			7 days		42.1 MPa
			28 days		50.3 MPa

Norcem A.S R&amp;D 05.aug.03

 po.  
 PD

 E. Aaroldsen  
 Laboratory Manager

## NORCEM A.S R&amp;D

 Address: Setreveien 2  
 P.O. Box 38  
 N-3991 Brevik

 Phone: +47 35 57 20 00  
 Telefax: +47 35 57 04 00

 Ent.no: NO 934 949 145 VAT  
 Bank account: 6003 06 12488

 Head Office: Lilleakerveien 2b  
 P.O.Box 143 Lilleaker  
 0216 Oslo

# Appendix B

## Sand Grading Curve



Testrapport nr. : 465/03		Skjema nr. :	
Sted	: NorStone Årdal	Kunde	: Ferdigvarekontroll
Uttak	: <u>Big-bags til NORCEM</u>		
Vare	: 0/8mm NSBR		
Dato	: 23-04-03		
Kiokka	:		

ISO sikt	0.063	0.125	0.250	0.50	1.00	2.00	4.0	8.0	F.M.
Min.:									
Max.:									
Sikterst.	97.5	94.0	87.4	74.5	55.0	34.8	16.8	1.1	3.17

**FAX** *Knut O. Kjellson*  
*35 57 04 00*  
*NorStone / Forsh*

*24104103*

		<i>T.R</i>	
Dato	Anmerkn.	Sign.	Kontroll



# Appendix C

## Data Sheet, Scanflux AD18

## SAFETY DATA SHEET

### MATERIAL SAFETY DATA SHEET

Last changed: 2002/11/08

Internal No.: 2177

Replaces date: 2002/01/15

# SCANFLUX AD 18

**EXPOSURE CONTROL**

Usual rules for handling of chemicals must be observed. Eyewash facilities must be available at the workplace. Wash hands and face after using the product. Wash skin at the end of each work shift and before eating, smoking and using the toilet. Keep away from food, drink and animal feed.

**RESPIRATORY PROTECTION**

Not required, except in case of aerosol formation.

**EYE PROTECTION**

Wear splash-proof eye goggles to protect against possible eye contact.

**HAND PROTECTION**

Safety-gloves made of neopren-, nitril-rubber, vinyl or other type of a resistant material.

**PROTECTIVE CLOTHING**

Protective clothing should be worn if there is a possibility of direct contact or splashes.

## 9. PHYSICAL AND CHEMICAL PROPERTIES

Physical State:	Liquid		
Colour:	Light brown		
Odour:	Slight		
Solubility:	Completely miscible/Water		
Melting point/range:	ca 0°C	Density:	1045
Exp. limit LEL-UFL%:		Solubility in water:	Soluble
Vapour pressure:		Saturation conc.:	
Decomposition temp.:		Rel. dens. sat. air (air=1):	
pH solution:		Boiling point/range:	ca 100°C
Flash point:		pH concentrate:	6 - 7
Molar weight:		Viscosity:	25 mPas
Ignition temp.:		Odour threshold value:	
Rel.vap.dens. (air=1):		Rel. evap. velocity:	
Air reactive:		Water reactive:	

## 10. STABILITY AND REACTIVITY

**STABILITY**

Stable under recommended storage and handling conditions.

**MATERIALS TO AVOID**

No hazardous reactions known.

**HAZARDOUS DECOMPOSITION PRODUCTS**

No decomposition if used as directed. See section 5.

## 11. TOXICOLOGICAL INFORMATION

Acute oral tox.	LD50 (oral, rat)	>2000 mg/kg
Acute derm. tox.		
Inh. toxicity		

**OTHER TOXICOLOGICAL INFORMATION**

no data available

**GENERAL**

Not known or expected to be harmful to health in normal use.

**INHALATION**

Not relevant.

**SKIN CONTACT**

Repeated contact may cause some drying of the skin.

**EYE CONTACT**

# Appendix D

## Description of Equipment, Made by the Participants

Dilation Rigs, totally 12, are described in the following pages. The 10 first rigs are those participating in the Round Robin tests. The two last ones (SINTEF, Nantes) did not participate, but is included as extra information since descriptions were submitted.

### D.1 Description of Equipment/Procedures

Company/Institution:	Delft University of Technology
Department:	Civil Engineering and Geosciences/Concrete Structures group
Information filled in by:	Eddy Koenders
E-mail address:	E.A.B.Koenders@citg.tudelft.nl

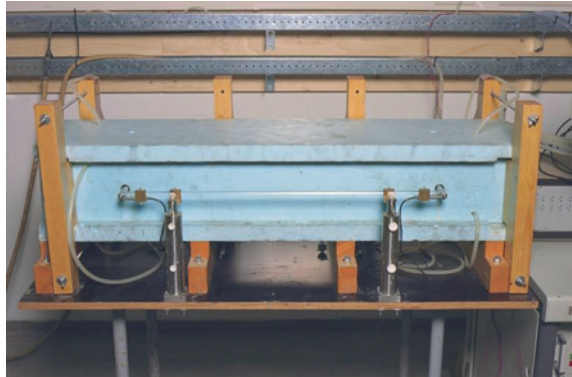
Name of rig:	ADTM
Designed to measure on: (concrete, mortar, paste, etc.)	Concrete, mortar and paste (reinforced and non-reinforced)
Specimen geometry:	Cross-section up to $150 \times 150 \text{ mm}^2$ . Measuring distance 750 mm
Specimen orientation: (horizontal/vertical)	Horizontal
Start of measurement: (hours after mixing)	After setting, from 3 h on
Type of measuring device: (LVDT, strain gauge, laser, thermocouples, etc.)	4 LVDT's and 3 thermocouple

Name of rig:	ADTM
Temperature control (yes/no):	Yes
<i>Designed to measure</i>	
(a) AD at isothermal temperatures (yes/no):	Yes
(b) Coupled AD and TD at semi-adiabatic temperature histories (yes/no):	Yes
(c) CTE during rapid temperature changes (yes/no):	Yes
Additional info.:	Thermal controlled Elastic modulus measurements can also be performed simultaneously

### ***D.1.1 Description of ADTM Rig and Specimen***

The Autogenous Deformation Testing Machine (ADTM) is a horizontal positioned temperature controlled mould with which linear hardening deformations of concrete specimens can be determined, under sealed and various thermal boundary conditions (see Fig. D.1). The ADTM is situated in a climate-controlled room (see Fig. D.2) and is part the Thermal Stress Testing Machine configuration (TSTM).

**Fig. D.1** Front view of the ADTM specimen



**Fig. D.2** Survey photo of the ADTM/TSTM climate room



For the ADTM measurements, moulds with different dimensions are available for mixtures that develop different temperature rates during hardening.

Type of mix	Dimensions of mould	Note
Concrete	150 × 150 × 1,000 mm	Moderate temperature development
Mortar and HPC	100 × 100 × 1,000 mm	High temperature development
Pastes	40 × 150 × 1,000 mm	Extreme temperature development

The specimen in the ADTM should experience the thermal hardening conditions as imposed prior to testing. In order to achieve this, a thermally controlled insulated mould and one or more cryostat units can be applied to keep temperature differences between the imposed thermal hardening condition and the ADTM specimen within negligible ranges. With this configuration, any desired thermal path can be imposed to the specimen during hardening.

The ADTM specimen experience no external restrained while hardening. This is obtained by application of a plastic cover foil attached to the inner sides of the thermally insulated moulds with lubricating grease. The deformations measured from the hardening specimen can therefore be considered as the autogenous deformations.

### D.1.2 Casting and Test Procedure

For the proposed RR-tests on mortar, the autogenous deformations will be measured from large specimens with dimensions of 100 × 100 × 1,000 mm<sup>3</sup> (Fig. D.3). The mould can be dismantled into several parts. These parts are made of 40 mm foam plastic with a low coefficient of thermal conductivity ( $\lambda = 0.03 \text{ W/m}^2 \text{ K}$ ). On one side a 1 mm thick steel plate is glued to the foam to ensure a smooth surface and to cover the “canals” that are cut in the foam. These canals enable cooling or heating of the concrete surface. The canals are connected to a cryostat, one cryostat for the top part of the mould and another cryostat for the bottom part of the mould. Both cryostats control the water temperature and

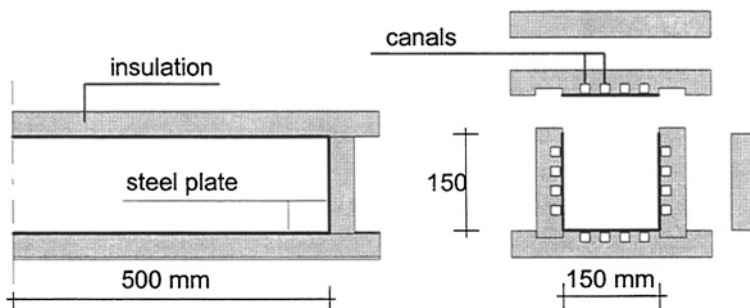
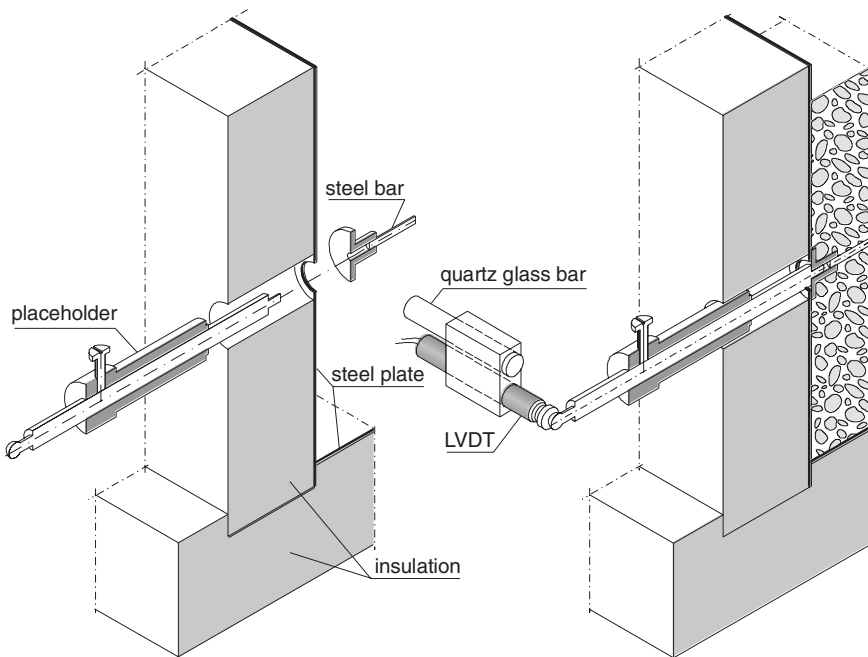


Fig. D.3 Schematic representation of the ADTM thermally insulated mould

pump the water through the canals. Before casting, the bottom part and the four side-parts are put together. A wooden frame is used to support the mould during casting and setting of the paste. The inside of the bottom of the mould is covered with a sheet of plastic foil and a sheet of felt. A second sheet of felt covers the bottom and the vertical sides of the mould. Together these three sheets allow the paste to deform without almost any restraint. The latter foil also prevents leakage of paste and it also prevents drying shrinkage of the hardening paste. Thermocouples are placed at three different locations at half the height of the specimen. After casting, the topside of the paste is covered by a layer of foil. After that, the top part of the mould is installed. During hardening, the temperature and the load-independent deformation of the paste are measured. The deformations of the cement paste are measured with LVDT's on two sides exterior of the mould, over a length of 750 mm between two steel bars (that pass through the mould), which are embedded in the paste during casting (see Fig. D.4). As soon as the setting period of the paste has ended, measurements can start.

At this moment the paste has built up negligible strength. This is mostly a few hours after casting, depending on the length of the dormant stage of the paste. In this way, the load-independent deformations (autogenous deformation) can be measured soon after the beginning of the hydration process.



**Fig. D.4** Installation of measuring bars and placeholders before casting (*left*) and installation of the LVDT's after casting (*right*)

### ***D.1.3 Measuring System and Data Presentation***

The measuring signals gained from the LVDT's and the thermocouples are continuously processed by means of a computer unit in conjunction with a data processing control unit. Tests are performed in a climate-controlled room that implicitly determines the thermal reference conditions. With the LVDT's, the deformational changes of the ADTM are measured continuously throughout the testing period. The thermal conditions of the specimen are controlled all-around the specimen by means of the thermally controlled mould, in order to achieve a uniform thermal profile within the specimen, resembling a one-dimensional loading situation (linear measurement). The presented deformation measurements, therefore, represent one-dimensional hardening deformations while submitted to predefined thermal conditions.

## **References**

1. Lokhorst, S.J.: Deformational behaviour of concrete influenced by hydration-related changes of the microstructure. Research Report, Delft University of Technology, Delft, The Netherlands (1998)
2. Koenders, E.A.B.: Simulation of volume changes in hardening cement-based materials. PhD thesis, Delft University of Technology, Delft, The Netherlands (1997)
3. Lura, P.: Autogenous deformation and internal curing of concrete. PhD thesis, Delft University of Technology, Delft, The Netherlands (2003)
4. Sule, M.S.: Effect of reinforcement on early-age cracking in high strength concrete. PhD thesis, Delft University of Technology, Delft, The Netherlands (2003)

## D.2 Description of Equipment/Procedures

Company/Institution:	Technical University of Denmark
Department:	Department of Civil Engineering
Information filled in by:	Ole Mejlhede Jensen
E-mail address:	omj@civil.auc.dk—to be changed during summer 2003

Name of rig:	Automatic dilatometer
Designed to measure on: (concrete, mortar, paste, etc.)	Primarily Paste, but mortar with 1–2 mm aggregate is possible as well
Specimen geometry:	Approx. $\varnothing 25 \times 300$ mm
Specimen orientation: (horizontal/vertical)	Horizontal
Start of measurement: (hours after mixing)	A few minutes
Type of measuring device: (LVDT, strain gauge, laser, thermocouples, etc.)	LVDT
Temperature control (yes/no):	Submerged in thermostatically controlled bath

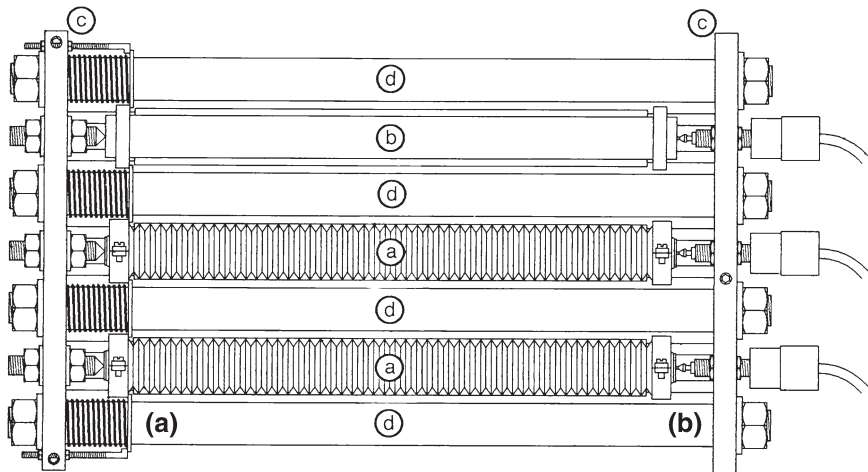
### *Designed to measure*

(a) AD at isothermal temperatures (yes/no):	Yes
(b) Coupled AD and TD at semi-adiabatic temperature histories (yes/no):	Yes
(c) CTE during rapid temperature changes (yes/no):	Yes
Additional info.:	Corrugated moulds enables linear measurements to commence before set

### D.2.1 Description of Rig and Specimen

The dilatometer consists of an invar measuring frame and special corrugated moulds for encapsulation of the cement paste. During the tests the dilatometer is submerged in a thermostatically controlled glycol bath. The proposed measuring technique permits: (i) commencement of the measurements a few minutes after casting; (ii) insignificant restraint of the hardening cement paste; (iii) accurate control of the temperature of the dilatometer and of the hardening cement paste; and (iv) efficient sealing of the cement paste.





**Fig. D.5** Early version of the dilatometer as given in Ref. [2]. Dilatometer frame with two test specimens (a) and an invar reference specimen (b). The lengths of the specimens are approximately 300 mm

### D.2.2 Casting and Test Procedure

The corrugated tube with one end closure mounted is filled with the material to be tested. The casting is done on a vibrating table. The top end closure is mounted, the sample is inserted into the dilatometer, the dilatometer is lowered into a thermostatically controlled bath and measurements are started.

### D.2.3 Measuring System and Data Presentation

Typically measurements are saved every 15 min, and typically also measurements of autogenous relative humidity change are recorded simultaneously (Fig. D.5).

## References

1. Jensen, O.M.: Dilatometer—calibration and testing (in Danish). Ph.D. project, Building Materials Laboratory, The Technical University of Denmark, Technical report 261/92 (1992)
2. Jensen, O.M., Hansen, P.F.: A dilatometer for measuring autogenous deformation in hardening Portland cement paste. *Mater. Struct.* **28**(181), 406–409 (1995)
3. Jensen, O.M.: Dilatometer—further development. Department of Structural Engineering and Materials, The Technical University of Denmark, June 1996

### D.3 Description of Equipment/Procedures

Company/Institution:	Technical University of Denmark
Department:	Department of Civil Engineering
Information filled in by:	Ole Mejlhede Jensen
E-mail address:	omj@civil.auc.dk—to be changed during summer 2003

Name of rig	Thermal comparator dilatometer
Designed to measure on: (concrete, mortar, paste, etc.)	Primarily paste, but mortar with 1–2 mm aggregate is possible as well
Specimen geometry:	Approx. $\varnothing 25 \times 300$ mm
Specimen orientation: (horizontal/vertical)	Horizontal
Start of measurement: (hours after mixing)	0.5 h
Type of measuring device: (LVDT, strain gauge, laser, thermocouples, etc.)	Thermal comparator
Temperature control (yes/no):	Submerged in thermostatically controlled flowing water

#### *Designed to measure*

(a) AD at isothermal temperatures (yes/no):	Yes
(b) Coupled AD and TD at semi-adiabatic temperature histories (yes/no):	Yes
(c) CTE during rapid temperature changes (yes/no):	Yes
Additional info.:	Corrugated moulds enables linear measurements to commence before set. Very fast temperature changes are possible

#### ***D.3.1 Description of Rig and Specimen***

The dilatometer consists of a thermal comparator sensor which is fixed directly on top of special corrugated moulds that encapsulates the cement paste. During the tests the corrugated mould is submerged in thermostatically controlled flowing water. The proposed measuring technique permits: (i) commencement of the measurements shortly after casting; (ii) insignificant restraint of the hardening cement paste; (iii) very fast and accurate control of the temperature of the hardening cement paste; and (iv) efficient sealing of the cement paste.

### ***D.3.2 Casting and Test Procedure***

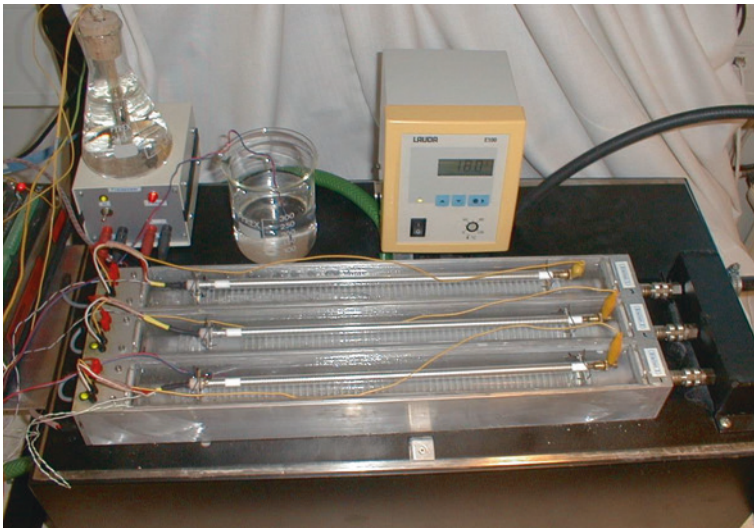
The corrugated tube with one end closure mounted is filled with the material to be tested. The casting is done on a vibrating table. The top end closure is mounted, the thermal comparator sensor is mounted, the sample is lowered into a thermostatically controlled, flowing water bath and measurements are started.

### ***D.3.3 Measuring System and Data Presentation***

Typically measurements are saved every 15 min.

## **Reference**

1. Østergaard, T., Jensen, O.M.: A thermal comparator sensor for measuring autogenous deformation in hardening Portland cement paste (paper under preparation)



Three measuring units with thermal comparators. Each module can be operated individually.

## D.4 Description of Equipment/Procedures

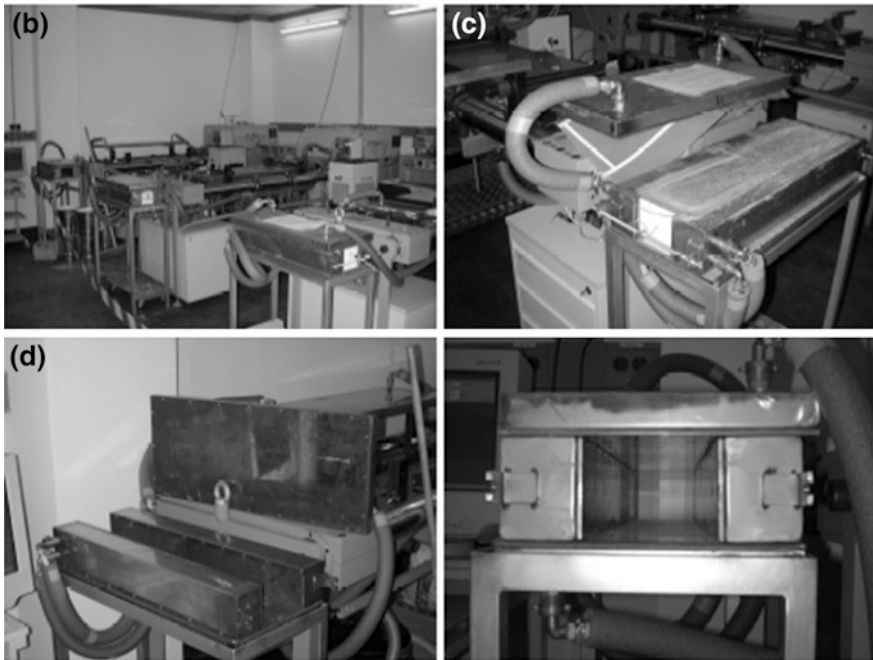
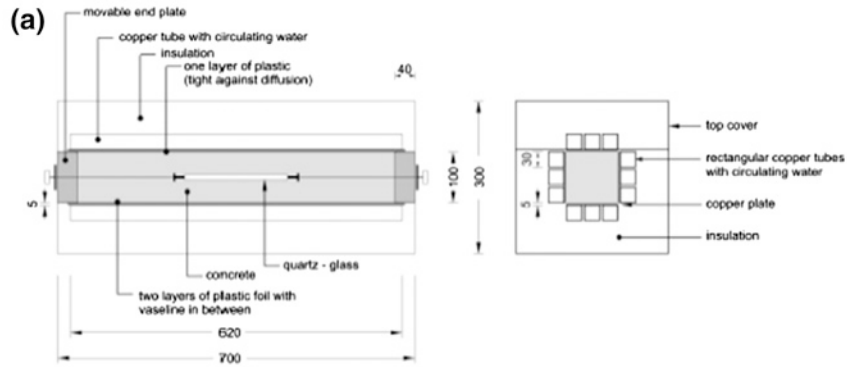
Company/Institution:	Technical University of Braunschweig
Department:	Institute of Building Materials. Concrete Construction and Fire Protection
Information filled in by:	Matias Krauß? Reinhard Nothnagel
E-mail address:	m.krauss@tu-bs.de, r.nothnagel@tu-bs.de

Name of rig:	TSTM K7
Designed to measure on: (concrete, mortar, paste, etc.)	Concrete and mortar
Specimen geometry:	100 × 100/620 mm
Specimen orientation: (horizontal/vertical)	Horizontal
Start of measurement: (hours after mixing)	~30 min after concrete placing and compaction
Type of measuring device: (LVDT, strain guage, laser, thermocouples, etc.)	Glued strain gauge on quartz-glass tubes, glued strain gauge on copper foil, thermocouples
Temperature control (yes/no):	Yes
<i>Designed to measure</i>	
(a) AD at isothermal temperatures (yes/no):	Yes
(b) Coupled AD and TD at semi-adiabatic temperature histories (yes/no):	Yes
(c) CTE during rapid temperature changes (yes/no):	Yes
Additional info.:	Two independent rigs

### D.4.1 Description of Rig and Specimen

The autogenous deformation is measured on the companion specimen of temperature–stress testing machine (TSTM). This TSTM is build up by two independent test rigs. Fig. D.6 shows the geometry of the specimen.

The mould is constructed of 5 mm thick copper plates. Rectangular copper tubes are connected to these plates in order to maintain a prescribed temperature in the test items. All specimens are embedded in insulating material with a total thickness of 100 mm on the length and 40 mm on the face surface. Arbitrary temperature histories in a range between 5 and 60 °C can be realized in the specimens, provided by a computer controlled cryostat.



**Fig. D.6** a Test specimen for autogenous shrinkage rig: *left* longitudinal view; *right* cross-section. **b** TSTM K7—overview of all rigs. **c** Test specimen ready for testing. **d** Mould of test specimen, *left* overview; *right* front face

### D.4.2 Casting and Test Procedure

The mould is lined with two layers of plastic sheets with Vaseline in between in order to minimize friction. All measuring devices are placed and fixed in the mould. After concrete is cast and compacted, the top surface is covered with thin plastic foil to prevent the lost of moisture. When the top cover is put into place, the measurements starts. Typically 30 min after mixing.

### ***D.4.3 Measuring System and Data Presentation***

Two types of devices to depict the strain development are used. The first one is electric strain gauges glued on quartz-glass tubes cf.[4]. The second one are also electric strain gauges glued on pre-stressed copper straps embedded in brass tubes can fixed with endplates. These endplates have a diameter of 200 mm. The strain measured in the middle of cross-section.

Amplifier and computer provide a continuously recording of all measured data. All measured strains are temperature compensated. The climate of the laboratory is controlled by air condition (23 °C/65 % r.h). All data are presented from time after placing.

## **References**

1. Rostásy, F.S., Krauß, M.: Frühe Risse in massigen Betonbauteilen—Ingenieurmodelle für die Planung von Gegenmaßnahmen. DAFStb-Heft 520. Beuth, Berlin (2001)
2. Springenschmid, R. (Hrsg.): Prevention of thermal cracking in concrete at early ages. RILEM Report 15 (1998)
3. Gutsch, A.W.: Stoffeigenschaften junger Betons—Versuche und Modelle. DAFStb-Heft 495, Beuth, Berlin (1999)
4. Morabito, P.: Round robin testing programme: equipments, testing methods, test results. IPACS Report, TU Lulea, Sweden (2001). ISBN 91-89580-42-7

## D.5 Description of Equipment/Procedures

Company/Institution:	Kanazawa University
Department:	Department of Civil Engineering
Information filled in by:	Shin-ichi Igarashi
E-mail address:	igarashi@t.kanazawa-u.ac.jp
<hr/>	
Name of rig:	Shrinkage testing apparatus
Designed to measure on: (concrete, mortar, paste, etc.)	Concrete, mortar and cement pastes at early ages
Specimen geometry:	50 × 50 × 1,018 mm
Specimen orientation: (horizontal/vertical)	Horizontal
Start of measurement: (hours after mixing)	10–12 h after mixing
Type of measuring device: (LVDT, strain gauge, laser, thermocouples, etc.)	2 × LVDT
Temperature control (yes/no):	No
<i>Designed to measure</i>	
(a) AD at isothermal temperatures (yes/no):	No
(b) Coupled AD and TD at semi-adiabatic temperature histories (yes/no):	No
(c) CTE during rapid temperature changes (yes/no):	No
Additional info.:	Temperature effects are ignored because of the small cross section of specimen

### D.5.1 Description of Rig and Specimen

The restrained and free shrinkage tests can be simultaneously carried out by the use of uniaxial restrained shrinkage testing apparatus. The apparatus is placed in the room at 18 °C. Concretes are directly cast into the molds for the restrained and free shrinkage measurements (Fig. D.7). In order to reduce friction between the cast concrete and the mould, the mold is lined with thin plastic sheets (Teflon). This computer controlled testing system, developed by Kovler [1] can be used to determine free shrinkage, restraining stresses and visco-elastic responses using the procedures outlined in [1]. The specimens are sealed immediately after casting.

The testing apparatus consisted of two identical specimens and the measuring devices. In the restrained shrinkage specimen, when shrinkage occurs and its level

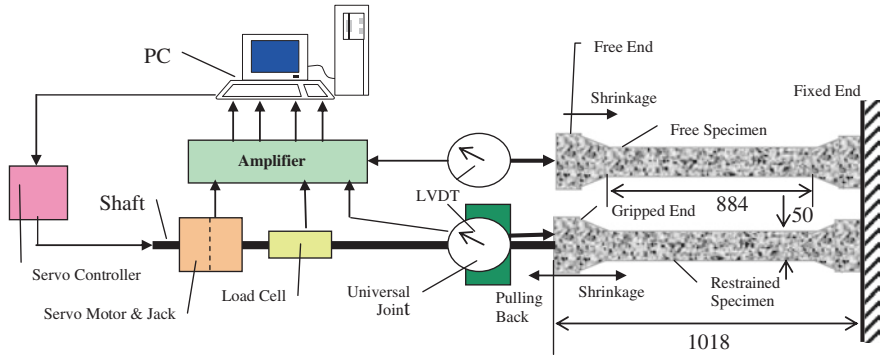


Fig. D.7 Restrained shrinkage testing apparatus

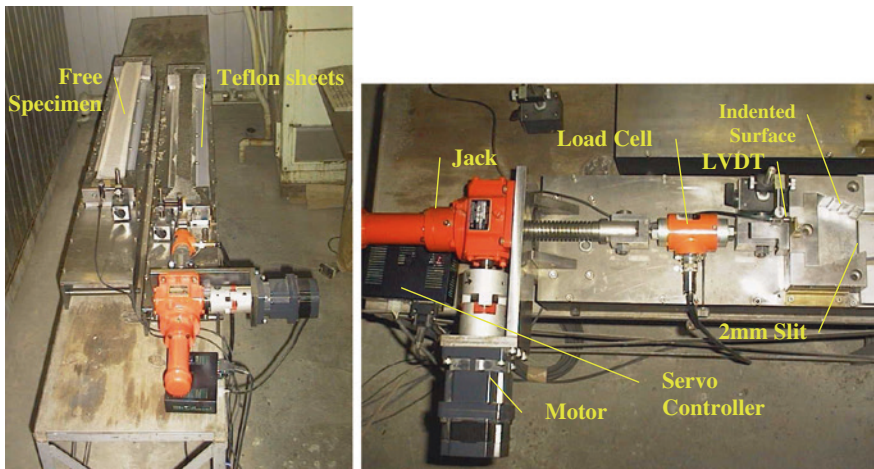


Fig. D.8 Left Cover shot of the apparatus. Right Details of restraining system

is beyond a strain of  $10 \times 10^{-6}$ , the servo motor automatically starts working to pull the specimen back to the initial position. Length changes of both specimens and the restraining load generated by the restrained shrinkage specimen are continuously recorded. The capacity of the load cell is 10,000 N. Because of the limited capacity of load, this apparatus can be used only for early age cementitious materials. The restraint is given the specimen after allowing it to shrink for the first 12 h after casting. Effects of thermal expansion are ignored since the increase in temperature is at most 1–2 °C in the specimens with small cross sections. The test is usually conducted for 7 days after casting (Fig. D.8).



## References

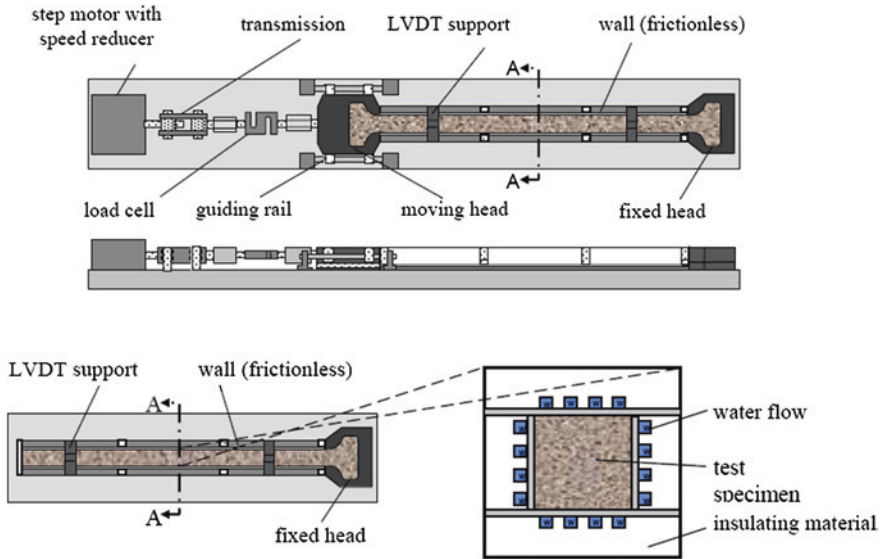
1. Kovler, K.: Testing system for determining the mechanical behavior of early age concrete under restrained and free uniaxial shrinkage. *Mater. Struct.* **27**(170), 324–330 (1994)
2. Igarashi, S., Kawamura, M.: Effects of microstructure on restrained autogenous shrinkage behavior in high strength concretes at early ages. *Mater. Struct.* **35**(3), 80–84 (2002)

Company/Institution:	Laval University, Canada
Department:	CRIB—Department of civil engineering
Responsible person:	Fabien Perez
E-mail address:	fabien.perez@gci.ulaval.ca

Name of rig	Free shrinkage apparatus
Designed to measure on: (concrete, mortar, paste, etc.)	Cement paste, mortar, mini-concrete
Specimen geometry:	50 × 50 × 1,000 mm
Specimen orientation: (horizontal/vertical)	Horizontal
Start of measurement: (hours after mixing)	11 h
Type of measuring device: (LVDT, strain gauge, lacer, thermo-couples, etc.)	LVDT
Temperature control (yes/no):	Yes
<i>Designed to measure</i>	
(a) AD at isothermal temperatures (yes/no):	Yes
(b) Coupled AD and TD at semi-adiabatic temperature histories (yes/no):	Yes
(c) CTE during rapid temperature changes (yes/no):	Yes
Additional info.:	–

### D.5.2 Description of Rig and Specimen

The operating principle of the DRS test setup is similar to that of longitudinal instrumented testing rigs originally developed by Bloom and Bentur [2], Kovler [3] and Bjøntegaard [1, 4, 5]. A comprehensive review of various equipments that have been developed to investigate the early age behavior of concrete can be found elsewhere [6].



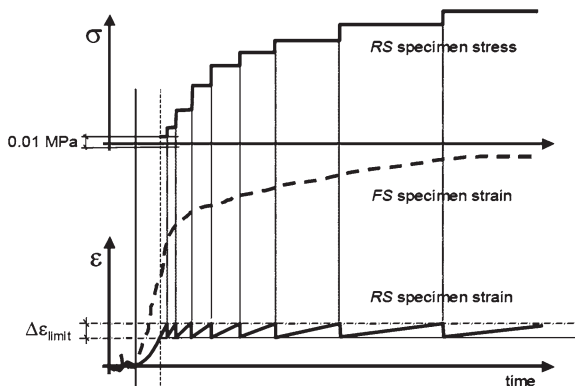
**Fig. D.9** Schematic configuration of the discretized restrained shrinkage (DRS) test setup. **a** Restrained shrinkage (RS) apparatus. **b** Free shrinkage (FS) apparatus. **c** RS and FS apparatus cross-section A-A

The DRS setup used in this investigation is composed of two independent fully automated instrumented pieces of equipment: a free shrinkage (FS) apparatus and a restrained shrinkage (RS) apparatus. In the former, one end of the specimen is restrained against movement by a fixed steel head, and the other is free to move (Fig. D.9b), whereas in the latter one end is restrained by a fixed steel head, and the displacement of the other end is controlled by a motor-driven moving steel head (Fig. D.9a).

As can be seen in Fig. D.9, both of pieces of equipment were designed to test slender dog-bone shape specimens, with a 1-m long straight central portion of the specimen having a  $50 \times 50$  mm cross section. Depending on the apparatus, the specimen width at one (for the FS apparatus) or at both ends (for the RS test rig) increases from 50 to 150 mm with 25-mm radii (on both sides) to provide the load-bearing abutments. The specimen dimensions were selected to allow testing a broad variety of cement-based materials (cement paste, mortar and small aggregate concrete mixtures) and to minimize as much as possible internal temperature gradients. In addition, the lateral walls and the horizontal contact surface, which serve as formwork at the time of casting, are made of aluminum. The high thermal conductivity ( $k = 34.1$  W/m °C) of aluminum greatly facilitates the temperature control of the specimen, while its low density helps in limiting the total mass of the system.

The loading (restraining) mechanism of the RS apparatus is depicted in Fig. D.9a. The rotating motion produced by a step-motor is transformed into linear

**Fig. D.10** Schematic representation of DRs procedure



displacement through a transmission shaft coupled to a stiff sliding unit. This unit is itself connected to the moving head with a load cell. The displacement of the moving head allows the specimen to deform during the different phases of the DRS experiment, as explained in the next section.

As concrete hydrates, it readily undergoes significant volume changes (see Fig. D.10). After casting, the specimen placed in the closed-loop instrumented RS test rig is initially restrained by the setup self-rigidity, the motor being turned off until the recorded load reaches a critical stress value of 0.01 MPa (tension or compression, i.e., +0.01 or -0.01 MPa). At that moment, the LVDTs readings are zeroed. Thereafter, the load is continually adjusted to maintain a constant stress (i.e., within a  $\pm 0.01$  MPa range) and the specimen is allowed to deform until the recorded strain in its straight part reaches a critical deformation (i.e.,  $\pm 6 \times 10^{-6}$  for this study). This coincides with the end of the first cycle, at which time the load is adjusted to pull (or push) the specimen back to its original length. The applied load at the end of the adjustment process is then kept constant throughout the following cycle, until the strain in the specimen again reaches the limit value. The test then goes on in a stepwise fashion until it is stopped (typically at 7 days). The stress generation in the test specimen is thus discretized and allows the determination of the stress build-up and the corresponding elastic and creep strains in the specimen as a function of time. In a perfectly restrained specimen, the above mentioned threshold value becomes infinitely small. In parallel with the restrained shrinkage experiment, a test is conducted in the free shrinkage (FS) apparatus for the determination of the free shrinkage curve.

The cross-section of both DRS test apparatus is illustrated in Fig. D.9c. The inner surface of the aluminum walls are covered with a thin plastic sheet (UHMW) and an ultra thin paraffin film is installed prior to the placement of concrete. This is essentially intended to minimize friction between the walls and the specimens. The conditioning system is located on the outer face of the panels and it consists of grooved (6-mm channels) insulating plastic panels glued against the aluminum

plates in which temperature-controlled water is circulated (thermal conduction water—aluminum—concrete). The channels are connected in closed loop to a thermal bath that controls temperature in a range between 5 and 50 °C with a precision of  $\pm 0.05$  °C [7]. The material (Delrin) used for the water-circulating system was selected mostly on the basis of its insulating properties ( $k = 0.23$  W/m °C) to minimize thermal losses.

## References

1. Bjøntegaard, Ø.: Thermal dilation and autogenous deformation as driving forces to self-induced stresses in high performance concrete, 253 p. Ph.D. thesis, Norwegian University of Science and Technology, Norway (1999)
2. Bloom, R., Bentur, A.: Free and restrained shrinkage of normal and high-strength concretes. *Am. Concr. Inst. Mater. J.* **92**(2), 211–217 (1995)
3. Kovler, K.: Testing system for determining the mechanical behaviour of early-age concrete under restrained and free uniaxial shrinkage. *Mater. Struct.* **27**(170), 324–330 (1994)
4. Bjøntegaard, Ø., Sellevold, E.J.: Thermal dilation—autogenous shrinkage: how to separate? In: *Autogeneous Shrinkage of Concrete*, E & FN Spon, London, pp. 233–244 (1998)
5. Bjøntegaard, Ø., Sellevold, E.J.: Interaction between thermal dilation and autogenous deformation in high-performance. *Mater. Struct.* **34**, 266–272 (2001)
6. Bentur, A., Kovler, K.: Evaluation of early-age cracking characteristics in cementitious systems. *Concr. Sci. Eng./Mater. Struct.* **36**(257), 183–189 (2003)

## D.6 Description of Equipment/Procedures

Company/Institution:	Laboratoire Central des Ponts et Chaussées (LCPC)
Department:	Concrete and cementitious composites
Information filled in by:	Véronique Baroghel-Bouny
E-mail address:	baroghel@lcpc.fr
<hr/>	
Name of rig	LCPC autogenous shrinkage rig (concrete)
Designed to measure on: (concrete, mortar, paste, etc.)	Concrete
Specimen geometry:	h: 250 mm diameter: 120 mm
Specimen orientation: (horizontal/vertical)	Vertical
Start of measurement: (hours after mixing)	~1 h
Type of measuring device: (LVDT, strain gauge, laser, thermocouples, etc.)	Digital displacement LE12 SOLARTRON transducer
Temperature control (yes/no):	Yes
<i>Designed to measure</i>	
(a) AD at isothermal temperatures (yes/no):	Yes
(b) Coupled AD and TD at semi-adiabatic temperature histories (yes/no):	Yes in the future
(c) CTE during rapid temperature changes (yes/no):	Yes
Additional info.:	Heat measurement?
	Longitudinal wave dynamical sound velocity
	Setting time (by means of mechanical low cyclic solicitation)?

### D.6.1 Description of Rig and Specimen

The device is performed in stainless steel (bars made of invar) and includes a non-rigid corrugated mould (which ensures low friction and appropriate sealing) and a data-logger system (computer). The rig (see figure) allows autogenous length change measurement in isothermal conditions. The rig is entirely immersed in a thermo-regulated bath at the required temperature (e.g.  $T = 21\text{ }^{\circ}\text{C}$ , accuracy =  $0.1\text{ }^{\circ}\text{C}$ ).

The test duration is 15 days.

### D.6.2 Casting and Test Procedure

The concrete is prepared in a room regulated at  $T = 21\text{ }^{\circ}\text{C}$ . The sample is cast in the mould immediately after mixing.

Measurement start at  $\sim 1\text{ h}$ .

Deformations and temperature (internal zone of the specimen, bath and room) are recorded every 15 min (the frequency can be modified).

Temperature corrections can be made from the temperature measurement of the frame.

### D.6.3 Measuring System and Data Presentation

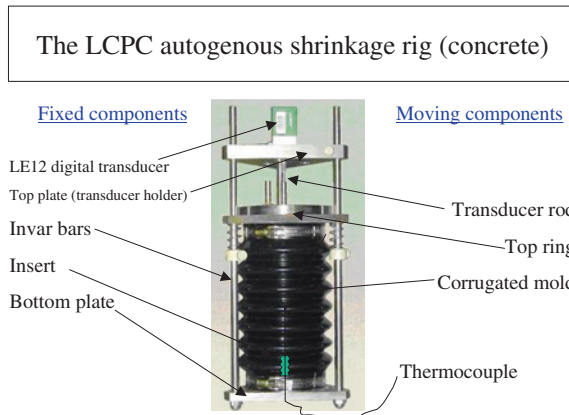
Accuracy of the digital SOLARTRON LE12 displacement transducer:  $0.3\text{ }\mu\text{m}$ .

Measuring length: 25 mm.

Resolution:  $5/100\text{ }\mu\text{m}$ .

## Reference

1. Boulay, C., Le Roy, R., Le Maou, F.: Etude du retrait et du fluage des bétons M100 et M120. BHP 2000 National Project, LCPC Report, February 1999



## D.7 Description of Equipment/Procedures

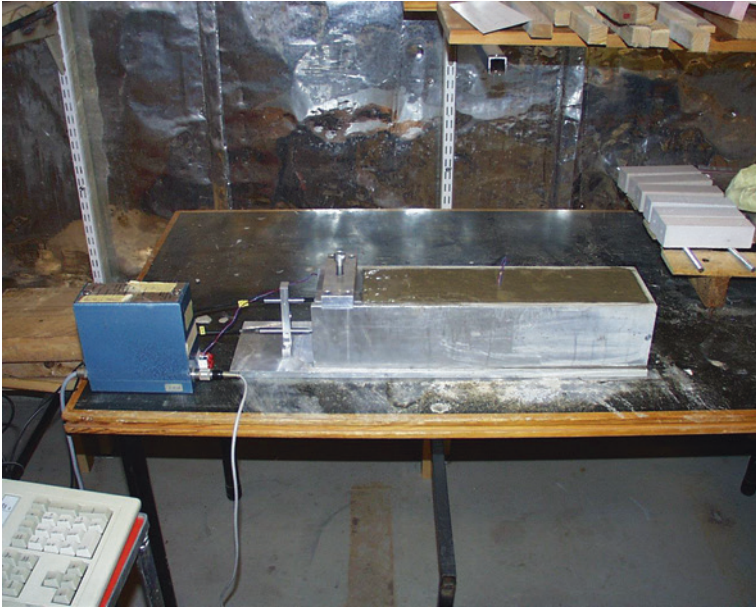
Company/Institution:	Lund Institute of Technology
Department:	Building Materials
Information filled in by:	Persson, Bertil
E-mail address:	Bertil.Persson@byggtek.lth.se
<hr/>	
Name of rig:	LTH shrink rig 1–3
Designed to measure on: (concrete, mortar, paste, etc.)	Autogenous, plastic or wet shrinkage at two levels
Specimen geometry:	100 × 100 × 400 mm
Specimen orientation: (horizontal/vertical)	Horizontal
Start of measurement: (hours after mixing)	0.25 h
Type of measuring device: (LVDT, strain gauge, laser, thermocouples, etc.)	3 × 2 LVDTs
Temperature control (yes/no):	Yes
<i>Designed to measure</i>	
(a) AD at isothermal temperatures (yes/no):	AD?
(b) Coupled AD and TD at semi-adiabatic temperature histories (yes/no):	TD?
(c) CTE during rapid temperature changes (yes/no):	CTE?
Additional info.	Ongoing projects on self-compacting concrete

### D.7.1 Description of Rig and Specimen

The equipment is performed in stainless steel except for the end block which is aluminium. All part of the rig may be demounted in order to maintain, see Figs. D.11 and D.12.

### D.7.2 Casting and Test Procedure

The concrete is cast in a high relative humidity, RH, room and initially treated with air, curing compound or wet clothes as requested. RH = 95 % at casting. The temperature and deformations measurements start at 0.25-h-age. In case of



**Fig. D.11** The LTH shrink rig in detail with two LVDTs in order to measure the shrinkage profile



**Fig. D.12** An overview of the LTH shrink rig



autogenous shrinkage measurements a small amount of moisture onto the surface is required in order to obtain a vertical shrinkage profile. Otherwise the results with the double LVDTs always show an inclined profile from the surface even though the surface is sealed immediately after casting of the concrete. All other kinds of treatment the very first minutes after casting always causing a small drying of the surface which always gives plastic shrinkage assumed to be an autogenous one by many researchers before. A constant wind speed of 4 m/s is used above the specimen.

### ***D.7.3 Measuring System and Data Presentation***

LVDTs, thermocouples and computers, Figs. [D.11](#) and [D.12](#).

## **References**

1. Friberg, P.: Plastic shrinkage of self-compacting concrete. Plastisk krympning hos självkompakterande betong. TVBM-5051, Lund Institute of Technology, Lund University, Lund. Preliminary, 45 p. (2002). (In Swedish with English summary)
2. Hugas, P.A.: Mix proportions and properties of self-compacting concrete. Sammansättning och egenskaper hos självkompakterande betong. TVBM-5041, 56 p. Division of Building Materials, Lund Institute of Technology, Lund University, Lund (1999)
3. Charkas, M., Fayli, W.: Self-compacting concrete with glass filler—studies on aspects on materials and production. Material- och produktionstekniska studier av självkompakterande betong med glasfiller. Report TVBM-5042, 80 p. Division of Building Materials, Lund Institute of Technology, Lund University, Lund (1999). (In Swedish with English summary)

## D.8 Description of Equipment/Procedures

Company/Institution:	Munich Technical University
Department:	CBM—centrum baustoffe und materialprüfung
Information given by:	Jürgen Huber
E-mail address:	jhuber@cbm.tum.de

Name of rig	
Designed to measure on: (concrete, mortar, paste, etc.)	
Specimen geometry:	Cylindrical, $D = 30$ mm, $L = 140$ mm
Specimen orientation: (horizontal/vertical)	Horizontal
Start of measurement: (hours after mixing)	8 h
Type of measuring device: (LVDT, strain gauge, laser, thermocouples, etc.)	LVDT, p 100
Temperature control (yes/no):	No
<i>Designed to measure</i>	
(a) AD at isothermal temperatures (yes/no):	No
(b) Coupled AD and TD at semi-adiabatic temperature histories (yes/no):	No
(c) CTE during rapid temperature changes (yes/no):	No
Additional info.:	

### D.8.1 Description of Rig and Specimen

The fresh concrete is filled into a plastic cylinder covered by a Teflon foil on the inside. The length change is measured by position encoders at both ends of the specimen. The ends are sealed with (greased) steel caps (Figs. [D.13](#) and [D.14](#)).

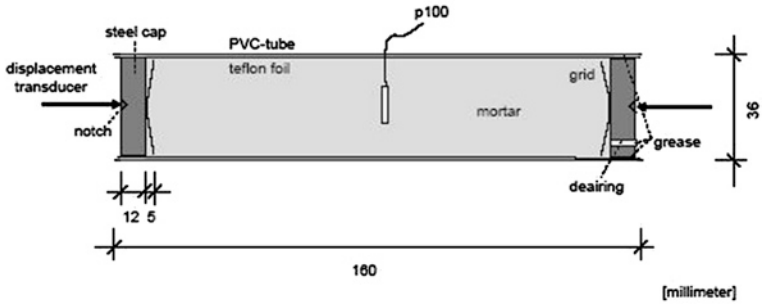


Fig. D.13 Dilation rig, principle sketch

Fig. D.14 Dilation rig,  
picture



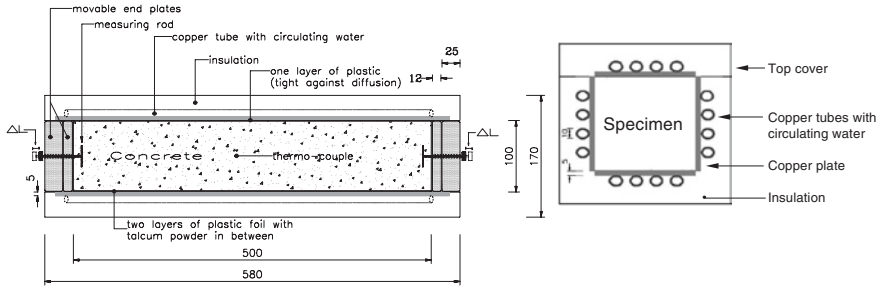
## D.9 Description of Equipment/Procedures

Company/Institution:	The Norwegian University of Science and Technology
Department:	Department of Structural Engineering
Information filled in by:	Øyvind Bjøntegaard
E-mail address:	oyvind.bjontegaard@bygg.ntnu.no
<hr/>	
Name of rig:	Dilation rig
Designed to measure on: (concrete, mortar, paste, etc.)	Concrete and mortar (can be modified to handle paste)
Specimen geometry:	100 × 100 × 500 mm
Specimen orientation: (horizontal/vertical)	Horizontal
Start of measurement: (hours after mixing)	~1 h
Type of measuring device: (LVDT, strain gauge, laser, thermocouples, etc.)	2 × LVDT and thermocouple
Temperature control (yes/no):	Yes
<i>Designed to measure</i>	
(a) AD at isothermal temperatures (yes/no):	Yes
(b) Coupled AD and TD at semi-adiabatic temperature histories (yes/no):	Yes
(c) CTE during rapid temperature changes (yes/no):	Yes
Additional info.:	A separate bleeding measurement is often performed

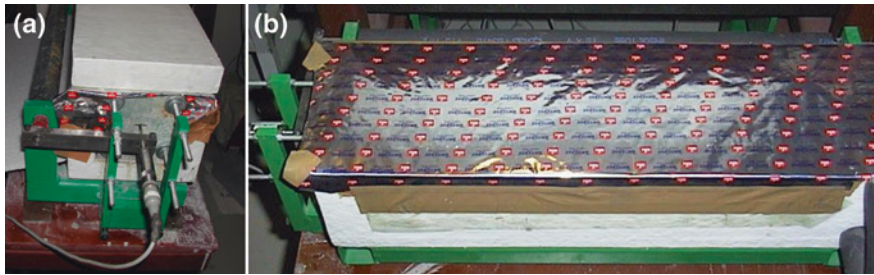
### D.9.1 Description of Rig and Specimen

The mould is constructed of 5 mm thick copper plates, to which copper tubes are fixed, and an outer insulating material, giving a total thickness is 35 mm, see Fig. D.15. The copper tubes are connected to a central bath, which circulates temperature-controlled water through the tubes and, thus, controls the temperature of the specimen during testing. The water temperature can be controlled from the computer (from a pre-prepared data file) or from a controller mounted directly on the bath. The system has shown to give very good temperature control of the specimen in the range 2–65 °C.

Each of the two ends of the mould consists of plates of insulating material (total thickness 37 mm) where centric holes are made for a measuring rod to enter, see Fig. D.16 (left). The end plates are held in place during the early period when



**Fig. D.15** The dilation rig: longitudinal view (*left*) and cross-section (*right*)



**Fig. D.16** *Left* End of specimen. The LVDTs are connected to each other by an invar steel bar (*left*) and connected to the specimen with invar rods. *Right* The dilation rig before placing of *top cover*. A foil to prevent water loss is wrapped around the top surface of the specimen

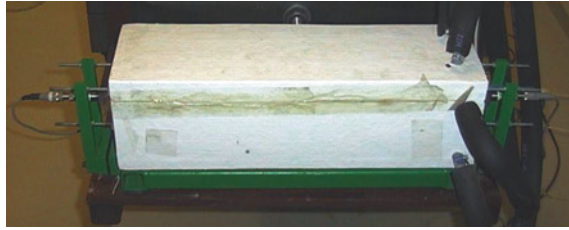
the concrete exerts hydrostatic pressure. After setting, the end plates may be gently moved a few millimeter away from the specimen to allow the specimen to expand freely. Length change ( $\Delta L$ ) is measured centrally at both ends by LVDTs. The LVDTs are connected to each other by an invar steel bar and connected to the specimen by 70 mm long invar steel rods (going through the holes in the end plates) with discs at the end. The rods extends  $\sim 15$  mm into the sample, hence the measuring length is  $\sim 470$  mm (the exact length is measured before each test).

The rig can also be modified to handle cement paste. The cross-section is then reduced to  $50 \times 50$  mm by placing massive steel plates into the larger mould chamber. A smaller cross-section is needed to maintain good temperature control when cement paste is tested since more heat is generated during hydration.

### D.9.2 Casting and Test Procedure

Before casting, the mould (bottom and all sides) is lined with two layers of plastic sheets with talcum powder in between in order to minimize friction. When the concrete is cast (and generally vibrated), the surface is trowelled and a thermocouple is put in the centre of the specimen. The top surface is tightly covered with aluminium foil to prevent loss of water, see Fig. D.16 (right), and, finally, the top cover is

**Fig. D.17** The dilation rig during measurement



put in place, Fig. D.17. The temperature measurement is started at this point (typically  $\frac{1}{2}$  h after mixing), while the LVDTs are activated somewhat later: During casting the LVDTs are at the end of the measuring range due a small spring load (corresponds to a concrete stress of  $\sim 0.001$  MPa) inside the LVDT. The LVDTs are activated (i.e., adjusted to the middle of the measuring range) when the concrete has lost some consistency and, thus, can resist the spring load. This time may vary from  $\frac{1}{2}$  h to some hours depending on the concrete composition.

Bleed water collected on the surface of the specimen is generally removed before setting in order to prevent it to be reabsorbed after setting, which may influence the result. The bleeding of the concrete is often measured in a parallel experiment.

### ***D.9.3 Measuring System and Data Presentation***

The signals from the two LVDTs and the thermocouple are recorded continuously by means of a signal amplifier and a computer during each test (the surrounding air temperature is also measured as control). The LVDT signals are added to give the total length change ( $\Delta L$ ). Presented data (strains) are always compensated for the thermal movement of the end steel rods, which is caused by heat transmission from the specimen. A relation between concrete temperature and the temperature of the steel rods is established. The compensation constitutes around 2–3 % of the measured length change in the rig. Data are generally presented from around setting (i.e., when stresses are recorded in a parallel TSTM-test).

## **References**

1. Bjøntegaard, Ø.: Thermal dilation and autogenous deformation as driving forces to self-induced stresses in high performance concrete. Doctoral thesis, NTNU (1999). ISBN 82-7984-002-8
2. Morabito, P.: IPACS report. Round Robin Testing Programme. Contribution from 13 authors within the IPACS consortium, TU Luleå, Sweden (2001). ISBN 91-89580-42-7
3. Bjøntegaard, Ø., Hammer, T.A., Sellevold, E.J.: On the Measurement of Free Deformation of Early Age Cement Paste and Concrete, Cement and Concrete Composites (2003) (accepted for publication)

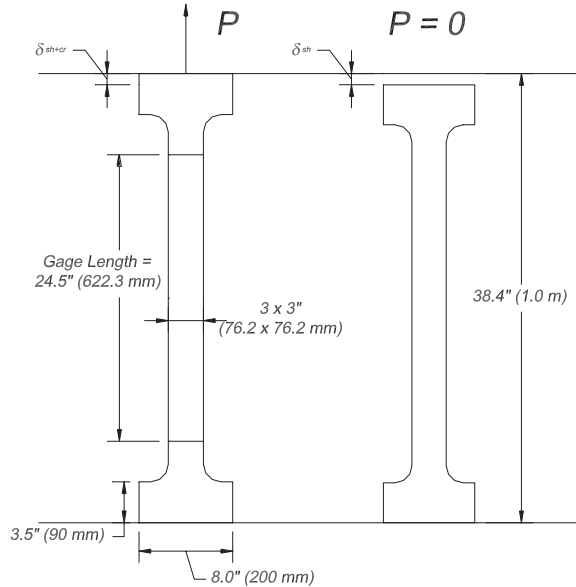
## D.10 Description of Equipment/Procedures

Company/Institution:	University of Illinois at Urbana-Champaign
Department:	Department of Civil and Environmental Engineering
Information filled in by:	Matthew D' Ambrosia
E-mail address:	dambrosi@uiuc.edu
<hr/>	
Name of rig:	Uniaxial Creep-Shrinkage Device
Designed to measure on: (concrete, mortar, paste, etc.)	Concrete and mortar
Specimen geometry:	76.2 × 76.2 × 1,000 mm
Specimen orientation: (horizontal/vertical)	Horizontal
Start of measurement: (hours after mixing)	8–10 h for LVDT, 1 h for embedded strain gages
Type of measuring device: (LVDT, strain gauge, laser, thermocouples, etc.)	2 × LVDT, 2 × embedded strain gage, thermocouples
Temperature control (yes/no):	Room control only
<i>Designed to measure</i>	
(a) AD at isothermal temperatures (yes/no):	Yes
(b) Coupled AD and TD at semi-adiabatic temperature histories (yes/no):	No
(c) CTE during rapid temperature changes (yes/no):	No
Additional info.:	Additional specimens for internal relative humidity and semi-adiabatic calorimetry measurements

### D.10.1 Description of Rig and Specimen

The uniaxial test technique allows for simultaneous measurement of free shrinkage and deformation under restrained or constant tensile load [1]. Two companion specimens were cast in a temperature and humidity controlled environmental chamber. The conditions during testing were 23 °C (±0.5 °C) and 50 % (±5 %) relative humidity. The dimensions of each specimen are given in Fig. D.18. The steel end grips, which transmit the applied load, remained in place for the duration of the test. Steel formwork was removed from the sides of the specimen at 23 h. A barrier of self-adhesive aluminum foil was used to impose a sealed condition. Formwork was lined with foil prior to casting and sealed immediately after placement.

**Fig. D.18** Companion specimen diagram



A rounded transition in specimen geometry minimizes stress concentrations and interactions between the specimen and the end grip. To minimize friction between the specimen and the table surface, a 3 mm (1/8") thick plastic sheet was used.

### D.10.2 Casting and Test Procedure

The unrestrained specimen, shown in Fig. D.19, was used to measure free shrinkage and not subject to external loading or restraint. The restrained specimen, shown in Fig. D.20, was connected to the actuator and tested in a computer controlled closed-loop configuration. This configuration can be used to conduct two different tests. A constant load test can be performed or a restrained load condition can be imposed. The specimen was allowed to deform within a threshold strain value and then restrained by applying a load to compensate for this deformation once the threshold value was reached. For measuring tensile creep, compressive loads did not compensate for expansion. The applied load was feedback controlled and stopped once the specimen returned to its original length. A threshold value of 0.005 mm (8  $\mu\epsilon$ ) was used to simulate restraint. This value was determined experimentally to be the minimum effective value within the limitations of the measuring equipment.

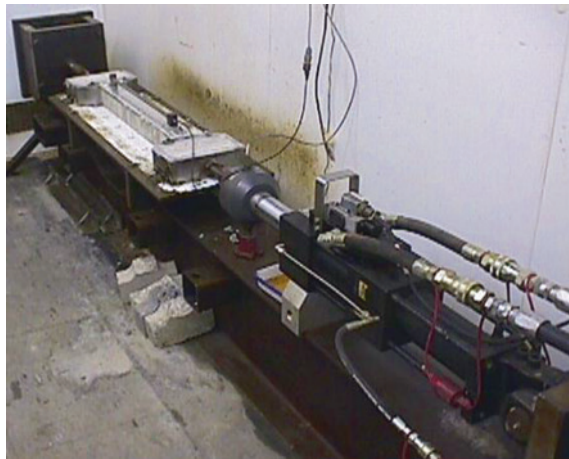
### D.10.3 Measuring System and Data Presentation

A 20 kN (5 kip) load cell in line with a 90 kN (20 kip) servo-hydraulic actuator controlled the load applied to the specimen. Deformation was measured using an extensometer consisting of a linear variable differential transformer (LVDT) and a





**Fig. D.19** Unrestrained uniaxial test specimen



**Fig. D.20** Restrained uniaxial test specimen with servo-hydraulic system

steel rod positioned on the top of the concrete specimen for a total gage length of 622.3 mm (24.5 in.). Steel brackets with bolts anchored into the concrete specimen supported the measurement assembly. The test measurements began at 9 h for this study.

Data collection is performed using LabView and Instron controller in a closed loop feedback controlled system. The system operates in load control until the restrained specimen reaches a threshold deformation (typically 0.005 mm), then transfers to strain control to apply load to the restrained specimen until the LVDT reads 0.000 mm deformation (Figs. [D.21](#), [D.22](#), [D.23](#), [D.24](#), [D.25](#), [D.26](#) and [D.27](#)).

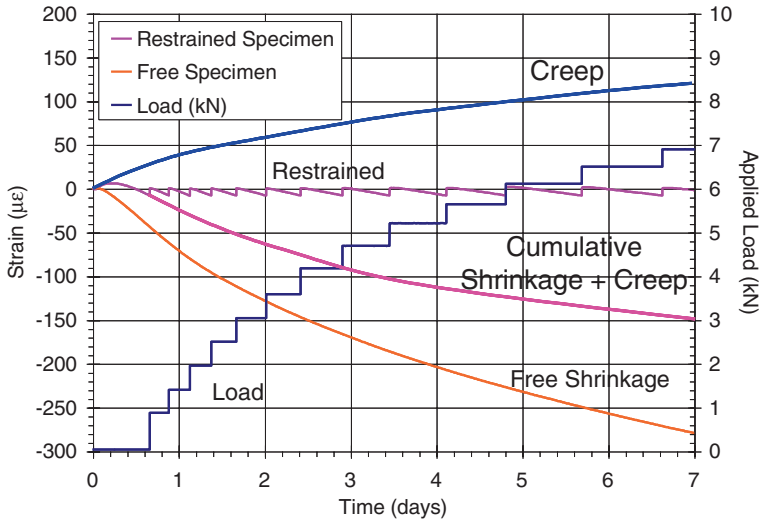


Fig. D.21 Typical restrained test data

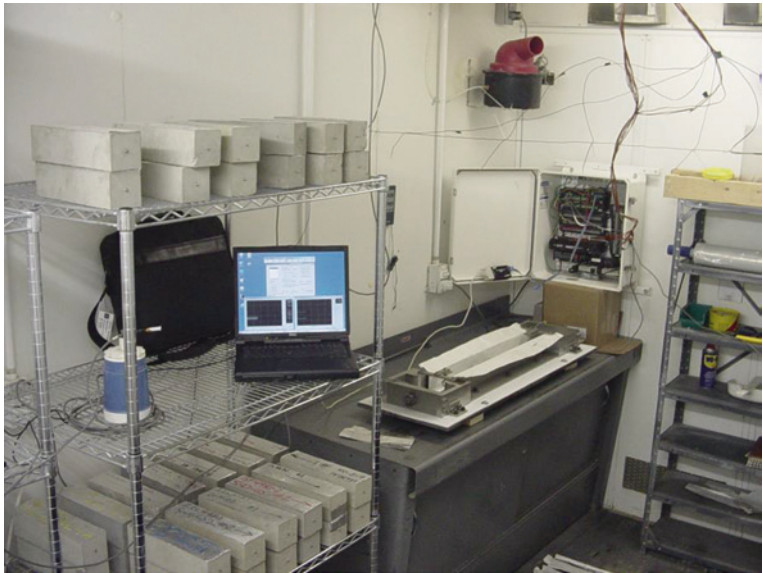


Fig. D.22 Free shrinkage specimens



Fig. D.23 Environmental chamber and relative humidity system



Fig. D.24 LabView program and controller



**Fig. D.25** Autogenous deformation measurement in sealed samples

**Fig. D.26** Embedment strain gage measurement



**Fig. D.27** Restrained system with embedment gage



## References

1. Altoubat, S.A.: Early age stresses and creep-shrinkage interaction of restrained concrete. Ph.D. thesis, Department of Civil and Environmental Engineering, University of Illinois at Urbana-Champaign (2000)
2. Altoubat, S.A., Lange, D.A.: Grip-specimen interaction in uniaxial restrained test. ACI SP-206, Concrete: Material Science to Application—A Tribute to Surendra P. Shah (2002)

### D.11 Description of Equipment/Procedures

Company/Institution:	SINTEF Civil and Environmental Engineering
Department:	Cement and Concrete
Information filled in by:	Tor Arne Hammer
E-mail address:	Tor.hammer@sintef.no
<hr/>	
Name of rig:	Plastic shrinkage rig
Designed to measure on: (concrete, mortar, paste, etc.)	Concrete, mortar and paste
Specimen geometry:	Slab, 100 × 100 × 280 mm or 50 × 50 × 280 mm
Specimen orientation: (horizontal/vertical)	Horizontal
Start of measurement: (hours after mixing)	Immediately after placing
Type of measuring device: (LVDT, strain gauge, laser, thermocouples, etc.)	LVDT
Temperature control (yes/no):	No
<i>Designed to measure</i>	
(a) AD at isothermal temperatures (yes/no):	Yes
(b) Coupled AD and TD at semi-adiabatic temperature histories (yes/no):	No
(c) CTE during rapid temperature changes (yes/no):	No
Additional info.:	Originally designed to measure settlement, shrinkage, pore water pressure, weight loss and temperature evolution before and during time of setting

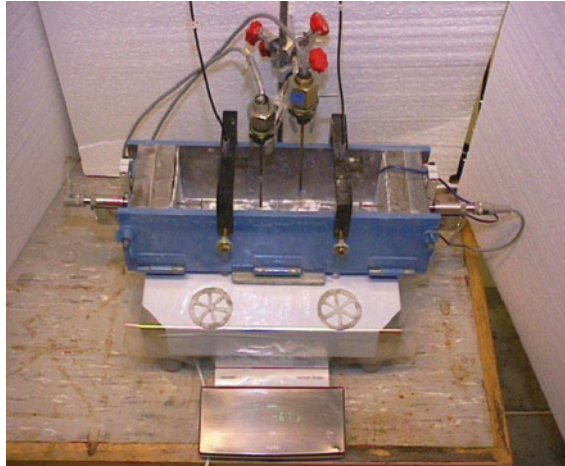
Shrinkage and settlement is measured on a slab in a steel mould with length/thickness/height of 280/100/100 mm, see Figure. A double layer of plastic sheets with talc powder in between is used inside the mould in order to keep the friction between the concrete and the mould as low as possible. The shrinkage is measured as the horizontal movement of two “nails” placed centric in both ends of the specimen. The nails are made of 3 mm thick steel rods with a 15 × 15 mm steel plate soldered to the end, placed 30 mm in the concrete. The other end is wedged and screwed into inductive displacement transducers through a hole in the ends of the mould. The transducers are fixed to the mould. The measurements have shown acceptable reproducibility.

The settlement is measured as the vertical movement of two circular plastic meshes with diameter of 50 mm, placed with its centre approximately 70 mm from the ends



of the mould. In order to prevent any external load from the inductive displacement transducer, the movable part of it resting on the mesh was very light. The meshes penetrate any bleed water. All data (settlement, shrinkage and pore water pressure) are recorded every second minute by the use of an electronic data logger. The rig is placed on a balance so that the water loss may be recorded (in tests with external drying).

The pore water pressure is measured by pressure transducer connected to a water filled tube with inner diameter of 3 mm, see figure. Two tubes are placed vertically in the concrete with the ends at 5 and 50 mm depths, respectively.



Picture of the rig with devices used to measure settlement, shrinkage, pore water pressure and weight loss in concrete before and during setting.

## References

1. Hammer, T.A.: On the strain capacity and cracking mechanisms of high strength concrete at very early age. In: Proceedings of the Sixth International Conference on Creep, Shrinkage and Durability of Mechanics of Concrete and Other Quasi-brittle Materials, pp. 657–662, Cambridge (MA), USA (2001). ISBN: 0-08-044002-9
2. Hammer, T.A.: The relationship between settlement and plastic shrinkage of high strength concrete. In: Pre-proceedings of the RILEM International Conference on Early Age Cracking of Cementitious Systems, National Building Research Institute/Technion, Haifa, Israel (2001)
3. Radocea, A.: A study on the mechanism of plastic shrinkage of cement-based materials. Thesis for the Degree of Doctor of Engineering from Chalmers Technical University, Gothenburg, Sweden (1992)

## D.12 Description of Equipment/Procedures

Company/Institution:	Ecole Centrale Nantes/Laboratoire de Génie Civil
Department:	Civil engineering
Information filled in by:	Loukili, Ahmed
E-mail address:	Ahmed.loukili@ec-nantes.fr
<hr/>	
Name of rig	Nantes—R&DO SHRINK RIG
Designed to measure on: (concrete, mortar, paste, etc.)	Autogenous, plastic shrinkage and settlement Mortar and concrete
Specimen geometry:	70 × 70 × 280 mm
Specimen orientation: (horizontal/vertical)	Horizontal
Start of measurement: (hours after mixing)	0.3 h
Type of measuring device: (LVDT, strain gauge, laser, thermocouples, etc.)	2 lasers for horizontal shrinkage and 1 laser for settlement, thermocouple
Temperature control (yes/no):	Yes
<i>Designed to measure</i>	
(a) AD at isothermal temperatures (yes/no):	(a) yes
(b) Coupled AD and TD at semi-adiabatic temperature histories (yes/no):	(b) it is under development. This was done with volumetric measurements on mortar [1]and paste [2]
(c) CTE during rapid temperature changes (yes/no):	(c) no
Additional info.:	Studies in progress within the framework of the French National project on self-compacting concrete

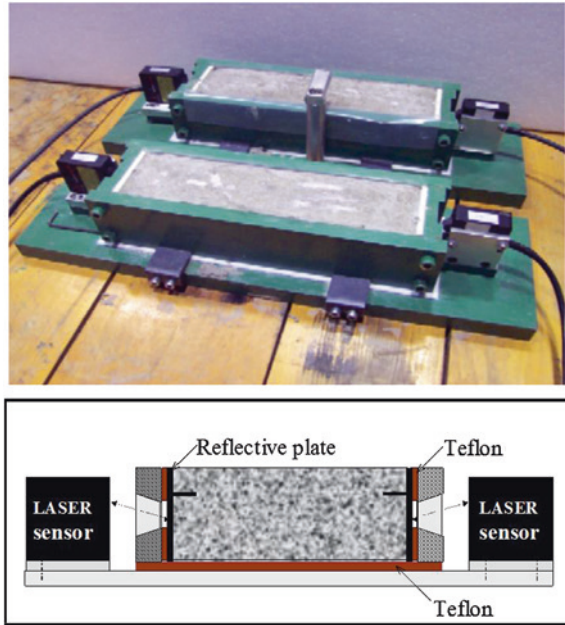
### D.12.1 Description of Rig and Specimen

The device schematized on Fig. D.28 was used to measure plastic shrinkage (with or without drying) before the final setting. The equipment is performed in stainless steel with a Teflon plate in the lower part to reduce friction between the concrete and the mould (Fig. D.28).

After mixing, mixture was placed in a 7 × 7 × 28 cm mold. Two laser transducers were used to measure the movement of the two short sidewalls, which can follow the specimen shrinkage. Tests were performed at constant temperature and 50 ± 5 % Relative Humidity (HR) and began 20 mn after casting. A constant wind speed of 5 m/s can be applied above the specimen. All data are logged on computer.



**Fig. D.28** The Nantes—  
R&DO SHRINK RIG in  
detail with two laser sensors



## References

1. Turcry, P., Loukili, A., Barcelo, L., Casabonne, J.M.: Can the maturity concept be used for separating autogenous shrinkage and thermal deformation of a cement paste at early age? *Cem. Concr. Res.* **32**(9), 1443–1450
2. Loukili, A., Chopin, D., Khelidj, A., Le Touzo, J-Y.: A new approach to determine autogenous shrinkage of mortar at early age considering temperature history. *Cem. Concr. Res.* **30**(6), 915–922 (2000)